CHALMERS
UNIVERSITY OF TECHNOLOGY

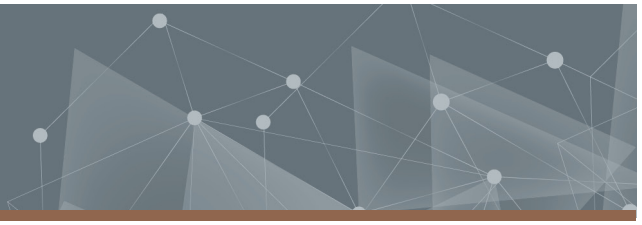

The Environmental Opportunities and Challenges of Composite Cars

Master's thesis in Industrial Ecology

Ivan Berg
Kevin Sandberg

DEPARTMENT OF TECHNOLOGY MANAGEMENT AND ECONOMICS
DIVISION OF ENVIRONMENTAL SYSTEMS ANALYSIS

CHALMERS UNIVERSITY OF TECHNOLOGY
Gothenburg, Sweden 2021
www.chalmers.se
Report No. E2021:065

Report No. E2021:065

The Environmental Opportunities and Challenges of Composite Cars

Ivan Berg
Kevin Sandberg

Department of Technology Management and Economics
Division of Environmental Systems Analysis
Chalmers University of Technology
Gothenburg, Sweden 2021

The environmental opportunities and challenges of Composite cars
Ivan Berg
Kevin Sandberg

Supervisor: Frida Hermansson, Technology Management and Economics
Examiner: Magdalena Svanström, Technology Management and Economics

Report No. E2021:065
Department of Technology Management and Economics
Division of Environmental Systems Analysis
Chalmers University of Technology
SE-412 96 Gothenburg
Sweden
Telephone +46 31 772 1000

Gothenburg, Sweden 2021

The environmental opportunities and challenges of Composite cars

Ivan Berg
Kevin Sandberg
Department of Technology Management and Economics
Chalmers University of Technology

Abstract

The transport sector faces several challenges when it comes to reducing its contribution to global warming and dependence on fossil fuels. This means that the transport sector needs to find alternative energy sources for its vehicles as well as to decrease the energy use in the use phase of the life cycle. This can be achieved by turning from vehicles with conventional internal combustion engines to electrical vehicles as well as to reduce the weight of the vehicles. The latter can be accomplished by substituting conventional materials with lightweight materials such as carbon fiber composites. However, there are also solutions on how to combine these strategies where the energy is stored in the body, which will reduce the mass of the vehicle as a consequence of reduced battery size.

The aim of the thesis was to assess the environmental impact of two composite vehicles based on either carbon fiber reinforced polymers or structural batteries as well as to give suggestion on how these materials can substitute conventional materials to reduce the weight while keeping or increasing the system performance. This implied a conceptual design of a conventional battery electric vehicle where the components were replaced with either carbon fiber reinforced polymers or structural batteries. This resulted in three conceptual vehicles based on different materials which functioned as input data to the inventory analysis of a cradle-to-grave life cycle assessment where the vehicles were assessed according to global warming potential, crustal scarcity indicator and cumulative energy demand.

The result showed that both carbon fiber reinforced polymers and structural batteries have the potential to reduce the weight of a conventional battery electric vehicle of approximately 30-50% while keeping or increasing the mechanical and electrochemical performance of the vehicle. The result showed that the vehicle based on carbon fiber reinforced polymers provides environmental benefits over a conventional electric vehicle, while structural batteries cause more environmental impact. However, the result indicated that the carbon fiber reinforced polymers and structural batteries could decrease its environmental impact drastically if the energy use was reduced in the carbon fiber production as well as the structural batteries manufacturing process in addition to using fossil carbon lean energy system.

Keywords: Multifunctionality, Lightweight Materials, Structural Batteries, Carbon Fiber Reinforced Polymers, Life Cycle Assessment

Acknowledgements

We wish to express our sincere appreciation to our supervisor, PhD student Frida Hermansson, for guiding us through the whole process of writing the master's thesis. We would also like to thank, Professor Leif Asp, for all the insights regarding structural batteries. Our examiner, Professor Magdalena Svanström, also deserves a big thank you for all the nuanced discussions. Lastly a great thank you to Fredrik Edgren, Technical Expert – Structural Composites at Volvo Car Corporation, for validating our conventional BEV model and providing us with input.

The result of the thesis is the outcome of a cooperation between the authors where the workload has been split equally.

Ivan Berg, Kevin Sandberg, Gothenburg, June 2021

Glossary

BEV Battery electric vehicle. 3

CFRPs Carbon fiber reinforced polymers. 1
CLT Classical lamination theory. 9

ERV Electric reduction value. 25
EU European Union. 1
EVs Electric vehicles. 1

GHG Greenhouse gas. 2

LCA Life cycle assessment. 2
Li-ion Lithium ion. 2

NEDC New European driving cycle. 25

PAN Polyacrylonitrile. 5
PVDF Polyvinylidenfluride film. 31

RTM Resin transfer moulding. 25

SBs Structural batteries. 1

WLTC Worldwide harmonised light-duty vehicles test procedure. 25

Contents

List of Figures **xv**

List of Tables **xxiii**

1 Introduction **1**
1.1 Background . . . 1
1.2 Objectives . . . 2
1.2.1 Specification of the Issue Under Investigation . . . 3
1.3 Limitations . . . 3

2 Theory **5**
2.1 Monofunctional Materials Design . . . 5
2.1.1 Carbon Fibers . . . 5
2.1.2 Carbon Fibers Reinforced Polymers . . . 6
2.2 Multifunctional Materials Design . . . 6
2.3 Structural Batteries . . . 7
2.3.1 Carbon Fibres in Structural Batteries . . . 7
2.3.2 Architectures for structural batteries . . . 8
2.3.3 Case-studies on Structural Batteries . . . 8
2.4 Classical Laminate Theory . . . 9
2.4.1 Volume and Weight Fractions . . . 9
2.4.2 Longitudinal Strength . . . 10
2.4.3 Tensile Strength . . . 10
2.4.4 Poission's Ratio . . . 10
2.4.5 Macromechanics of a Lamina . . . 11
2.5 Life Cycle Assessment . . . 13

3 Methodology **15**
3.1 Multifunctional Design Analysis . . . 15
3.2 The Conventional BEV . . . 17
3.2.1 Design of the Conventional BEV . . . 17
3.3 The CFRP car . . . 18
3.3.1 Design of the CFRP car . . . 18
3.4 The SB car . . . 19
3.4.1 Cell Design . . . 19
3.4.2 Design of the SB car . . . 20
3.5 Summary of the Design Processes . . . 21

3.6 Life Cycle Assessment . . . 21
3.6.1 Goal of the Study . . . 21
3.6.2 Scope of the Study . . . 22
3.6.2.1 Functional Unit . . . 22
3.6.2.2 Data Quality Requirements . . . 22
3.6.2.3 System Boundaries . . . 22
3.6.2.4 Impact Categories . . . 23
3.6.2.5 Allocation . . . 24
3.6.2.6 Limitations . . . 24
3.6.2.7 Assumptions . . . 25
3.6.3 Inventory Analysis . . . 26
3.6.3.1 Modelling of the Conventional BEV . . . 26
3.6.3.2 Modelling of the CFRP car . . . 28
3.6.3.3 Modelling of the SB car . . . 29
3.6.3.4 Modelling of the Use Phase . . . 32
3.6.4 Sensitivity Analysis . . . 32

4 Result and Discussion **35**
4.1 Design of the Conceptual Vehicles . . . 35
4.2 Global Warming Potential . . . 37
4.3 Crustal Scarcity Indicator . . . 39
4.4 Cumulative Energy Demand . . . 41
4.5 Hotspot Analysis . . . 42
4.5.1 The Conventional BEV . . . 42
4.5.2 The CFRP car . . . 45
4.5.3 The SB car . . . 50
4.6 Sensitivity Analysis . . . 56
4.6.1 The Result of Lightweighting Normalized to Swedish and Global data . . . 56
4.6.2 Break-even Analysis of the Use Phase of Global Warming Potential . . . 57
4.6.3 Hotspots in the CFRP Car and the SB Car . . . 58
4.6.3.1 Global Warming Potential . . . 58
4.6.3.2 Crustal Scarcity Indicator . . . 58
4.6.3.3 Cumulative Energy Demand . . . 59

5 Conclusion **61**
5.1 Future Research . . . 62

Bibliography **63**

A Calculations of the Effective Modulus of Elasticity **I**
A.1 Cell Design with 8 laminates . . . I

B Inventory Analysis **III**
B.1 Modelling of the conventional BEV . . . III
B.2 Modelling of the CFRP car . . . IV

B.3 Modelling of the SB car . . . V
B.4 Modelling of the Use Phase . . . VI

C Sensitivity Analysis **VII**
C.1 Adjustments in the Sensitivity Analysis based on Swedish data . . . VII
C.1.1 The Conventional BEV . . . VII
C.1.2 The CFRP car . . . VIII
C.1.3 The SB car . . . VIII

D Global Warming Potential **IX**
D.1 European data . . . IX
D.1.1 The SB car . . . IX
D.2 Global data . . . X
D.2.1 The conventional BEV . . . XI
D.2.2 The CFRP car . . . XII
D.2.3 The SB car . . . XIV
D.3 Swedish data . . . XVI
D.3.1 The conventional BEV . . . XVII
D.3.2 The CFRP car . . . XVIII
D.3.3 The SB car . . . XX

E Crustal Scarcity Indicator **XXIII**
E.1 European data . . . XXIII
E.1.1 The SB car . . . XXIII
E.2 Global Data . . . XXIV
E.2.1 The conventional BEV . . . XXV
E.2.2 The CFRP car . . . XXVI
E.2.3 The SB Car . . . XXVIII
E.3 Swedish Data . . . XXX
E.3.1 The conventional BEV . . . XXXI
E.3.2 The CFRP car . . . XXXII
E.3.3 The SB Car . . . XXXIV

F Cumulative Energy Demand **XXXVII**
F.1 European data . . . XXXVII
F.2 Global Data . . . XXXVIII
F.2.1 The conventional BEV . . . XXXIX
F.2.2 The CFRP car . . . XL
F.2.3 The SB Car . . . XLII
F.3 Swedish Data . . . XLIV
F.3.1 The conventional BEV . . . XLV
F.3.2 The CFRP car . . . XLVI
F.3.3 The SB Car . . . XLVIII

List of Figures

2.1 Structural battery laminated design, cross sectional view. 8
2.2 The LCA procedure where solid and dashed arrows indicates the order and possible iterations, respectively. 13

3.1 Multifunctional design requirements for a) the BMW i3 and b) the Tesla Model S. The dashed blue line for both figures represent the nominal weight of the two vehicles. The purple, yellow and red lines represent different values of electrochemical properties. 16
3.2 Cell with 6 laminates and laminate orientation code $[0/60/\text{-}60]_s$. . . . 20
3.3 Simplified flowchart of the processes including input and output flows. 23
3.4 Flowchart of the conventional BEV. Solid lines represent processes included in the system, while dashed lines represents processes excluded in the system. 27
3.5 Flowchart of the CFRP car. Solid lines represent processes included in the system, while dashed lines represents processes excluded in the system. 29
3.6 Flowchart of the SB car. Solid lines represent processes included in the system, while dashed lines represents processes excluded in the system. 30

4.1 The climate impact of the three vehicles. The black bars represent the net climate impact of the vehicles. 38
4.2 The crustal scarcity impact of the three vehicles. The black bars represent the net crustal scarcity impact. 40
4.3 The cumulative energy demand of the three vehicles. The black bars represent the net cumulative energy demand. 41
4.4 GWP 100 of the processes in the conventional BEV. 42
4.5 Crustal scarcity indicator of the processes in the conventional BEV. . 43
4.6 Cumulative energy demand of the processes in the conventional BEV. 43
4.7 GWP 100 of the processes in the CFRP car. 45
4.8 Crustal scarcity indicator of the processes in the CFRP car. 46
4.9 Cumulative energy demand of the processes in the CFRP car. 46
4.10 Cumulative energy demand of the processes in the CFRP car. 48
4.11 Crustal scarcity indicator of the processes in the CFRP car. 48
4.12 Cumulative energy demand of the processes in the CFRP car. 49
4.13 GWP 100 of the processes in the SB car. 50
4.14 Crustal scarcity indicator of the processes in the SB car. 51

4.15 Cumulative energy demand of the processes in the SB car. 51
4.16 GWP 100 of the processes in the SB car. 53
4.17 Crustal scarcity indicator of the processes in the SB car. 54
4.18 Cumulative energy demand of the processes in the SB car. 55
4.19 Break-even analysis of the global warming potential for the CFRP car and the SB car. Data is based on European data. 57

A.1 Cell with 8 laminates and laminate orientation code $[0/-45/45/90]_s$. . I

D.1 Contribution graph for global warming potential of the carbon fiber production for the SB car based on European data. The result was achieved by an LCA where the inventory was based on a conceptual design of the vehicle. The functional unit included the function of the car components as well as the battery of the electric vehicle where the lifetime was set to 200,000 km. IX
D.2 Global warming potential of the three vehicles based on global data. Black bars shows the net climate impact. The result was achieved by an LCA where the inventory was based on a conceptual design of the three vehicles. The functional unit included the function of the car components as well as the battery of the electric vehicle where the lifetime was set to 200,000 km. X
D.3 Global warming potential per process for the conventional BEV based on global data. The result was achieved by an LCA where the inventory was based on a conceptual design of the vehicle. The functional unit included the function of the car components as well as the battery of the electric vehicle where the lifetime was set to 200,000 km. XI
D.4 Global warming potential per process for the CFRP car based on global data. The result was achieved by an LCA where the inventory was based on a conceptual design of the vehicle. The functional unit included the function of the car components as well as the battery of the electric vehicle where the lifetime was set to 200,000 km. XII
D.5 Contribution graph for global warming potential of the carbon fiber production for the CRFP car based on global data. The result was achieved by an LCA where the inventory was based on a conceptual design of the vehicle. The functional unit included the function of the car components as well as the battery of the electric vehicle where the lifetime was set to 200,000 km. XIII
D.6 Global warming potential per process for the SB car based on global data. The result was achieved by an LCA where the inventory was based on a conceptual design of the vehicle. The functional unit included the function of the car components as well as the battery of the electric vehicle where the lifetime was set to 200,000 km. XIV

D.7 Contribution graphs for global warming potential of the carbon fiber production and the SB manufacturing for the SB car based on global data. The result was achieved by an LCA where the inventory was based on a conceptual design of the vehicle. The functional unit included the function of the car components as well as the battery of the electric vehicle where the lifetime was set to 200,000 km. XV
D.8 Global warming potential of the three vehicles based on Swedish data. Black bars shows the net climate impact. The result was achieved by an LCA where the inventory was based on a conceptual design of the vehicles. The functional unit included the function of the car components as well as the battery of the electric vehicle where the lifetime was set to 200,000 km. XVI
D.9 Global warming potential per process for the conventional BEV based on Swedish data. The result was achieved by an LCA where the inventory was based on a conceptual design of the vehicle. The functional unit included the function of the car components as well as the battery of the electric vehicle where the lifetime was set to 200,000 km.XVII
D.10 Global warming potential per process for the CFRP car based on Swedish data. The result was achieved by an LCA where the inventory was based on a conceptual design of the vehicle. The functional unit included the function of the car components as well as the battery of the electric vehicle where the lifetime was set to 200,000 km. XVIII
D.11 Contribution graph for global warming potential of the carbon fiber production for the CRFP car based on Swedish data. The result was achieved by an LCA where the inventory was based on a conceptual design of the vehicle. The functional unit included the function of the car components as well as the battery of the electric vehicle where the lifetime was set to 200,000 km. XIX
D.12 Global warming potential per process for the SB car based on Swedish data. The result was achieved by an LCA where the inventory was based on a conceptual design of the vehicle. The functional unit included the function of the car components as well as the battery of the electric vehicle where the lifetime was set to 200,000 km. XX
D.13 Contribution graphs for global warming potential of the carbon fiber production and the SB manufacturing for the SB car based on Swedish data. The result was achieved by an LCA where the inventory was based on a conceptual design of the vehicle. The functional unit included the function of the car components as well as the battery of the electric vehicle where the lifetime was set to 200,000 km. XXI

E.1 Contribution graph for crustal scarcity indicator of the carbon fiber production for the SB car based on European data. The result was achieved by an LCA where the inventory was based on a conceptual design of the vehicle. The functional unit included the function of the car components as well as the battery of the electric vehicle where the lifetime was set to 200,000 km. XXIII

E.2 Crustal scarcity impact of the three vehicles based on global data. Black bars shows the net climate impact. The result was achieved by an LCA where the inventory was based on a conceptual design of the vehicles. The functional unit included the function of the car components as well as the battery of the electric vehicle where the lifetime was set to 200,000 km. XXIV
E.3 Crustal scarcity impact per process for the conventional BEV based on global data. The result was achieved by an LCA where the inventory was based on a conceptual design of the vehicle. The functional unit included the function of the car components as well as the battery of the electric vehicle where the lifetime was set to 200,000 km. XXV
E.4 Crustal scarcity impact per process for the CFRP car based on global data. The result was achieved by an LCA where the inventory was based on a conceptual design of the vehicle. The functional unit included the function of the car components as well as the battery of the electric vehicle where the lifetime was set to 200,000 km. XXVI
E.5 Contribution graph for crustal scarcity indicator of the carbon fiber production for the CRFP car based on global data. The result was achieved by an LCA where the inventory was based on a conceptual design of the vehicle. The functional unit included the function of the car components as well as the battery of the electric vehicle where the lifetime was set to 200,000 km. XXVII
E.6 Crustal scarcity impact per process for the SB car based on global data. The result was achieved by an LCA where the inventory was based on a conceptual design of the vehicle. The functional unit included the function of the car components as well as the battery of the electric vehicle where the lifetime was set to 200,000 km. XXVIII
E.7 Contribution graphs for crustal scarcity indicator of the carbon fiber production and the SB manufacturing for the SB car based on global data. The result was achieved by an LCA where the inventory was based on a conceptual design of the vehicle. The functional unit included the function of the car components as well as the battery of the electric vehicle where the lifetime was set to 200,000 km. XXIX
E.8 Crustal scarcity impact of the three vehicles based on Swedish data. Black bars shows the net climate impact. The result was achieved by an LCA where the inventory was based on a conceptual design of the vehicles. The functional unit included the function of the car components as well as the battery of the electric vehicle where the lifetime was set to 200,000 km. XXX
E.9 Crustal scarcity impact per process for the conventional BEV based on Swedish data. The result was achieved by an LCA where the inventory was based on a conceptual design of the vehicle. The functional unit included the function of the car components as well as the battery of the electric vehicle where the lifetime was set to 200,000 km.XXXI

E.10 Crustal scarcity impact per process for the CFRP car based on Swedish data. The result was achieved by an LCA where the inventory was based on a conceptual design of the vehicle. The functional unit included the function of the car components as well as the battery of the electric vehicle where the lifetime was set to 200,000 km. XXXII
E.11 Contribution graph for crustal scarcity indicator of the carbon fiber production for the CRFP car based on Swedish data. The result was achieved by an LCA where the inventory was based on a conceptual design of the vehicle. The functional unit included the function of the car components as well as the battery of the electric vehicle where the lifetime was set to 200,000 km. XXXIII
E.12 Crustal scarcity impact per process for the SB car based on Swedish data. The result was achieved by an LCA where the inventory was based on a conceptual design of the vehicle. The functional unit included the function of the car components as well as the battery of the electric vehicle where the lifetime was set to 200,000 km. XXXIV
E.13 Contribution graphs for crustal scarcity indicator of the carbon fiber production and the SB manufacturing based on Swedish data. The result was achieved by an LCA where the inventory was based on a conceptual design of the vehicle. The functional unit included the function of the car components as well as the battery of the electric vehicle where the lifetime was set to 200,000 km. XXXV

F.1 Contribution graph for cumulative energy demand of the carbon fiber production for the SB car based on European data. The result was achieved by an LCA where the inventory was based on a conceptual design of the vehicle. The functional unit included the function of the car components as well as the battery of the electric vehicle where the lifetime was set to 200,000 km. XXXVII
F.2 Cumulative energy demand of the three vehicles based on global data. Black bars shows the net climate impact. The result was achieved by an LCA where the inventory was based on a conceptual design of the vehicles. The functional unit included the function of the car components as well as the battery of the electric vehicle where the lifetime was set to 200,000 km. XXXVIII
F.3 Cumulative energy demand per process for the conventional BEV based on global data. The result was achieved by an LCA where the inventory was based on a conceptual design of the vehicle. The functional unit included the function of the car components as well as the battery of the electric vehicle where the lifetime was set to 200,000 km. XXXIX
F.4 Cumulative energy demand per process for the CFRP car based on global data. The result was achieved by an LCA where the inventory was based on a conceptual design of the vehicle. The functional unit included the function of the car components as well as the battery of the electric vehicle where the lifetime was set to 200,000 km. XL

F.5 Contribution graph for cumulative energy demand of the carbon fiber production for the CRFP car based on global data. The result was achieved by an LCA where the inventory was based on a conceptual design of the vehicle. The functional unit included the function of the car components as well as the battery of the electric vehicle where the lifetime was set to 200,000 km. XLI
F.6 Cumulative energy demand per process for the SB car based on global data. The result was achieved by an LCA where the inventory was based on a conceptual design of the vehicle. The functional unit included the function of the car components as well as the battery of the electric vehicle where the lifetime was set to 200,000 km. XLII
F.7 Contribution graphs for cumulative energy demand of the carbon fiber production and the SB manufacturing for the SB car based on global data. The result was achieved by an LCA where the inventory was based on a conceptual design of the vehicle. The functional unit included the function of the car components as well as the battery of the electric vehicle where the lifetime was set to 200,000 km. XLIII
F.8 Cumulative energy demand of the three vehicles based on Swedish data. Black bars shows the net climate impact. The result was achieved by an LCA where the inventory was based on a conceptual design of the vehicles. The functional unit included the function of the car components as well as the battery of the electric vehicle where the lifetime was set to 200,000 km. XLIV
F.9 Cumulative energy demand per process for the conventional BEV based on Swedish data. The result was achieved by an LCA where the inventory was based on a conceptual design of the vehicle. The functional unit included the function of the car components as well as the battery of the electric vehicle where the lifetime was set to 200,000 km. XLV
F.10 Cumulative energy demand per process for the CFRP car based on Swedish data. The result was achieved by an LCA where the inventory was based on a conceptual design of the vehicle. The functional unit included the function of the car components as well as the battery of the electric vehicle where the lifetime was set to 200,000 km. XLVI
F.11 Contribution graph for cumulative energy demand of the carbon fiber production for the CRFP car based on Swedish data. The result was achieved by an LCA where the inventory was based on a conceptual design of the vehicle. The functional unit included the function of the car components as well as the battery of the electric vehicle where the lifetime was set to 200,000 km. XLVII
F.12 Cumulative energy demand per process for the SB car based on Swedish data. The result was achieved by an LCA where the inventory was based on a conceptual design of the vehicle. The functional unit included the function of the car components as well as the battery of the electric vehicle where the lifetime was set to 200,000 km. XLVIII

F.13 Contribution graphs for cumulative energy demand of the carbon fiber production and the SB manufacturing for the SB car based on Swedish data. The result was achieved by an LCA where the inventory was based on a conceptual design of the vehicle. The functional unit included the function of the car components as well as the battery of the electric vehicle where the lifetime was set to 200,000 km. XLIX

List of Tables

3.1 Data on components in the conventional BEV including material type and properties as well as dimensions. Data is adapted with permission from Hermansson et al. [33]. Data for Li-ion battery is based on the findings in Asp et al. [7]. 17
3.2 Data on components in the CFRP car including material type and properties as well as dimensions. Data is based on MATLAB calculations and the findings in Asp et al. [7]. 19
3.3 Input data for calculations of the effective modulus of elasticity. Data was reprinted with permission from Hermansson et al. [33]. 19
3.4 Data on components in the SB car including material type and properties as well as dimensions. Data is based on MATLAB calculations and the findings in [7]. 21
3.5 The mass savings and change in mass of the battery for the conceptual vehicles. 21
3.6 Reference flow for the vehicles. 22
3.7 Data for structural battery cells was adapted from Zackrisson et al. [49]. 31
3.8 Data for structural battery electrolyte was adapted from Zackrisson et al. [49]. 31

4.1 Weight loss for the CFRP and SB car relative to the conventional BEV. 35
4.2 Compiled results from the weight reduction model. 36
4.3 Lightweighting normalized to Swedish and global data for global warming potential 100. 56
4.4 The climate impact for the hotspots in the CFRP and the SB car normalized to Swedish and global data. 58
4.5 The crustal scarcity impact for the hotspots in the CFRP car and the SB car normalized to Swedish and global data. 59
4.6 The cumulative energy demand for the hotspots in the CFRP and the SB car normalized to Swedish and global data. 59

B.1 Providers for the modelling of the conventional BEV including processes for production. Data is based on the database Ecoinvent APOS 3.7 and ELCD. III
B.2 Providers for the modelling of the conventional BEV including processes regarding recycling. Data is based on the database Ecoinvent APOS 3.7 and ELCD. IV

B.3 Providers for the modelling of the CFRP car. Data is based on the database Ecoinvent APOS 3.7 and ELCD. IV
B.4 Providers for the modelling of the SB car. Data is based on the database Ecoinvent APOS 3.7 and ELCD. V
B.5 Providers for the modelling of the SBE adapted from [49]. Data is based on providers in Ecoinvent APOS version 3.7. VI
B.6 Provider for the modelling of the use phase of the vehicles. Data is based on providers in Ecoinvent APOS version 3.7. VI

C.1 Manually changed in the processes for the sensitivity analysis of the conventional BEV. Data is based on Ecoinvent APOS version 3.7. . . VII
C.2 Manually changes in the processes for the sensitivity analysis of the CFRP car. VIII
C.3 Manually changes in the processes for the sensitivity analysis of the SB car. VIII

1
Introduction

1.1 Background

From 1970 until today, emissions from the transport sector have more than doubled and the emission intensity has increased faster than any other comparable sector [1]. The transport sector includes road vehicles such as cars, trucks and buses as well as aircraft, boats and trains [2]. Based on data from 2010, road vehicles (i.e. cars, trucks and buses) caused approximately 72 % of the total emissions at a global level, which corresponds to 5.04 $GtCO_2eq$ per year. This value equals approximately 0.38 round trips annually per person between Gothenburg and New York assuming a total population of 7.8 billion people and that a round trip emits 1.7 tCO_2eq. per person. Importantly, the value does not include indirect emissions such as fuel production, vehicle production and infrastructure construction [1]. Other sectors such as agriculture, industry and energy have seen a decline since the early 1990s in terms of emissions. However, the transport sector has not followed the same trend shift. Not until 2007 could the same type of shift be identified in the transport sector, though the emissions are still at higher levels than in 1990 [3]. The transport sector is central to Europe's economy. Consequently, the emission reduction is a critical issue to achieve the long-term objectives set by the European Union (EU), where the main objective is to reduce emissions by 60 % until 2050 compared to 1990 levels [2].

The transport industry has committed to reduce CO_2 emissions and improve energy use to meet future requirements on environmental impact, which can be accomplished in several ways [1]. One approach is to switch from traditional internal combustion engine vehicles to electric vehicles (EVs). The mass of the vehicle can also be reduced by substitution of conventional materials to lightweight and thereby reduce the energy use from the use phase. Carbon fiber reinforced polymers (CFRPs) is a monofunctional lightweight material with good mechanical properties that has the potential of increasing system performance of battery electrical vehicles. This can also be accomplished by a combination of these strategies by using structural batteries (SBs) where the energy is stored in the vehicle's components, which replaces the lithium-ion (Li-ion) batteries and the structural components. This concept is referred to as multifunctionality which means that two or more material properties are utilized simultaneously to support multiple functions in a single material.

Multifunctionality is a rather new concept that can be utilized to further improve the efficiency of different products. Increasing the energy storage while reducing the weight is one good example of an application area where multifunctionality can be utilized [4]. Multifunctionality implies that two or more conventional materials with their characteristics are combined to create a material which covers multiple functions. Some examples are load-bearing structures, thermal insulation, energy storage, self-repair, health monitoring or adaptive structures [5, 6].

Carbon fibre composites have suitable material properties to increase the appliance of multifunctionality in different products. This follows as a consequence of the microstructure of carbon fibre composites which entails great mechanical and electrochemical properties. SBs can be designed as either laminated or 3D-structured components where carbon fibres are enfolded in structural battery electrolytes (SBE) whose structure permits ionic redox reactions to occur while simultaneously ensuring structural stiffness [7, 8]. There are many similarities between SBs and lithium ion (Li-ion) batteries. The biggest being that they both have a positive (cathode) as well as negative (anode) electrode with a separator in between. The charging of SBs works in the same way as for regular Li-ion batteries, where current drives the lithium ions from the cathode to the anode. This creates an electrical potential that can be used to generate electrical power [6].

This type of solution was demonstrated in a case study where the roof of an EV was replaced with SBs. From the study, the main conclusion was that mass-savings could be achieved by using SBs. In addition, the researchers claimed that the roof is a suitable car component for SBs as the component should not bear any significant loads, which implies that the mechanical requirements can be lower in comparison to other more critical structural components [9]. Some studies have performed a life cycle assessment (LCA) of SBs. One study showed that with renewable energy systems providing the electricity for replacing steel and lithium-ion batteries with SBs, there is a positive effect on several environmental impact categories [10]. Additionally, another LCA indicated that carbon fibre composites can achieve significantly reductions in energy use and greenhouse gas (GHG) emissions due to its low weight [11]. However, the same result also showed that the potential is highly dependent on the energy requirements for producing the carbon fiber. However, to our best knowledge, research on this type of solutions is limited, especially when it comes to the environmental impact of SBs and how these would affect the overall life cycle of a vehicle. Therefore, this study aims at addressing the environmental challenges and opportunities of CFRPs and SBs by conducting an LCA based on a conceptual design.

1.2 Objectives

The purpose of the thesis is to assess the environmental impact of two conceptual composite vehicles with either CFRPs or SBs. The thesis also intends to examine monofunctional and multifunctional materials and give suggestions on how these materials can be utilized to improve the system performance. An LCA will be per-

formed on the conceptual composite vehicles where the environmental impacts will be assessed. The LCA result will include a basecase of a conventional battery electric vehicle (BEV) to make a comparative analysis. The LCA will identify challenges and opportunities of dominant phases, materials and design parameters. Issues regarding the methodologic assessment of technologies like composite cars with SBs will also be identified.

The outcome of the master thesis will function as a basis for future research on LCA of composite cars based on either CFRPs or SBs. Furthermore, the outcome should also raise awareness about design and technological lock-in´s in the automotive industry when it comes to multifunctionality.

1.2.1 Specification of the Issue Under Investigation

Given the previous research, this thesis aims at answering the following research questions:

1. Which car components in a conventional BEV are possible to replace with either CFRPs or SBs while keeping the same level of performance in terms of modulus of elasticity and energy storage?
2. What are the environmental impacts of a conceptual composite vehicle with either CFRPs or SBs?
3. What are the differences in environmental impacts of a conceptual composite vehicle with either CFRPs or SBs?
4. What are the challenges and opportunities of CFRPs and SBs in terms of dominant phases, materials and design parameters?
5. What are the main methodological issues in assessing technologies like CFRPs and SBs using LCA?

1.3 Limitations

The thesis is limited to the following points:

- There are other existing type of solutions for multifunctionality in road vehicles, including structural capacitors, structural supercapacitors and structural fuel cells [12]. These solutions are excluded from the study, which means that structural batteries only will be considered.
- The LCA is limited to components included in the conventional BEV as well as the conceptual composite vehicles with either CFRPs or SBs.
- The conceptual BEV as well as the composite vehicles with either CFRP or SBs will not be validated through data simulation.
- The modulus of elasticity was selected as the mechanical property for the study.

- The assessment of the SBs electrochemcial property will only consider energy density.
- The LCA is limited to only include three impact categories.
- The end-of-life treatment of the system will not be included in the sensitivity analysis.
- All type of transport except in the use phase is excluded from the LCA study.

2
Theory

This chapter presents the theory including multifunctional materials design, carbon fibers reinforced polymers, structural batteries, classical Laminate theory and life cycle assessment.

2.1 Monofunctional Materials Design

Monofunctional materials are materials that only has one function in a system. Monofunctional materials are nothing new and is what almost all systems consist of today where many different components are working together but only have one single function. However, a new interesting idea is to use lightweight monofunctional materials, that can increase the performance of a system by decreasing its weight without changing any other parameters. One material that has the potential of changing the automotive industry is CFRPs. According to some researchers, CFRPs has the potential of decreasing the weight of vehicles by 60 % [13]. CFRPs consists mostly of carbon fibers mixed with a polymer (e.g., epoxy), which creates the low density and relative high stiffness of the structure.

2.1.1 Carbon Fibers

Carbon fiber can either be pitch-based or polyacrylonitrile (PAN)-based fibres. The former is characterised by high stiffness and moderate strength as well as low failure strain. This type of carbon fiber usually have a high level of graphic content with large and oriented crystals. However, pitch-based fibres are much more rare to use compared to PAN-based fibres [14]. This is because PAN-based fibres microstructure can be varied much easier, which entails that the mechanical properties can be adapted to more specific application. The stiffness of PAN-based fibres ranges from 200-600 GPa, while its strength ranges from 3000-6000 MPa.

Carbon fibers are today mostly manufactured by stabilization and carbonization of the PAN-based fibers [15]. This is a highly energy intensive process in addition to the fact that the carbon fibers are fossil-based. New production methods can possibly decrease the energy use in the manufacturing process where one example is lignin-based carbon fibers, which could further decrease the environmental impact [16].

2.1.2 Carbon Fibers Reinforced Polymers

CFRP are widely used in many applications today. It has mechanical properties that is comparable to steel and aluminium when it comes to the weight ratio [17]. To create CFRPs with a thermoset (e.g., epoxy), the manufacturing method is usually injection moulding or pultrusion [17]. However, there are possibilities of using other materials than epoxy to create CFRPs which have similar mechanical properties.

2.2 Multifunctional Materials Design

Multifunctional materials seeks to improve the system performance while maintaining or reducing the weight. O'Brien et al. [18] developed a model for multifunctional materials design based on Ashby [19] and Thomas and Qidwai's [20] models regarding materials selection and flight time maximization, respectively. The purpose of the model is to determine the electrochemical and structural requirements for mass-savings in multifunctional design. O'brien et al. [18] model was constructed for a platform with both capacitive energy storage and structural requirements. However, the model can be extended and used for other similar multifunctional applications.

The total mass of the system is given in Equation (2.1).

$$M = m_e + m_s \tag{2.1}$$

where m_e represents the mass of the electrical element (kg) and m_s represents the mass of the structural element (kg).

The energy density for the capacitor can be defined as presented in Equation (2.2)

$$\bar{\Gamma} = \frac{\frac{1}{2}CS^2}{m_e} \tag{2.2}$$

where C represents the capacitance (F) and S represents the breakdown voltage of the capacitor (V).

The previous equations represents the conventional system. This system must be compared with a new system which also includes the mass of the structural capacitor.

$$M^* = m_e^* + m_s^* + m_{mf}^* \tag{2.3}$$

where $m_m^* f$ represents the mass of the structural capacitor (kg).

This system should be the same as the conventional system in terms of electrochemical and mechanical properties. However, the conditions presented in Equation (2.4) and (2.5) must be met for the properties to be the same.

$$\bar{\Gamma} m_e^* + \bar{\Gamma}_{mf} m_{mf}^* = \bar{\Gamma} m_e \tag{2.4}$$

and

$$\bar{E} m_s^* + \bar{E}_{mf} m_{mf}^* = \bar{E} m_s \tag{2.5}$$

where $\bar{\Gamma}_m f$ represents the energy density (Wh/kg) and $\bar{E}_m f$ represents the specific stiffness (N/m^2).

By combining Equation (2.1) and (2.3), the requirement for mass-saving can be found.

$$M^* < M \tag{2.6}$$

Equation (2.1), (2.2), (2.4) and (2.5) can be combined to express what requirements the structural capacitor must satisfy to achieve mass-saving.

$$(M - M^*) = \left(\frac{\bar{\Gamma}_{mf}}{\bar{\Gamma}} + \frac{\bar{E}_{mf}}{\bar{E}} - 1\right) m^*_{mf} \tag{2.7}$$

Equation (2.7) shows that the sum of the ratio for energy density and specific stiffness between the structural capacitor and the conventional system must be larger than 1 to achieve mass-savings.

$$\frac{\bar{\Gamma}_{mf}}{\bar{\Gamma}} + \frac{\bar{E}_{mf}}{\bar{E}} > 1 \tag{2.8}$$

The ratios can be expressed as efficiencies for simplicity as in Equation (2.9).

$$\eta_e = \frac{\bar{\Gamma}_{mf}}{\bar{\Gamma}} \quad \text{and} \quad \eta_s = \frac{\bar{E}_{mf}}{\bar{E}} \tag{2.9}$$

This provides the design requirement for mass-savings in multifunctional design. Equation (2.10) shows that if the capacitor can be produced such that the requirement is met, the new system will have less mass than the conventional system.

$$\eta_{mf} \equiv \eta_s + \eta_e > 1 \tag{2.10}$$

2.3 Structural Batteries

2.3.1 Carbon Fibres in Structural Batteries

Carbon fibres must carry mechanical loads and function as an active electrode simultaneously to achieve multifunctionality. The latter requirement implies that the carbon fibres have the possibility to store ions in its microstructure. The storage function is necessary when the ions are inserted into the fiber during charge (lithiation) and removed during discharge (delithiation). Kanno et al. [21] and Snyder et al. [22] showed that PAN-based fibres function as good electrodes, while pitch-based fibers exhibited the opposite behaviour. Kjell et al. [23] and Fredi et al. [24] have performed studies on PAN-based fibres to investigate the electrochemical properties. The carbon fibers under investigation ranged from low to high modulus. The results showed that all tested carbon fibers had some electrochemical performance. However, the fibers with high stiffness showed lower electrochemical performance than fibers with low and intermediate stiffness. The researchers explained that the electrochemical performance is negatively affected by large and highly oriented graphite crystals. Thus, the high modulus carbon fibers tend to have lower electrochemical

performance, while low and intermediate carbon fibers tend to have higher electrochemical performance.

Jacques et al. [25] study on carbon fibers investigated the effect lithiation has on the mechanical properties. The result indicated that the stiffness was not affected by lithiation. However, the strength was affected by lithiation, but it was returned once the carbon fibers were delithiated. Additionally, Jacques et al. [25] also investigated the effect on the electrochemical performance by mechanical loads. The result showed that the carbon fibers exhibited the same electrochemical performance regardless of whether the fibers were exposed to a mechanical load or not. Additionally, carbon fibers tend to expand when ions are moving between the electrodes during lithiation and delithiation. A study performed by Jacques et al. [26] concluded that the expansion depends on the amount of lithium inserted where low levels of lithium resulted in the larger carbon fiber expansions. Furthermore, carbon fibers do not have the piezo-electrochemical effect naturally. However, if lithium is inserted into the microstructure, carbon fibers become piezo-electrical.

2.3.2 Architectures for structural batteries

There are several designs for SBs, but the laminated and the 3D-fibre are the most common ones. The former design consists of a positive and a negative electrode separated from each other by an electrically insulating thin film (see Figure 2.1). The positive and the negative electrode are built up by carbon fibres, but the carbon fibers in the positive electrode are also coated with a thin-film of lithium metal oxide or phosphate. The SB is infused by an electrolyte, i.e., an in-homogeneous system such as the bi-continuous structural electrolytes. Asp et al. [14] constructed a semi-structural 3D-fibre battery. The result did not meet the theoretical values of $LiFePO_4$, but it gave a hint about the potential of this type of battery design. However, the solution is still at an innovative stage and extensive work still remains to scale up the battery design.

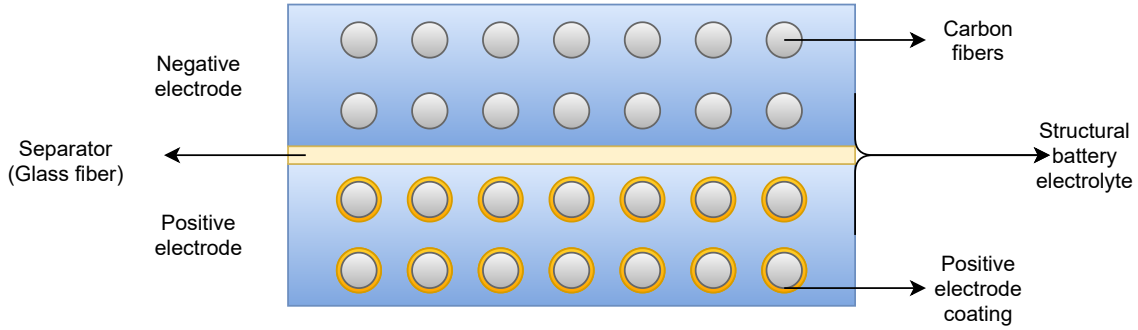

Figure 2.1: Structural battery laminated design, cross sectional view.

2.3.3 Case-studies on Structural Batteries

Research on SBs have intensified the last few years with the aim of improving the performance. Asp et al. [27] reported improvements in different multifunctionality

aspects of the SBs where most important conclusion was regarding the improvement of the mechanical and electrochemical properties of SBs [27]. The study used carbon fibers in both the positive and the negative electrodes where the carbon fibers in the positive one was draped in aluminium film in addition to two different separators in glass fiber (GF plain weave and GF/A Whatman). Asp and Carlstedt [7] have shown a non-linear relationship between the thickness of the separator and the driving range where conclusion was that a thinner separator improves the driving distance. The result also showed that implementing stiffer separators with warp and weft yarns in the same direction as the implemented forces increases the tensile strengths in those directions. One conclusion regarding SBs is that the electrochemical and mechanical properties can be tuned to specific area of application [14, 27]. Previous studies on SBs have either focused on improving the electrochemical or mechanical properties. Moyer et al. study showed electrochemical performance of 35 Wh kg^{-1} but with low mechanical performance with an Young´s modulus of about 2 GPa.

Case-studies have been performed on SBs to investigate its usefulness in different applications ranging from interior panels in aircraft to hull of electric ferry to laptop computer chassis. Johannisson et al. [9] performed a case-study on a roof of an electric vehicle made from a SB. The base case of the study was a roof in steel which was compared to a roof based on either carbon fiber composites and SBs, where the result indicated a mass-saving of 20 % and 62 % respectively. It is worth mentioning that a roof does not need to be designed to carry any heavy loads. However, the roof must be sufficiently stiff to not deform permanently due to pressure on the surface. In practice this translates to that the roof is not designed to withstand heavy forces upon a car accident unlike a door of a vehicle.

2.4 Classical Laminate Theory

In the following section, the theory of classical lamination theory (CLT) is presented. CLT can be used to calculate the effective modulus of elasticity of materials for composites. In order to determinate the effective modulus of elasticity of a composite, one need to determine the volume and weight fractions, longitudinal and tensile strength and Poisson's ration. All these parameters provides with information such that the effective modulus of elasticity can be found.

2.4.1 Volume and Weight Fractions

An important aspect of classical laminate theory is the fraction between the fibers ($_f$) and matrix ($_m$) of the composite material. The fractions can be expressed by either using weight (W_i) or volume (V_i) fraction for characterization as presented in Equation (2.11) and (2.12).

$$W_m = \frac{w_m}{w_c}, W_f = \frac{w_f}{w_c} \tag{2.11}$$

where w_c represents the total weight of the composite material, while w_f and w_m

represents the total weight fractions of the matrix (kg) and fibre material (kg), respectively.

$$V_m = \frac{v_m}{v_c}, V_f = \frac{v_f}{v_c} \tag{2.12}$$

where v_c represents the total volume of the composite material, while v_f and v_m represents the total volume fractions of the matrix (kg) and fibre material (kg), respectively.

2.4.2 Longitudinal Strength

The longitudinal strength of a unidirectional composite can be calculated given a number of assumptions. Firstly, the carbon fibres must be assumed to have the same size and properties, and act in parallel to each other. Secondly, there must exist a perfect bonding between the fibers and the matrix. This causes each longitudinal strain to be the same for the fibres, the matrix and the composite, which causes the longitudinal load carried by the composite to be shared between the fibres and the matrix. Based on these assumptions, the longitudinal load can be expressed by adding the respective forces as presented in Equation (2.13).

$$P_c = \sigma_c A_c = P_f + P_m = \sigma_f A_f + \sigma_m A_m \tag{2.13}$$

where σ_i represents the stress (N/m^2) and A_i represents the cross sectional area (m^2).

The composites longitudinal elastic stiffness can be obtained by assuming a linear elastic behaviour for the fibres and the matrix.

$$E_L = E_f V_f + E_m V_m \tag{2.14}$$

where E_i represents the longitudinal stiffness (N/m^2).

2.4.3 Tensile Strength

Failure occurs when the fibers are exposed to the critical fracture strain. However, this fact is based on the assumption that the fibre failure strain is less than the matrix failure strain. This means that the composite failure stress is dependent on fibre volume fraction. The critical volume fraction express when the failure strength of the fibres and the matrix are equal to each other and the parameter can be determined by comparing the failure strengths of the fibres and the matrix. In practical applications, the critical volume fraction is usually very low. Thus, the fibres volume fraction do not tend to be a problem.

2.4.4 Poission's Ratio

The longitudinal stress and the transverse strain can be related to each other by using the major Possion's ratio (ν_{LT}) and minor Poisson's ratio (ν_{TL}), respectively.

$$\nu_{LT} = \nu_f V_f + \nu_m V_m \quad \text{and} \quad \frac{\nu_{LT}}{E_L} = \frac{\nu_{TL}}{E_T} \Rightarrow \nu_{TL} = \nu_{LT}\frac{E_T}{E_L} \tag{2.15}$$

where E_L and E_T represents the longitudinal elastic stiffness (N/m^2) and the transverse elastic stiffness (/m^2), respectively.

2.4.5 Macromechanics of a Lamina

Hooke's law of a generally anisotropic material can be generalised to relate stresses and strains.

$$\sigma_i = C_{ij}\epsilon_j \qquad ijl = 1, 2..., 6 \tag{2.16}$$

where C_ij represents the stiffness matrix (N/m^2) and ϵ_j represents the strain components.
The constitutive relations for a fibre reinforced lamina is based on the assumption that the lamina is in the plane stress state. If a x_1,x_2,x_3 coordinate system is arranged such that the x_1-axis are parallel to to fibers direction and the x_3-axis points out of the plane, the stress in the x_3-direction and the shear stresses in the x_1,x_3-direction and x_2,x_3-direction will be equal to zero. This assumption is valid in most structural applications since the load is often applied in the plane of the laminate.

$$\begin{Bmatrix} \sigma_1 \\ \sigma_2 \\ \tau_{12} \end{Bmatrix} = \underbrace{\begin{bmatrix} Q_{11} & Q_{12} & 0 \\ Q_{12} & Q_{22} & 0 \\ 0 & 0 & Q_{66} \end{bmatrix}}_{[\mathbf{Q}]} \begin{Bmatrix} \varepsilon_1 \\ \varepsilon_2 \\ \gamma_{12} \end{Bmatrix} \tag{2.17}$$

The constitutive relations must be translated from a fibre oriented coordinate system (x_1,x_2,x_3) to a global coordinate system (xyz). This can be done by multiplying the reduced stiffness matrix (|$\mathbf{Q}$|) with the stress transformation matrix ([T_1]$^-$1) and the strain transformation matrix ([T_2]).

$$\begin{Bmatrix} \sigma_L \\ \sigma_T \\ \tau_{LT} \end{Bmatrix} = [T_1]^{-1} \begin{Bmatrix} \sigma_x \\ \sigma_y \\ \tau_{xy} \end{Bmatrix} \Longrightarrow [T_1]^{-1} = \begin{bmatrix} m^2 & n^2 & 2mn \\ n^2 & m^2 & -2mn \\ -mn & mn & m^2 - n^2 \end{bmatrix} \tag{2.18}$$

$$\begin{Bmatrix} \varepsilon_L \\ \varepsilon_T \\ \gamma_{LT} \end{Bmatrix} = [T_2] \begin{Bmatrix} \varepsilon_x \\ \varepsilon_y \\ \gamma_{xy} \end{Bmatrix} \Longrightarrow [T_2] = \begin{bmatrix} m^2 & n^2 & mn \\ n^2 & m^2 & -mn \\ -2mn & 2mn & m^2 - n^2 \end{bmatrix} \tag{2.19}$$

This implies that the relation between stresses and strains in a xyz coordinate system can be expressed as in Equation (2.20).

$$\begin{Bmatrix} \sigma_x \\ \sigma_y \\ \tau_{xy} \end{Bmatrix} = \underbrace{[T_1]^{-1}[\mathbf{Q}][T_2]}_{[\bar{\mathbf{Q}}]} \begin{Bmatrix} \varepsilon_x \\ \varepsilon_y \\ \gamma_{xy} \end{Bmatrix} = \begin{bmatrix} \bar{Q}_{11} & \bar{Q}_{12} & \bar{Q}_{16} \\ \bar{Q}_{12} & \bar{Q}_{22} & \bar{Q}_{26} \\ \bar{Q}_{16} & \bar{Q}_{26} & \bar{Q}_{66} \end{bmatrix} \begin{Bmatrix} \varepsilon_x \\ \varepsilon_y \\ \gamma_{xy} \end{Bmatrix} \tag{2.20}$$

The strain-displacement can be expressed as presented in Equation (2.21) where ϵ_s^0 and K_s represents the midplane strains and the plate curvatures, respectively, and the index (s) marks the present direction.

$$\epsilon_s = \epsilon_s^0 + zK_s \tag{2.21}$$

The stresses (i.e., stress and shear stress) can be expressed as normal forces and moments, which can be obtained by integrating the stresses over the thickness of the laminate.

$$N_i = \int_{-h/2}^{h/2} \sigma_i dz \qquad i = x, y \quad \text{and} \quad N_i = \int_{-h/2}^{h/2} \tau_{xy} dz \qquad i = xy, yx \tag{2.22}$$

$$M_i = \int_{-h/2}^{h/2} \sigma_i z dz \qquad i = x, y \quad \text{and} \quad M_i = \int_{-h/2}^{h/2} \tau_{xy} z dz \qquad i = xy, yx \tag{2.23}$$

The normal forces must be grouped into a single vector to be able to relate the normal forces with the midplane strains and the plate curvatures. This is done by integrating the stresses (i.e. stress and shear stress) over the thickness of the laminate.

$$\{\mathbf{N}\} = \begin{Bmatrix} N_x \\ N_y \\ N_{xy} \end{Bmatrix} = \int_{-h/2}^{h/2} \begin{Bmatrix} \sigma_x \\ \sigma_y \\ \tau_{xy} \end{Bmatrix} dz = \sum_{k=1}^{n} \int_{h_{k-1}}^{h_k} \begin{Bmatrix} \sigma_x \\ \sigma_y \\ \tau_{xy} \end{Bmatrix}_k dz \tag{2.24}$$

By combining Equation (2.21) and (2.24), the N vector can be expressed as presented in Equation (2.25).

$$\{\mathbf{N}\} = \sum_{k=1}^{n} \int_{h_{k-1}}^{h_k} [\overline{\mathbf{Q}}]_k \left\{\varepsilon^0 + z\mathbf{k}\right\} dz \tag{2.25}$$

Equation (2.25) can be rewritten as presented in Equation (2.26) given the fact that the midplane strains and the plate curvatures as well as the material properties are constant within each lamina.

$$\{\mathbf{N}\} = [\mathbf{A}] \left\{\varepsilon^0\right\} + [\mathbf{B}]\{\mathbf{k}\} \tag{2.26}$$

where

$$[\mathbf{A}] = \left[\sum_{k=1}^{n} [\mathbf{Q}]_k \left(h_k - h_{k-1}\right)\right] \quad \text{and} \quad [\mathbf{B}] = \frac{1}{2}\left[\sum_{k=1}^{n} [\mathbf{Q}]_k \left(h_k^2 - h_{k-1}^2\right)\right] \tag{2.27}$$

The same type of reasoning can be applied for the moments resulting in Equation (2.28).

$$\{\mathbf{M}\} = \begin{Bmatrix} M_x \\ M_y \\ M_{xy} \end{Bmatrix} = [\mathbf{B}] \left\{\varepsilon^0\right\} + [\mathbf{D}]\{\mathbf{k}\} \tag{2.28}$$

where

$$[\mathbf{D}] = \frac{1}{3}\left[\sum_{k=1}^{n} [\mathbf{Q}]_k \left(h_k^3 - h_{k-1}^3\right)\right] \tag{2.29}$$

By combining all these equations, the relationships between N-M and ϵ^0-k can be expressed as in Equation (2.30).

$$\begin{Bmatrix} \mathbf{N} \\ \mathbf{M} \end{Bmatrix} = \begin{bmatrix} \mathbf{A} & \mathbf{B} \\ \mathbf{B} & \mathbf{D} \end{bmatrix} \begin{Bmatrix} \varepsilon^0 \\ \mathbf{k} \end{Bmatrix} \tag{2.30}$$

2.5 Life Cycle Assessment

LCA was developed to assess the environmental impact of products and system. An LCA study is structured in four steps: goal and scope definition, inventory analysis, impact assessment and interpretation. The LCA procedure is presented in Figure 2.2 as described by Peters and Svanstrom [28].

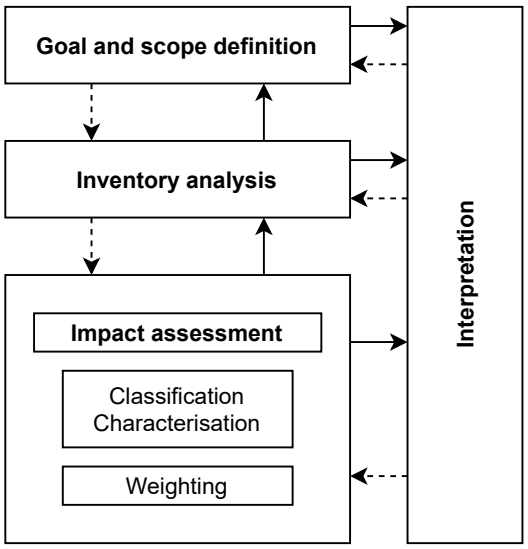

Figure 2.2: The LCA procedure where solid and dashed arrows indicates the order and possible iterations, respectively.

The first step includes a definition of the goal and scope of the study. This implies definition of how the results will be used, the reason for carrying it out well as the audience of the study. Additionally, this step also includes a specification of the modelling aspects such as the choice of functional unit. Technical aspects should also be defined in the scope such as flowcharts, system boundaries, allocation procedures and impact categories. This step is followed by an inventory analysis where the technical system is modelled according to the requirements defined in the step. This involves modelling of the technical system, data collection on inputs and outputs such as raw materials, products and solid waste as well as calculations of resource use and emission. The third step is the impact assessment where the inventory results are translated to environmentally understandable information. This includes activities such as classification and characterization. The findings are continuously interpreted during the study through identification of important environmental findings and critical methodological choices as well as evaluation of consistency and completeness, which will result in conclusions and recommendations.

3
Methodology

This chapter presents the methodology of the conceptual design of the conventional BEV as well as the composite vehicles where components are based on either CFRPs or SBs (Section 3.1-3.4). The result from the conceptual design is summarised in Section 3.5. The chapter also includes the methodology of the cradle-to-grave LCA of the conventional BEV and the composite vehicles (Section 3.6). The purpose of the conceptual design was to show the potential mass-savings while keeping or increasing the system performance by using CFRPs or SBs instead of conventional materials. The result functioned as input data for the inventory analysis of the LCA whose purpose was to assess the environmental impact of the conceptual composite vehicle (i.e., vehicles based on either CFRPs and SBs) as well as to identify key areas that need further research.

3.1 Multifunctional Design Analysis

The purpose of the multifunctional design analysis was to demonstrate the potential mass-savings while increasing the system performance by replacing monofunctional materials with multifunctional materials. By using multifunctional materials, a material is obtained that provides both mechanical and electrochemical properties. The properties can be varied such that the system performance increases while the vehicle receives a mass-saving. The result from the multifunctional design analysis was used as a basis for the design process of the conventional BEV (Section 3.2).

EVs based on lightweight materials are a rather new concept and there are various suggestions on how the concept should continue to be developed. BMW and Tesla are two pioneers in the matter and the car manufactures have chosen to develop the concept in different ways. The main difference lies in the material selection and the management of the consequences of the material selection. In the BMW case, the EVs are mainly built by CFRPs [29], which means that the EVs can be designed to use lighter and smaller batteries. Tesla has chosen to focus on aluminium instead [30], which is approximately twice as heavy as CFRPs. As a result, Tesla must design the EVs with a much heavier and larger battery to compensate for the additional mass in comparison to BMW EVs.

The multifunctional design analysis included the Tesla model S and the BMW i3 to see what implications the material selection have for the multifunctionality aspects of a vehicle. The analysis was based on O'brien et al. [18] model on multifunctional

materials design presented in Section 2.2. The original model was intended to examine the design requirements of structural capacitors for mass-savings. However, the same model was used for this analysis because the model was based on the same type of variables such as mass, modulus of elasticity and energy density. Data for construction and battery weight were obtained from Rangarajan [31].

Figure 3.1 presents the result from the multifunctional design analysis including (a) the BMW i3 and (b) the Tesla Model S. The blue dashed lines represents the nominal weight of the EVs based on current mechanical and electrochemical properties. The red, yellow and purple solid lines represents different values of electrochemical properties (Ω_e), which have been varied over different values of mechanical properties (Ω_s). The system performance can only be improved if the $\Omega_e + \Omega_s > 1$ and the ideal situation is achieved when $\Omega_e, \Omega_s = 1$.

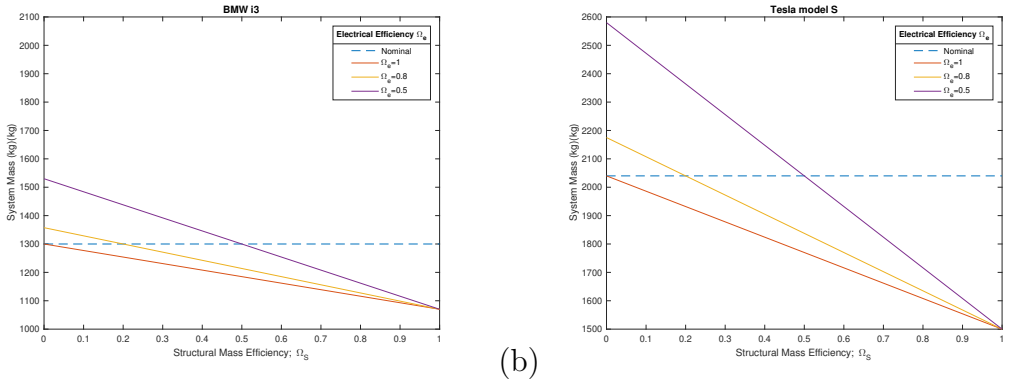

(a) (b)

Figure 3.1: Multifunctional design requirements for a) the BMW i3 and b) the Tesla Model S. The dashed blue line for both figures represent the nominal weight of the two vehicles. The purple, yellow and red lines represent different values of electrochemical properties.

Figure 3.1 shows that it is possible to achieve increased system performance while the mass is reduced by using multifunctional materials. The break-even point (i.e., the point just before the system performance starts to increase) for both the BMW i3 and the Tesla Model S occurs when the red, yellow or purple solid lines intersect with the blue dashed line, i.e., when $\Omega_e + \Omega_s = 1$. However, the break-even point does not imply any mass-savings for the vehicles. The mass savings can only be achieved when the system performance is increased, i.e., $\Omega_e + \Omega_s > 1$, which occurs when the red, yellow or purple lines are below the blue dashed line. For instance, in the BMW i3 case, when $\Omega_e = 0.5$ and $\Omega_s = 1.0$, the system performance is increased by 0.5 and the vehicle obtains a mass-saving of approximately 250 kg. The BMW i3 and the Tesla Model S can both achieve an increased system performance by using multifunctional materials, but it can be seen in Figure 3.1 that the effect of using multifunctional materials is larger on the Tesla Model S than the BMW i3. This can be identified by studying the slope of the curves for the different vehicles. For instance, if the mechanical performance increases from 0.5 to 0.6, the mass-savings would be approximately twice as much in absolute terms for Tesla Model S in comparison to the BMW i3. It is reasonable to imagine that this follows as

a consequence of the heavier and larger battery as well as heavier components. However, the key to the result is that both the vehicles have the possibility to increase the system performance while reducing the mass.

3.2 The Conventional BEV

The following section presents the design process of the conventional BEV where the result from the multifunctional design analysis functioned as the starting point.

3.2.1 Design of the Conventional BEV

The multifunctional design analysis resulted in some insights regarding the design process of the conventional BEV. For instance, the result showed that both the BMW i3 and Tesla Model S have potential to increase the system performance while the mass is reduced by replacing monofunctional materials with multifunctional materials. It therefore became interesting to examine different materials and car components to see what implications it has for multifunctionality. This resulted in a list of several components based on different materials including aluminium, steel, CFRPs and plastic as well as a Li-ion battery. Table 3.1 present the mechanical and electrochemical components in the conventional BEV. Aside from the Li-ion battery, the conventional BEV only includes a selected amount of components from a generic vehicle, which are static and only function as design elements or mechanical structures. The material types of the components in the conventional BEV were either based on [30] or discussions with technical experts. Polypropylene was selected as the material for all plastic components. However, in reality, different types of plastics are used depending on the component in question [32]. Data for material properties were adapted from Hermansson et al. [33], while data for the Li-ion battery was gathered from Asp et al. [7].

Table 3.1: Data on components in the conventional BEV including material type and properties as well as dimensions. Data is adapted with permission from Hermansson et al. [33]. Data for Li-ion battery is based on the findings in Asp et al. [7].

Component	Material	ρ (kg/m^3)	E (GPa)	l (m)	w (m)	t (mm)	m (kg)	Energy density (MJ/kg)
Outer door panels	Aluminium	2700	69.0	1.20	0.800	3.00	31.1	n/a
Roof	Steel	7800	206	2.20	1.10	0.800	15.1	n/a
Bumpers	Polypropylene	950	1.40	2.00	0.50	5.00	9.50	n/a
	CFRP	1310	50.0	2.00	0.50	2.00	5.20	n/a
A and B roof arches	Steel	7800	206	1.10	0.05	1.00	0.860	n/a
C roof arch	Steel	7800	206	1.10	0.05	5.00	2.10	n/a
Hood	Steel	7800	206	1.60	1.10	0.800	11.0	n/a
Dashboard	Polypropylene	950	1.40	1.80	0.50	2.00	1.70	n/a
Inner door panels	Polypropylene	950	1.40	1.00	0.60	2.00	4.60	n/a
Luggage floor	Polypropylene	950	1.40	1.00	0.88	2.00	1.70	n/a
Luggage wall (x2)	Polypropylene	950	1.40	0.500	0.880	2.00	1.70	n/a
Li-ion battery	n/a	n/a	n/a	n/a	n/a	n/a	540	0.570

The input data in Table 3.1 was used to create two composite vehicles with the same components, but where the materials were replaced with either CFRPs or SBs

(Section 3.3 and Section 3.4). To do this, the modulus of elasticity was chosen as reference point to be able to compare the materials mechanical performance. This gave data about the amount of CFRPs and SBs required to replace the components in the conventional BEV while maintaining the mechanical performance of the vehicles.

3.3 The CFRP car

This section includes the design process of the CFRP car. All calculations for the required amount of CFRPs were done in MATLAB.

3.3.1 Design of the CFRP car

In the design process of the CFRP car, the modulus of elasticity and the thickness of the components in the conventional BEV were compared to the CFRPs modulus of elasticity. Thereby, data could be obtained on what thicknesses the CFRPs need to maintain the mechanical performance of the components. Using the thicknesses of the CFRPs in the components, the total amount of CFRPs required to replace the components in the conventional BEV was determined. The calculations were done according to Equation 3.1 where $t_{component}$ and $E_{component}$ represent the thickness and modulus of elasticity of the component in question and t_{CFRP} and E_{CFRP} represent the thickness and the effective modulus of elasticity of the CFRPs.

$$t_{CFRP} = \frac{t_{component} E_{component}}{E_{CFRP}} \tag{3.1}$$

The modulus of elasticity of the CFRPs was assumed to 50 GPa after discussions with technical experts. The thickness of the CFRPs was found by multiplying the thickness of the particular component in the conventional BEV with its modulus of elasticity (Table 3.1) and divide the product with the modulus of elasticity of the CFRPs. To find to the total mass of CFRPs in the component, the thickness of the CFRPs was multiplied with its density as well as the length and width of the replaced component in the conventional BEV Table 3.1. The density of the CFRPs was assumed to 1310 kg/m^3 after discussions with technical experts. Table 3.2 presents the results for the CFRP car including material properties and dimensions. The CFRPs do not hold any electrochemical properties due to its monofunctional characteristics. This is why the CFRP car do not receive any battery weight reduction.

Table 3.2: Data on components in the CFRP car including material type and properties as well as dimensions. Data is based on MATLAB calculations and the findings in Asp et al. [7].

Component	Material	ρ (kg/m^3)	E (GPa)	l (m)	w (m)	t (mm)	m (kg)	Energy density (MJ/kg)
Outer door panels	CFRP	1310	50.0	1.20	0.80	4.14	20.8	n/a
Roof	CFRP	1310	50.0	2.20	1.10	3.30	10.5	n/a
Bumpers	CFRP	1310	50.0	2.00	0.500	0.140	0.370	n/a
	CFRP	1310	50.0	2.00	0.500	2.00	5.24	n/a
A and B roof arches	CFRP	1310	50.0	1.10	0.0500	4.12	0.590	n/a
C roof arch	CFRP	1310	50.0	1.10	0.0500	20.6	1.48	n/a
Hood	CFRP	1310	50.0	1.60	1.10	3.30	7.60	n/a
Dashboard	CFRP	1310	50.0	1.80	0.500	0.0600	0.0700	n/a
Inner door panels	CFRP	1310	50.0	1.00	0.600	0.0600	0.180	n/a
Luggage floor	CFRP	1310	50.0	1.00	0.880	0.0600	0.0700	n/a
Luggage wall (x2)	CFRP	1310	50.0	0.500	0.880	0.0600	0.0700	n/a
Li-ion battery	n/a	n/a	n/a	n/a	n/a	n/a	540	0.570

3.4 The SB car

This section presents the design process of the SB car including cell design and calculations of the effective modulus of elasticity as well as the design process. The calculations of the modulus of elasticity as well as the calculations for the required amount of SBs were done in MATLAB.

3.4.1 Cell Design

The energy density of the SBs was set to 75 Wh/kg after discussions with technical expert which is based on current state of the art of SBs. The effective modulus of elasticity was calculated based on classical laminate theory (Section 2.4.5). Input data for the calculations are presented in Table 3.3, which was adapted from Hermansson et al. [33].

Table 3.3: Input data for calculations of the effective modulus of elasticity. Data was reprinted with permission from Hermansson et al. [33].

Parameter	Metric	Unit
ν_{xy}	0.300	-
ν_{yx}	0.0500	-
E_x	75.0	GPa
E_y	10.0	GPa
G_{xy}	5.00	GPa
d	60.0	μm/*cell*

The cell was designed to include 6 laminates with a the orientation code of [0/60/60]s. Figure 3.2 present a sketch of the cell where the layers represent the laminates in the cell and the lines represent the carbon fibers. The cell was designed in this way to make the SBs isotropic, i.e., uniform regardless of the direction. An additional

cell design was tested where the cell included 8 laminates with a orientation code of $[0/\text{-}45/45/90]_s$. However, this cell design resulted in a lower effective modulus of elasticity. For further information about the cell design with 8 laminates, see Figure A.1. The calculations of the effective modulus of elasticity of the SBs were based on classical laminate theory and the cell design with 6 laminates as presented above. For more information regarding the calculations, see Hermansson et al. 2021 [33]. The calculations of the mechanical property resulted in a effective modulus of elasticity of 32.5 GPa.

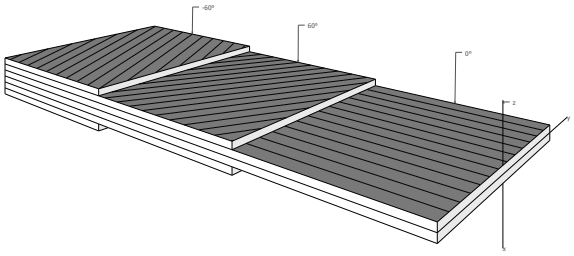

Figure 3.2: Cell with 6 laminates and laminate orientation code $[0/60/\text{-}60]_s$.

3.4.2 Design of the SB car

The design process of the SB car followed the same type of logic as for the CFRP car presented in Section 3.3.1 where the modulus of elasticity and the thickness of the components in the conventional BEV were compared to the SBs effective modulus of elasticity according to Equation 3.2. The density of the SBs was assumed to 1600 kg/m^3 after discussions with technical experts.

$$t_{SB} = \frac{t_{Component} E_{Component}}{E_{SB}} \tag{3.2}$$

The Table 3.4 presents the results for the SB car including data for material properties, dimensions and weight. Note that the total weight of the Li-ion battery has been reduced from 540 to 497 kg. The amount of SBs required to replace the components in the conventional BEV such that the mechanical performance was maintained resulted in a net increase of the components total weight. However, as already explained, SBs are multifunctional materials, which means that the materials can supply with both mechanical and electrochemical properties simultaneously. This means that the net increase of the components total weight plays less of a role because SBs provided with electrochemical properties that corresponds to approximately 43.0 kg, which resulted in a total net reduction of the vehicle by 38.0 kg.

Table 3.4: Data on components in the SB car including material type and properties as well as dimensions. Data is based on MATLAB calculations and the findings in [7].

Component	Material	ρ (kg/m^3)	E (GPa)	l (m)	w (m)	t (mm)	m (kg)	Energy density (MJ/kg)
Outer door panels	SB	1600	32.5	1.20	0.800	6.37	39.2	n/a
Roof	SB	1600	32.5	2.20	1.10	5.07	19.6	n/a
Bumpers	SB	1600	32.5	2.00	0.500	0.220	0.690	n/a
	SB	1600	32.5	2.00	0.500	3.08	9.85	n/a
A and B roof arches	SB	1600	32.5	1.10	0.0500	6.34	1.12	n/a
C roof arch	SB	1600	32.5	1.10	0.0500	31.7	2.79	n/a
Hood	SB	1600	32.5	1.60	1.10	5.07	14.3	n/a
Dashboard	SB	1600	32.5	1.80	0.500	0.0900	0.120	n/a
Inner door panels	SB	1600	32.5	1.00	0.600	0.0900	0.330	n/a
Luggage floor	SB	1600	32.5	1.00	0.880	0.0900	0.120	n/a
Luggage wall (x2)	SB	1600	32.5	0.500	0.880	0.0900	0.120	n/a
Li-ion battery	n/a	n/a	n/a	n/a	n/a	n/a	498	0.570

3.5 Summary of the Design Processes

Table 3.5 shows the weight loss of the CFRP car and the SB car compared to the conventional BEV. The result was used as input data for the inventory analysis. Note that the mass of SB changes as a consequence of a material substitution, but also as a consequence of a reduction of the battery size.

Table 3.5: The mass savings and change in mass of the battery for the conceptual vehicles.

Vehicle	Change in mass (kg)	Change in battery size (kg)	Total mass-savings (kg)
The conventional BEV	n/a	n/a	n/a
The CFRP car	-37.6	0	-37.6
The SB car	3.68	-42.0	-38.4

3.6 Life Cycle Assessment

The following sections presents the goal and scope of the study. This is followed by the inventory analysis including the modelling of the system before the methodology of the sensitivity analysis is presented.

3.6.1 Goal of the Study

The goal of this LCA study was to assess the environmental impact of two conceptual composite cars with either CFRPs or SBs. The outcome of the study should function as a basis for future research on composite vehicles. The LCA study has an attributional cradle-to-grave approach.

3.6.2 Scope of the Study

The following sections present the functional unit, system boundaries, impact categories, allocation, data quality requirements, limitations and assumptions.

3.6.2.1 Functional Unit

The functional was defined to include the function of the car components as well as the battery of the electric vehicle where the lifetime was set to 200,000 km. For further information about the reasoning behind the life, see Section 3.6.3.4. The functional unit was quantified per vehicle to include all components in the system, which is presented in Table 3.6.

Table 3.6: Reference flow for the vehicles.

Vehicle	Reference flow
The conventional BEV	The function of the components in the conventional BEV, except the Li-ion battery, with a lifetime of 200,000 km and a total mass of 84.54 kg (for more information about the components, mass and materials , see, Table 3.1).
The CFRP car	The function of the CFRP components, except the Li-ion battery, with a lifetime of 200,000 km and a total mass of 46.93 kg (for more information about the components, mass and materials, see, Table 3.2).
The SB car	The function of the SB components and the weight reduction of the Li-ion battery, with a lifetime of 200,000 km and a total mass 46.18 (for more information about the components, mass and materials, see, Table 3.4).

3.6.2.2 Data Quality Requirements

The LCA study only used average data where the data sources are essentially secondary data sources. A large part of the modelling is based on Ecoinvent APOS 3.7 [34] and ELCD [35] in addition to literature data. As mentioned in Section 3.3.1, the input data for inventory analysis (i.e., input data for all the conceptual vehicles) are based on estimations and assumptions. However, the inventory has been validated by a technical expert on composites at Volvo Cars in Gothenburg.

3.6.2.3 System Boundaries

The LCA study has a cradle-to-grave approach including raw material extraction, production processes, manufacturing of car, use phase and end-of-life treatment. The input and output flows consist of raw materials and energy as well as emissions and waste.

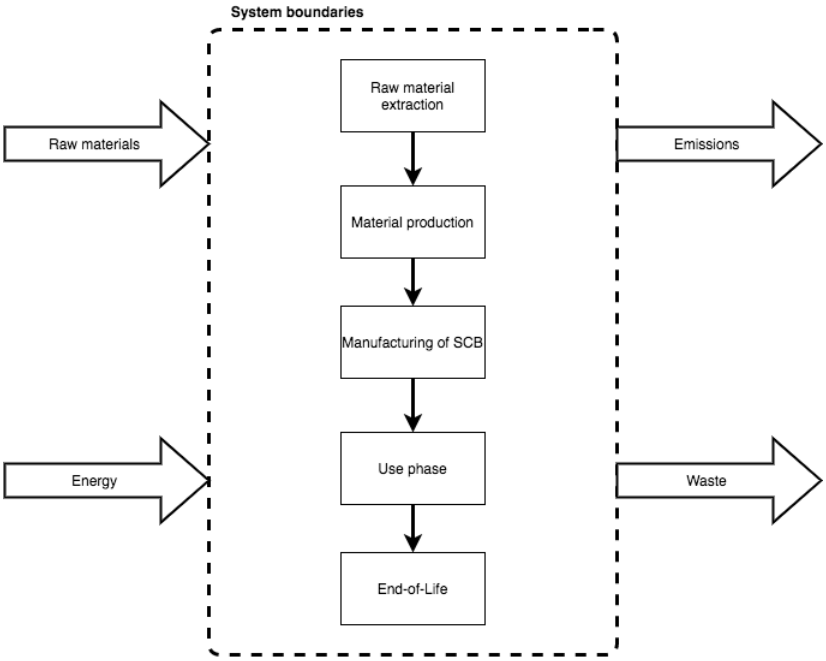

Figure 3.3: Simplified flowchart of the processes including input and output flows.

The LCA study did not include processes for RD activities, business travels and capital goods. The geographical boundaries were set to Europe, which means that only European data were used in the modelling. However, in some cases, the modelling was not possible with European data on the 1st provider in Ecoinvent APOS 3.7 [34]. For instance, standardized processes in Ecoinvent APOS 3.7 for both battery production and battery recycling are only available with global data. For these processes, the modelling was done with global data.

SBs is an emerging technology that has just been introduced. One can expect significant developments in the coming years for both production and manufacturing technology, but also for the SBs themselves. Additionally, carbon fiber has been relatively expensive for a long time, but the price is expected to decrease in the future. This means that a time horizon of 20 years is a reasonable limitation, which makes the result relevant to 2041.

3.6.2.4 Impact Categories

The LCA study had a midpoint approach and considered global warming potential and cumulative energy demand using the IPCC 2013 and the cumulative energy demand impact assessment methods as provided by Ecoinvent APOS database version 3.7 [34] as well as the crustal scarcity indicator made by Arvidsson et al. [36]. The amount of impact categories was limited to only a few categories. However, the correlation between the impact categories is generally high, making a limited set of impact categories sufficient [37]. For example, cumulative energy demand has a correlation to eutriphication, acidification and photochemcial ozone creation. This implies that the impact assessment should be sufficient and give a fair approximation. Furthermore, many of the environmental problems related to the transport

sector can be considered as global issues, which makes impact categories such as eutrophication and acidification less relevant.

Global warming potential was included as an impact category as it was expected that the life cycle impact of the vehicles contribute to global warming. Additionally, the impact category is also common and recognized among LCA practitioners.

Crustal scarcity indicator is included as it covers minerals in the electric vehicle batteries, but also other other materials in the vehicles.

Cumulative energy demand is an indicator in that calculates the direct and indirect energy use and presents them as either renewable (Wind, solar, water, biomass and geothermal) or non-renewable energy (fossil fuels, nuclear and primary forest). There is typically a correlation between global warming and cumulative energy demand. However, the impact categories do sometimes diverge from each other when there is a high portion of renewable resources, which is important to identify and further investigate.

3.6.2.5 Allocation

The LCA study has an attributional approach as mentioned in section 3.6.1. LCA proxy suggest partitioning as allocation procedure when allocation problems occurs such as when a process has single-input and multi-output. However, for this study, system expansion with substitution has been used for problems like this where a credit for avoided production and recycling have been given to the system.

There are arguments of dealing with allocation problems with both partitioning and system expansion with substitution. Hermansson et al. [38] performed an LCA study on lignin where different allocation approaches was examined to give a better understanding of how important the choice of allocation approach may be when assessing lignin as a substitute for other raw materials. The authors claimed that system expansion is more natural to consequential LCA studies, but that the allocation procedure also is applicable in attributional LCA studies where the main difference lies in the type of data that is selected. However, Hermansson et al. [38] study was based on processes with multi-output, but this thesis only covers recycling processes with single-output. It was therefore assumed that the same principles can be applied for single-output processes as well.

3.6.2.6 Limitations

The LCA study was limited to materials and components in Table 3.1, Table 3.2 and Table 3.4. This implied that other components of a vehicle was left out the study. The LCA study was limited to three impact categories: global warming potential, crustal scarcity indicator and cumulative energy demand. Toxicity could have worked as complement to the impact categories, but was not been included in the study. Zackrisson et al. [39] have concluded that toxicity evaluation is not currently reliable, particularly when it comes to metals such as lithium. This is ex-

plained by the lack of characterisation factors that translates these pollutants into toxic impacts.

All types of transport of goods and materials during the life cycle were excluded from the LCA study except from the use phase. However, it was found that some standard processes in Ecoinvent APOS version 3.7 had transport as a predetermined flow, but no manually changes were done to adjust these flows. Additionally, the assembly of the car components and the material sorting of the components before the recycling were also excluded. It was assumed that the impact from these processes are the same regardless of whether it is the conventional BEV, the CFRP car or the SB car, which means that the impact from each car take out each other.

3.6.2.7 Assumptions

EVs are associated with electricity losses as well as losses related to the mass of the battery. This type of reasoning for car batteries in the use phase has been used in other LCAs [40], who mainly used an energy reduction value (ERV) to compensate for the losses. For this LCA study, it is assumed that the influence of the electricity losses and the mass of the battery corresponds to 0.065 Wh/kg/km according to the New European Driving Cycle (NEDC). The NEDC gives a lower ERV in comparison to the worldwide harmonised light-duty vehicles test procedure (WLTC) value (0.069 Wh/kg/km). The NEDC and the WLTC have both been criticised for not representing the reality in a proper way and choosing the worst case scenario is therefore reasonable.

The components of the vehicle were assumed to not be fully recycled after the use phase. A recycling rate (i.e., the proportion of the material that is recycled and does not end up as landfill) of 95% was therefore assumed for all the materials. This assumption is in line with the European end-of-life vehicle directive [41]. Furthermore, all materials in the vehicles were assumed to be collected and undergo a material sorting process. However, the environmental impact of these steps was excluded from the study due to data uncertainties. The metals in the conventional BEV was assumed to have a recovery rate of 100% in addition to be reused in secondary applications. Additionally, the polypropylene was assumed to end up as waste in a municipal solid waste incinerator [42]. The polypropylene was assumed to have an energy content of 38 MJ/kg [42], which represents the lower heating value of the polymer. Additionally, it was assumed that all energy in the polypropylene was turned into heat without any losses. The CFRP production process was assumed to be resin transfer moulding (RTM). The energy requirement for this process was assumed to 12.8 MJ/kg of CFRP according to Suzuki [43] suggestion, while the recycling of the CFRP components was assumed to undergo a pyrolysis process to recover the carbon fibers where the energy requirements was assumed to 30 MJ/kg of CFRP according to Witik [44]. It was also assumed that all the energy used in the process was electricity in addition to a material degradation rate of 50% of the carbon fibers. Furthermore, recycling of SBs is not something that is currently going on. However, it was assumed that a pyrolysis process can be used to recover the carbon fibers and the glass fibers in the SBs. The same material degradation rate

was assumed for the carbon fibers in the SBs as for the carbon fibers in the CFRPs. Additionally, the glass fibers in the SBs was assumed to have material degradation rate of 50% [45]. The battery was assumed to be recycled via a hydrometallurgical process [46].

3.6.3 Inventory Analysis

The following sections present the modelling of the systems for the conventional BEV, the CFRP car and the SB car. The modelling was done in OpenLCA based on Ecoinvent APOS database version 3.7 [34]. If any other data sources were used, it has been stated in the text. For more information about the processes as well as the providers, see Appendix B.1-B.3. The modelling of the use phase for the three vehicles is presented in Section 3.6.3.4.

3.6.3.1 Modelling of the Conventional BEV

The conventional BEV includes car components made of aluminium, steel, polypropylene and CFRP presented in the flowchart of the system in Figure 3.4. Solid lines represent processes included in the system, while dashed lines represent processes excluded in the system. For a more detailed description about the modelling of the carbon fiber production, see Figure 3.5. For information about the modelling of the battery production and the battery recycling, see Section 3.6.3.3.

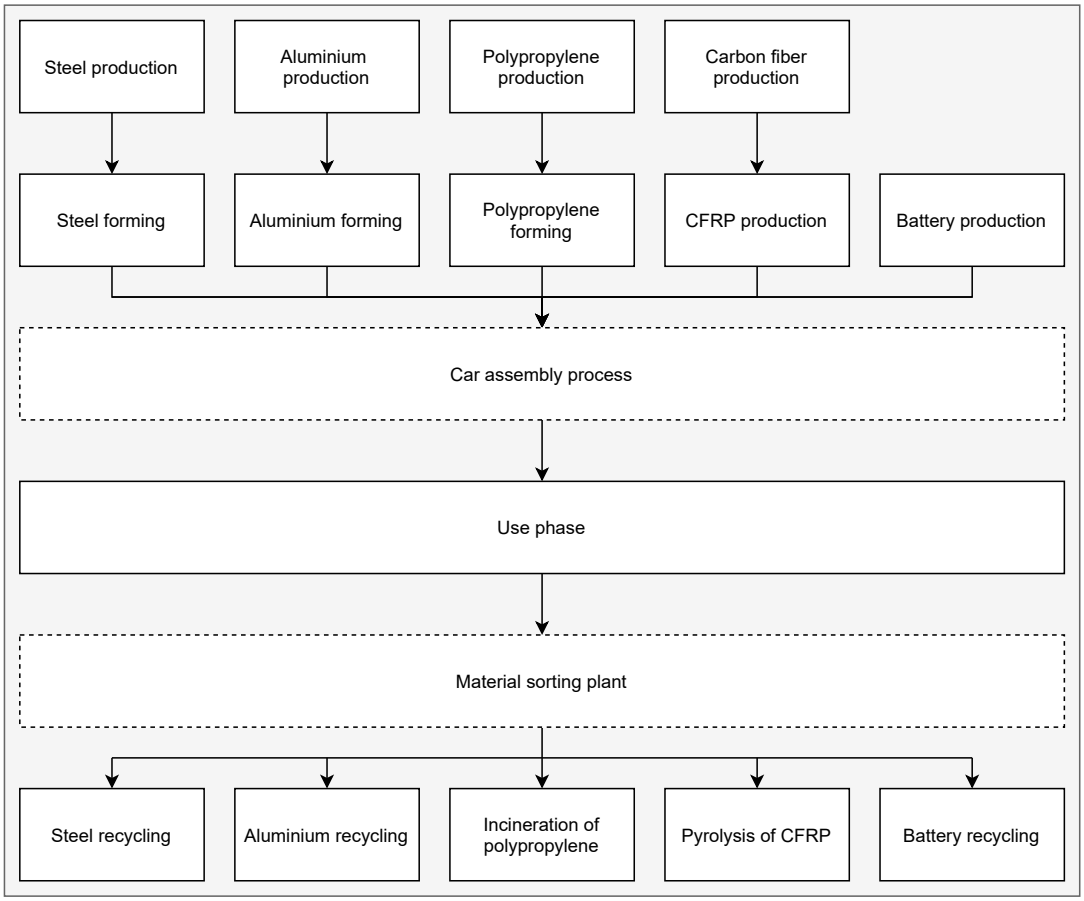

Figure 3.4: Flowchart of the conventional BEV. Solid lines represent processes included in the system, while dashed lines represents processes excluded in the system.

The aluminium components were modelled as aluminium alloys. The aluminium alloy was modelled to undergo a forming process before the use phase that included sheet rolling and impact extrusion with 5 strokes. The steel components were modelled as a hot-rolled alloy that also to underwent a forming process before the use phase. This step was modelled with the same impact extrusion process as for the aluminium alloy. The production of the polypropylene was modelled as polypropylene granulate and the forming polypropylene was modelled as injection moulding. The CFRP components includes processing processes for both carbon fiber production as well as CFRP production. The modelling of the carbon fiber production was based on a life cycle inventory by Romaniw [47]. The polyacrylonitrile precursor fiber production data was taken from Fazio and Pennington [35] and the data was found in the ELCD database [48]. The CFRP production process was modelled as resin transfer moulding (RTM) where the energy requirement for this process was set to 12.8 MJ/kg of CFRP. An electricity process with low voltage was used to supply the production process with energy.

Aluminium and steel components in the conventional BEV was modelled to be fully recovered after the use phase, which was modelled as a credit to the system. The

polypropylene components were modelled to end up in incineration where the heat from the treatment process resulted in a credit to the system. The energy content of the polypropylene was set to 38 MJ/kg. Additionally, all the energy content in the polypropylene was turned into heat in the incineration process. The CFRP production process used a resin transfer moulding (RTM) and the energy requirement of the process was set to 12.8 MJ/kg of CFRP where all energy was modelled as electricity. The recycling of the CFRP components to recover carbon fibers was modelled as a pyrolysis process, where the energy requirement was set 30 MJ/kg of CFRP [44]. This implied that the modelling only included emissions from the energy use, which meant that other potential emissions from the pyrolysis process were excluded. The energy use in the reycycling process of CFRP was modelled as electricity and the recovery rate was set to 50%.

3.6.3.2 Modelling of the CFRP car

The flowchart for the CFRP car are presented in Figure 3.5. Production of the car components for the CFRP car includes processing processes for carbon fiber production and CFRP production. The modelling followed the same logic as for the CFRP components in the conventional BEV presented in Section 3.6.3.1. The same applies for the recycling of the CFRP car components, which can be found in the same section. For information about the modelling of the battery production and the battery recycling, see Section 3.6.3.3.

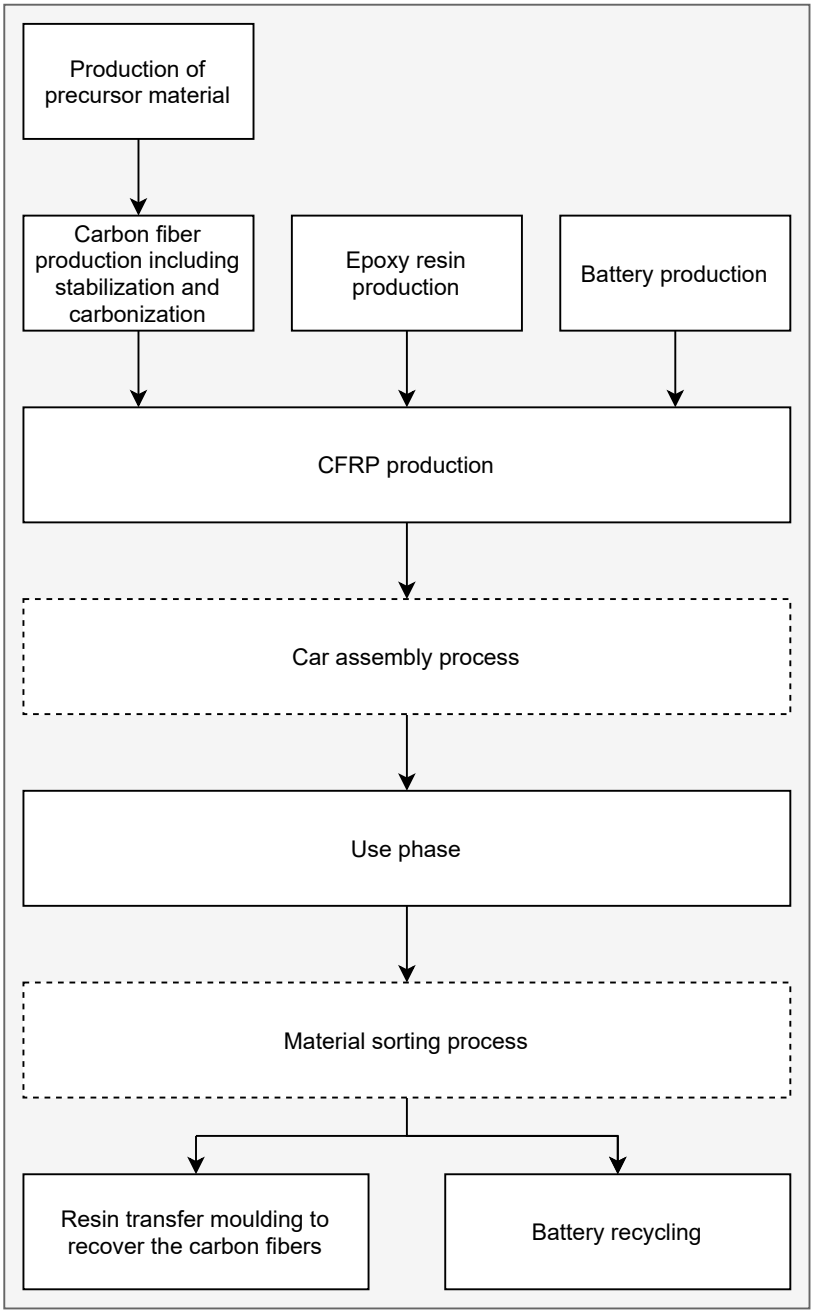

Figure 3.5: Flowchart of the CFRP car. Solid lines represent processes included in the system, while dashed lines represents processes excluded in the system.

3.6.3.3 Modelling of the SB car

Figure 3.6 presents the flowchart of the SB car including the production processes and the use phase as well as the recycling processes. Solid lines represent processes included in the system, while dashed lines represent processes excluded in the system. For further information about the modelling of the carbon fiber production, see Figure 3.5.

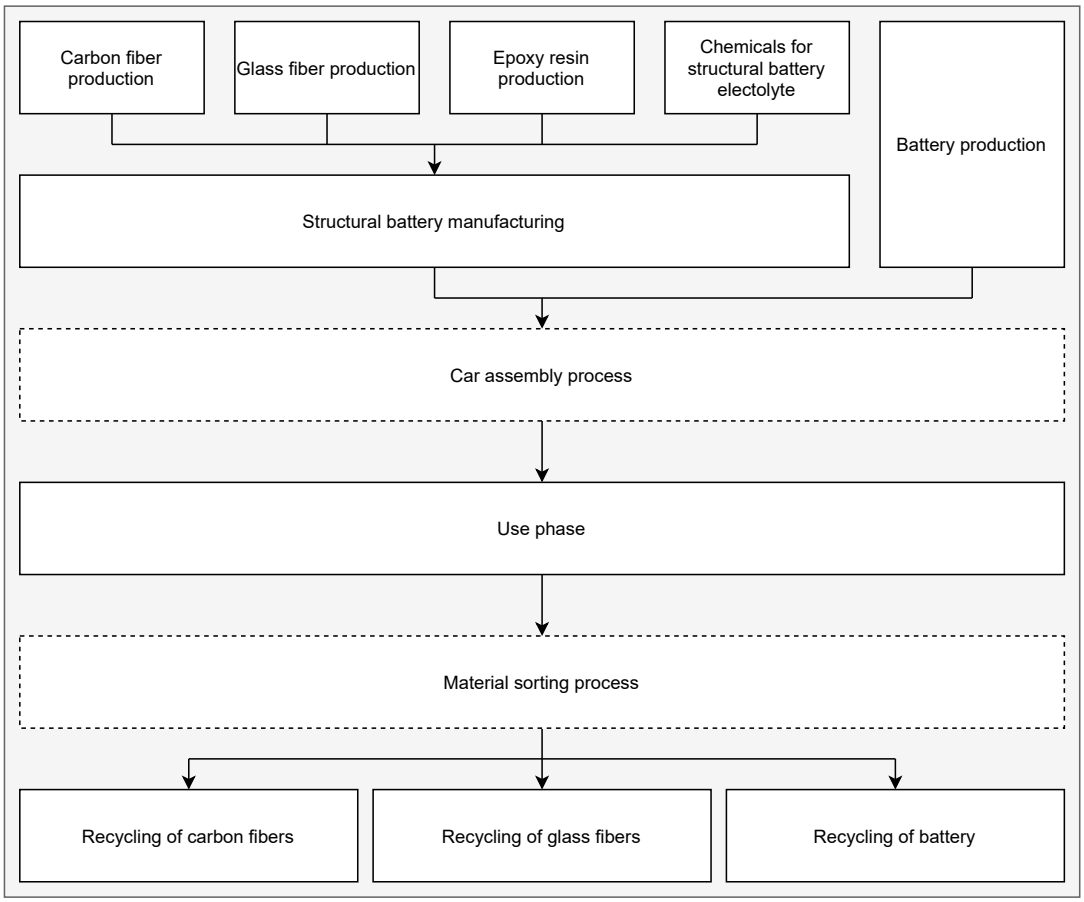

Figure 3.6: Flowchart of the SB car. Solid lines represent processes included in the system, while dashed lines represents processes excluded in the system.

The SBs was modelled as battery cells with an external casing made of glass fibers and epoxy resin based on Zackrisson et al. [49]. The bill of materials are presented in Table 3.7 including data for constituents and mass. The modelling of the carbon fiber production process follows the same logic as for the carbon fiber production in the conventional BEV presented in section 3.6.3.1. The battery cells was modelled with a negative and positive electrode, where the negative electrode was made of carbon fibers impregnated with SBE. Input data for the SBE is presented in Table 3.8, which is based on [49]. The main constituents in the SBE was bisphenol A dimethacrylate and ethylene carbonate. These constituents were modelled with processes taken from Ecoinvent APOS 3.7. However, the remaining constituents in the SBE could not be found in the database, so these materials were modeled as either organic or inorganic chemicals. See Table B.5 in Appendix B.1 for further information.

Table 3.7: Data for structural battery cells was adapted from Zackrisson et al. [49].

Part	Constituent	Mass (%)	Mass (g)
Negative electrode	Carbon fibers	13.08	12.3
Positive electrode	Carbon fibers	13.08	12.3
	LiFePO4	40.8	38.5
	PVDF	1.94	1.83
	Carbon black	2.34	2.19
Separator	Glass fibers	0.160	0.15
Casing	Glass fibers	8.53	8.04
	Epoxy resin	4.01	3.78
Electrolyte	SBE (see Table 3.8)	16.4	17.4
	Total	100	94.7

Table 3.8: Data for structural battery electrolyte was adapted from Zackrisson et al. [49].

Part	Constituent	Mass (%)	Mass (kg)
SBE	Bisphenol A dimethacrylate	9.26	8.77
	Lithium trifluoromethanesulfonate	0.813	0.77
	Ethylene carbonate	2.84	2.69
	Dimethyl methylphosphonate	2.84	2.69
	2,2'(Ethylenedioxy)diethanethiol	0.581	0.55
	Tris(N-nitroso-N-phenyl-hydroxylaminato)al.	0.0106	0.01
	2,2'-Azobis(2-methylpropionitrile)	0.095	0.09
	Total	16.4	17.4

The positive electrode was modelled as carbon fibers coated with LiFePO4, polyvinylidenfluride film (PVDF) and carbon black. LiFePO4 was modelled as diammonium phosphate production and data was taken from Manjare and Mohite [50]. Zackrisson et al. [49] used another type of PVDF in the modelling, but that process could not be found in the Ecoinvent 3.7 database. However, the processes are similar to each other and the impact was assumed to be negligible. Furthermore, the separator was made of glass fibers impregnated with SBE where the manufacturing process was assumed to be injection moulding. The casing was modelled to both include glass fibers and epoxy resin.

The energy requirements for battery cell manufacturing and battery assembly are dependent on several factors, such as dry or clean room conditions and plant throughput [51]. The modelling was been based on the assumption that it takes 11.7 kWh electricity and 8.8 kWh gas per kg of structural battery. Zackrisson et al. [10] used the same set up to model the SBs in their study.

The SBs were assumed to be partly recovered after the use phase. A material degradation rate of 50% as well as a recycling rate of 95% was taken in the mod-

elling for both carbon and glass fibers. The SBs were recycled by means of pyrolysis to recover carbon and glass fibers. The same energy requirement as for the pyrolysis process in the CFRP recycling was used (Section 3.6.3.1)

The battery of the electric vehicle was modelled as a rechargeable prismatic Li-ion battery, which could be used for mechanical drive of an electrical vehicle. The avoided battery production was modelled as a credit for the SB car where the avoided mass of the Li-ion battery, due to the SBs multifunctionality, set the size of the credit (Table 3.5). The recycling of the Li-ion battery was modelled as a hydrometallurgical process [46]. The same reasoning about the credits applies for the battery recycling as for the battery production.

3.6.3.4 Modelling of the Use Phase

The energy use in the use phase of the conventional BEV, the CFRP car and SB car was modelled with electricity low voltage, see Table B.6 for further information about provider. The use phase was modelled with an energy reduction value of 0.065 Wh/kg/km according to the NEDC with a lifetime of 200,000 km where the reference flow for each case was used to calculate the energy savings for all impact categories. Hottle et al. [52] showed that LCAs typically model the use phase of a vehicle with a wide range of lifetimes ranging from 150,000 km to 322,000 km. However, the authors stated that two distinct groupings could be identified: 190,000 km to 210,000 km and 231,000 to 250,000 km.

There are also regional differences of modelling the use phase of a vehicle. For example, the US vehicles are usually modelled with a lifetime from 190,000 km to 290,000 km, while the Japanese vehicles are modeled with a travel distance half to the US vehicles. One could argue that there are differences in lifetime between US and European vehicles. However, it is reasonable to think that the approximation is much similar than the Japanese one. Furthermore, the lifetime will affect the credit from using lightweight materials, which motivates the 200,000 km considered as a worse case scenario. Additionally, the energy use in the use phase was modelled with electricity with low voltage in Europe.

3.6.4 Sensitivity Analysis

A sensitivity analysis was performed on the vehicles for all impact categories where Swedish and global was used. All used processes modelling had providers based on global data as an option, which only necessitated adjustments from European to global data in the first process with its provider. However, there was a lack of Swedish data in the corresponding processes and providers. In these cases, the input data for the processes and providers were changed manually two steps down in the processes. For further information, see Appendix C.1-C.3.

A sensitivity analysis for the use phase was also performed where the lifetime of the CFRP car and SB car was varied until the break-even point was identified. For this sensitivity analysis, the break-even point represent the point when the environ-

mental impact for the CFRP car and the SB car is the same as for the conventional BEV. The break-even analysis was only done for global warming potential based on European data.

4
Result and Discussion

This chapter begins with the results from the conceptual design of the vehicles (Section 4.1) followed by a brief presentation of the LCA results where the vehicles are compared to each other per impact category: global warming potential (Section 4.2), crustal scarcity indicator (Section 4.3), cumulative energy demand (Section 4.4). The vehicles are individually examined in a hotspots analysis (Section 4.5) where each process of the vehicles is investigated. This is followed by a sensitivity analysis (Section 4.6) where a break-even analysis is performed on the lifetime of the vehicles. Additionally, the hotspots in the CFRP car and the SB car are also re-calculated, but based on either Swedish or global data.

4.1 Design of the Conceptual Vehicles

The design process of the SB car resulted in a weight reduction of 6% (Table 4.1) compared to the conventional BEV. The weight reduction was achieved without reducing the electrochemical or the mechanical performance in regards to the energy storage and the modulus of elasticity of the replaced car components. The result for the CFRP car showed that the system received a mass-saving of approximately 6%. This was also achieved without reducing the electrochemical or the mechanical performance of the vehicle.

Table 4.1: Weight loss for the CFRP and SB car relative to the conventional BEV.

	The CFRP car (%)	The SB car (%)
Weight loss of the total system (battery 540 kg)	6.02	6.14
Weight loss with reduced battery size (battery 28.18 kg)	33.37	46.73

The weight reduction of the vehicles are heavily affected by the fact that the weight of the Li-ion battery in the study was assumed to 540 kg. This means that the weight of the Li-ion battery constitutes approximately 87% of the total weight in the conventional BEV (Table 3.1). Translating this to the CFRP car and SB car the Li-ion battery still consist of a large part of the total weight. This is why the total weight reduction of the CFRP car and SB car are so similar, Table 4.1. However, in a generic BEV including all the components, a battery typically constitute 25% of the total weight. If the battery weight in the conventional BEV is scaled down such that it constitutes a 25% of the total weight, the new battery weight would be 28.18 kg, which result in a total weight of 112.73 kg for the conventional BEV. By scaling down the battery weight, the actual weight reduction can be found. For the

SB car, this gives a weight reduction of 46.73%, while for the CFRP car, this result in a weight reduction of 33.37%. However, the SBs provides the system with electrochemical performance that corresponds to 42.04 kg of battery, but in this case, the system only have 28.18 kg of Li-ion battery to replace, which means that the system receives a surplus of energy storage. Although a surplus of energy storage has a positive impact on the electrochemical performance of the vehicle, which can increase the driving range, the mass-savings cannot fully be exploited. The result for the SB car is similar to findings by Asp et al. [7] who concluded weight reductions of 20-30%.

Other similar studies that have examined the opportunities and benefits of multifunctionality have also come to the same results. Johanisson et al. replaced a steel roof with SBs and achieved an increased system performance of the vehicle [9]. However, this study distinguishes itself from the previous one because of the fact that different components of a vehicle based on monofunctional materials were replaced with SBs in addition to the number of different materials that were tested. Cars have a complex structure with many different components and materials that are collaborative and have different functions. Thus, increasing the number of components and materials will provide more comprehensive results and hence a more reality-based conclusions. Although, an increase of the complexity of the system can lead to more uncertainties and in the end affect the results.

In Table 4.2, the results from the calculations using the weight reduction model are presented including the mass for all component in the three conceptual vehicles and the relative weight loss for the CFRP car and SB car in comparison to the conventional BEV. The relative weight loss for the SB car also includes the weight reduction of the battery that originates from the electrochemical properties of the SBs.

Table 4.2: Compiled results from the weight reduction model.

	Conventional BEV		CFRP car		SB car		
Component	Material	Mass (kg)	Mass (kg)	Relative weight loss (%)	Mass (kg)	Weight reduction battery	Relative weight loss (%)
Outer door panels	Aluminium	31.1	20.8	33.0	39.2	18.7	34.1
Roof	Steel	15.1	10.5	30.8	19.6	9.40	31.9
Bumpers	PP	9.50	0.370	96.1	0.690	0.330	96.2
	CFRP	5.24	5.24	0	9.85	4.69	1.58
A and B roof arches	Steel	0.860	0.590	30.8	1.12	0.530	31.9
C roof arch	Steel	2.15	1.48	30.8	2.79	1.33	31.9
Hood	Steel	11.0	7.60	30.8	14.3	6.81	31.9
Dashboard	PP	4.56	0.180	96.1	0.330	0.160	96.2
Inner door panels	PP	1.71	0.0700	96.1	0.120	0.0600	96.2
Luggage floor	PP	1.67	0.0600	96.1	0.120	0.0600	96.2
Luggage wall	PP	1.67	0.0600	96.1	0.120	0.0600	96.2
Li-ion battery	$LiFePO_4$	540	540	0	498	n/a	7.79
All components (Total)		625	587	6.02	586	42.0	6.14

The conventional BEV includes many different components and materials and the required amount of either CFRPs or SBs to replace the components are decided by the effective elastic modulus and the density of the materials for all parts except the battery. The results show that the best material to substitute is polypropylene which achieves a relative weight loss of 96.14% for the CFRP car and 96.16% for the

SB car. According to Emilsson et al. [32], plastic constitute around 20% of the total weight of a generic BEV after-pre-treatment (i.e., the weight after the batteries, tires, and liquids are removed). In this model, the polypropylene was set to approximately 13% of the total mass of the components (excluding the battery). This means that the possibilities of replacing SBs with plastics in a conventional BEV are even bigger than shown in this study. Plastics are often used in components where there are no or small requirements for good mechanical properties, hence, the possibilities of replacing the structure with SBs are favorable. The relative weight loss for aluminum (34.10%) and steel (31.90%) are almost equal for the CFRP car and the SB car. Steel is the most used material in the automotive industry today, mainly because of its outstanding mechanical properties. However, the results from this study demonstrates that it is possible to replace aluminium and steel components with either CFRPs or SBs while keeping the mechanical performance. Additionally, the result indicates that replacing a lightweight material (i.e., the CFRPs in the bumper) with SBs does not increase the system performance. Instead of a weight loss, the vehicle received a weight gain of 58%. This is due to the higher effective modulus of elasticity in the CFRP compared to the SBs and that the density of the two materials are almost equal.

The weight reduction model can be improved by adding other mechanical properties, but to do that successfully, the model requires specific primary data, particularly for specific load cases. The model can be developed and extended with more parameters to the calculations. For example, the input data for the effective modulus of elasticity can be varied to handle future improvements of the SBs. As an example, Johannisson et al. [9] suggest that the volume fractions of the carbon fibers in the electrodes can be increased to improve the mechanical performance of the SBs.

4.2 Global Warming Potential

Figure 4.1 shows the result for global warming potential with a time horizon of 100 years. For a more detailed explanation of the vehicles, see Section 4.5.1 (the conventional BEV), Section 4.5.2 (the CFRP car) and Section 4.5.3 (the SB car). The figure presents three different vehicles: the conventional BEV, the CFRP car and the SB car. Grey bars represent CO_2-eq for the car components in the vehicles, while credits for avoided battery production and lightweighting are represented by dark grey and light grey bars, respectively. The black bars represent the net climate impact for all the three different vehicles.

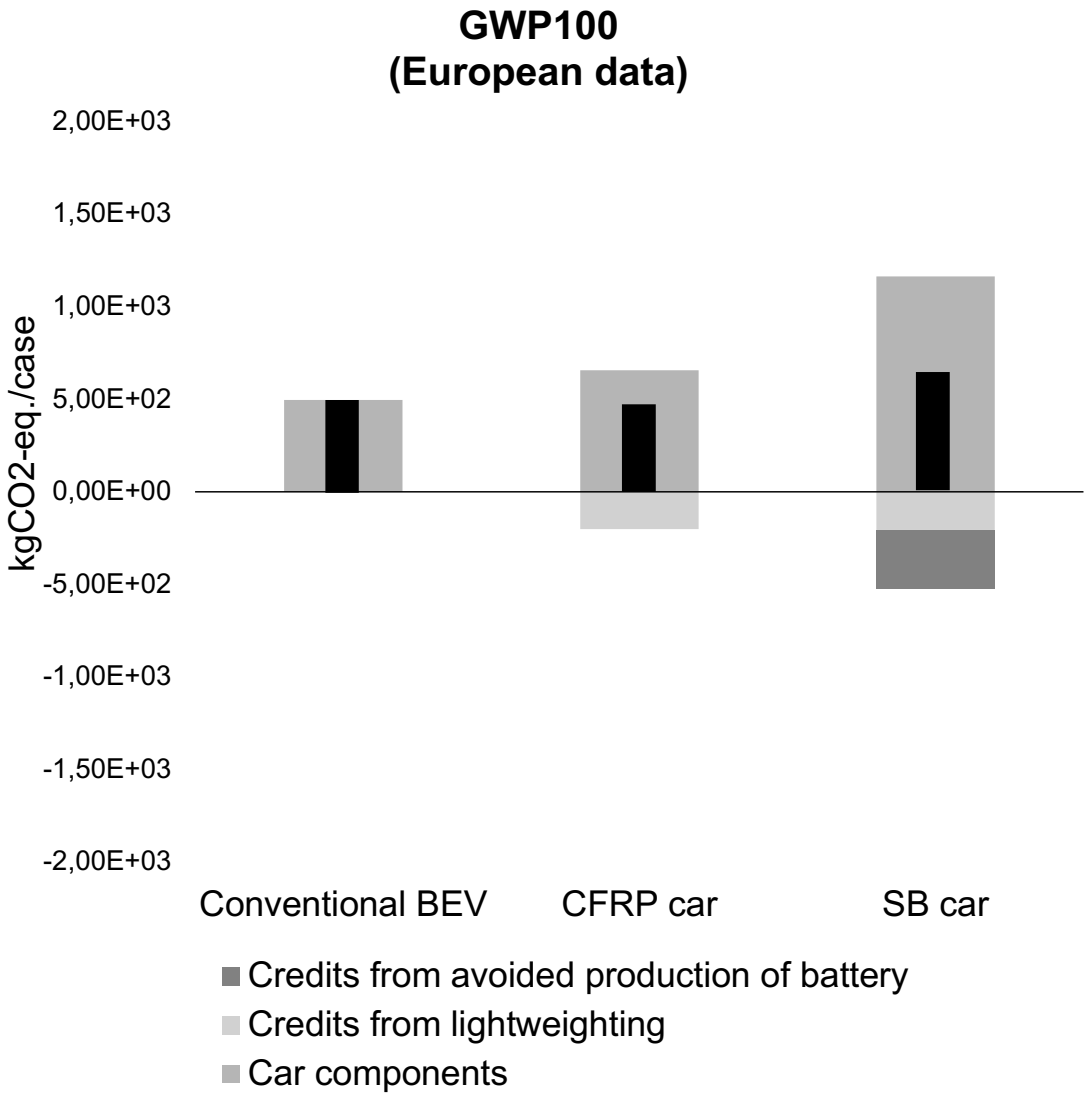

Figure 4.1: The climate impact of the three vehicles. The black bars represent the net climate impact of the vehicles.

The result shows that the conventional BEV and the CFRP car have similar net climate impact. However, the climate impact of the car components in the CFRP car is higher in comparison to the conventional BEV, but the CFRP car is credited from using lightweight materials in the use phase, which results in a lower net climate impact for the CFRP car. The SB car has the highest net climate impact of the three vehicles despite the credits from avoided battery production and lightweighting.

Credits from using lightweighting materials was based on the New European Driving Cycle (NEDC), which is dependent on the vehicle's mass as well as the lifetime of the vehicle. For this study, the lifetime of the vehicle was set to 200,000 km. The credits from lightweighting is also dependent on the electricity mix. A vehicle propelled in Europe will result in more credits than a vehicle propelled in Sweden. This is the same reasoning and results as Zackrisson et al. [10]. The credits for avoiding production of battery are slightly larger then the credits for lightweight-

ing. As mention in Section 3.6.3.3, only global data is available for modelling the Li-ion battery in Ecoinvent APOS version 3.7. This has consequences for the credits size, which probably would be smaller if the data for the battery production was based on European data. However, the major part of the battery production is currently taking place on a global scale [53], which makes the result more representative.

It should be mentioned that the technology maturity level between the vehicles is very different, where the conventional BEV and the SB car are having the highest and the lowest technology maturity level, respectively. Up to this point, SBs have only been manufactured in a small scale lab environment [27], even though SBs are facing several developments in material properties and composition. However, the difference in technology maturity level have implications for the comparison between the vehicles. For example, it is uncertain to compare technologies where one technology has been used for a very long time while the other has just been introduced.

4.3 Crustal Scarcity Indicator

Figure 4.2 presents the result for crustal scarcity impact. For a more detailed explanation regarding crustal scarcity impact for the separate vehicles see, conventional BEV (Section 4.5.1), CFRP car (Section 4.5.2) and SB car (Section 4.5.3). The figure is structured in the same way as Figure 4.1 where grey, dark grey and light grey bars represent the car components and the credits from avoided production of battery as well as lightweighting. The same applies for the black bars, which represent the net impact between the car components and the potential credits.

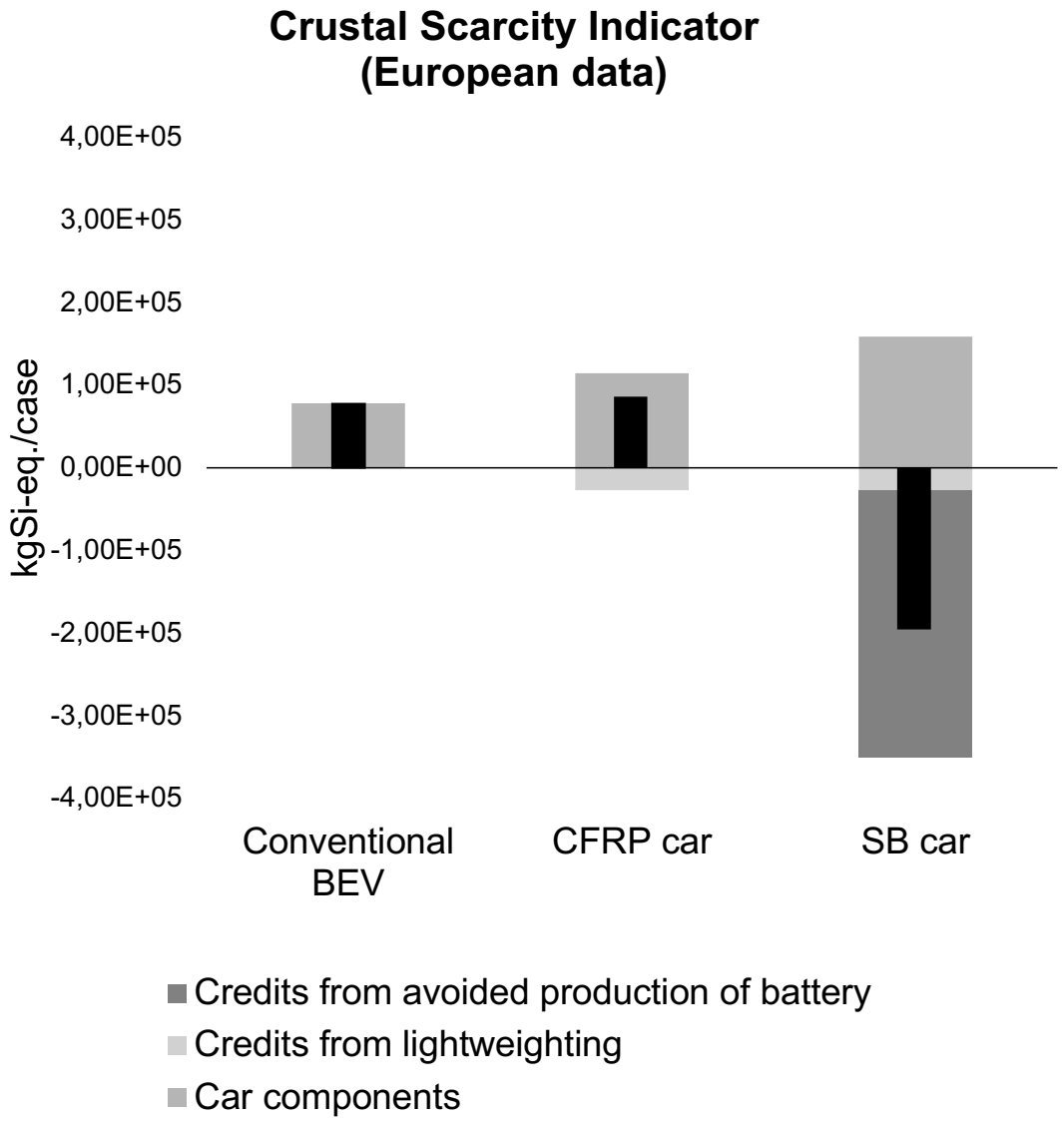

Figure 4.2: The crustal scarcity impact of the three vehicles. The black bars represent the net crustal scarcity impact.

The net crustal scarcity impact is similar between the conventional BEV and the CFRP car where the CFRP car is credited from using lightweight materials in the use phase. The SB car outperform both the conventional BEV and the CFRP car, which is mainly explained by the credit from the avoided battery production, but also the credit from lightweighting. It should be mentioned that the production of the battery cell and the battery itself accounts for approximately 80% of the credit from avoided battery production. These processes are resource intensive and that is why the SB car receives a large credit from the avoided battery production. Additionally, the battery production is based on global data, which also probably contributes to the large credit from avoided battery production. This is further explained Section 4.5.3.

4.4 Cumulative Energy Demand

Figure 4.3 shows the result for the cumulative energy demand. For a more detailed explanation regarding cumulative energy demand for the separate vehicles see, the conventional BEV (Section 4.5.1), the CFRP car (Section 4.5.2) and the SB car (Section 4.5.3). The figure is structured in the same way as Figure 4.1 and Figure 4.2 where grey, dark grey and light grey bars represent car components and credits from avoided production of battery as well as lightweighting. The same applies to the black bars, which represent the net impact between car components and potential credits.

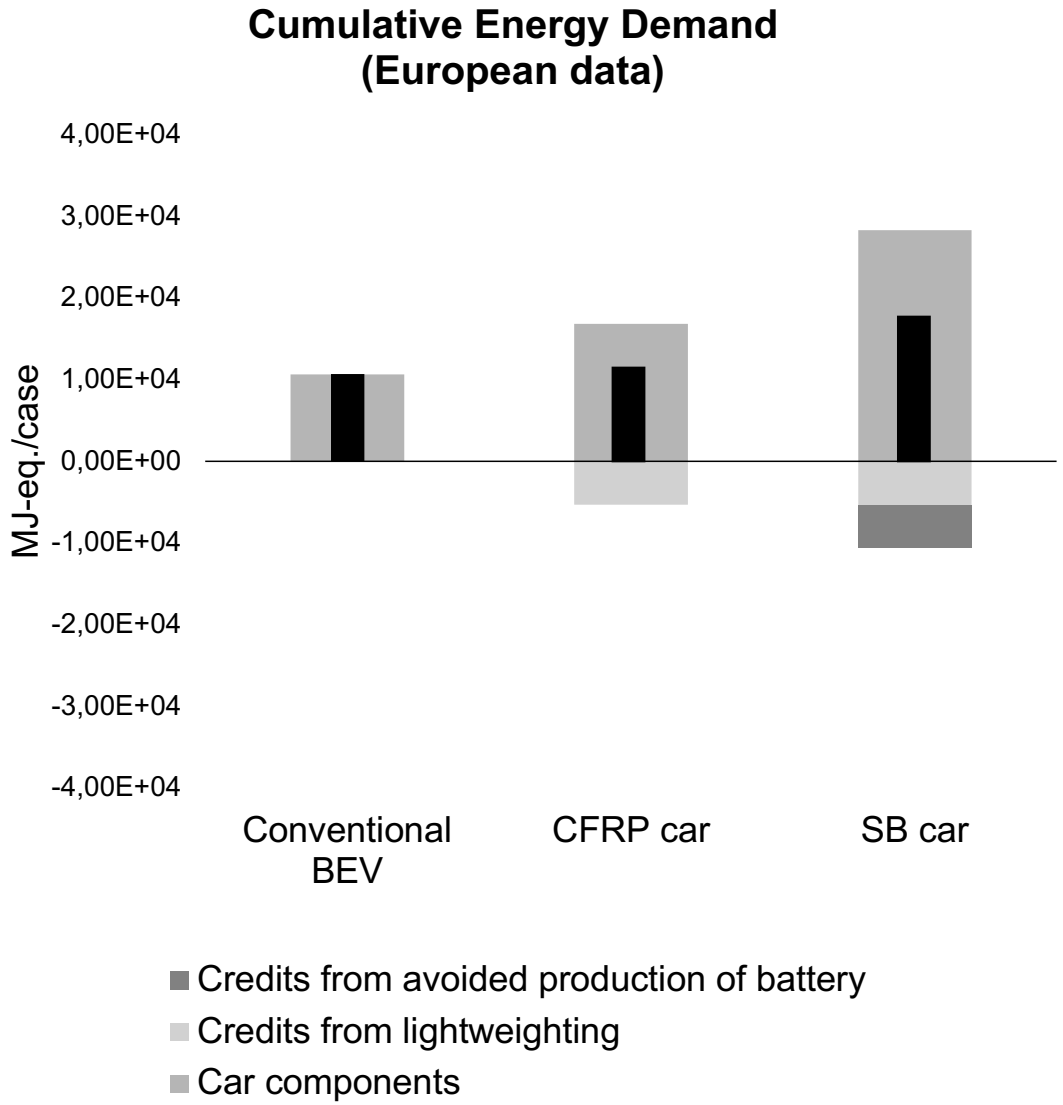

Figure 4.3: The cumulative energy demand of the three vehicles. The black bars represent the net cumulative energy demand.

The result for the cumulative energy demand are similar to the results from the global warming potential where the conventional BEV and the CFRP car have

resembling net impacts, while the SB car have a slightly higher energy demand. Car components for both the CFRP car and the SB car are produced with energy intensive processes, which despite the credits from avoided production of battery for the SB car and credits for lightweighting for both the vehicles are more energy demanding.

4.5 Hotspot Analysis

The following sections includes hotspot analyzes of the processes included in the conventional BEV, the CFRP car and the SB car.

4.5.1 The Conventional BEV

Figure 4.4, Figure 4.5 and Figure 4.6 present the impact categories for global warming potential, crustal scarcity indicator and cumulative energy demand per process of the conventional BEV (excl. the use phase of the vehicle). The conventional BEV was modelled as a reference point to the CFRP car and the SB car. This means that the analysis of the conventional BEV will only be general and not include any further investigations of potential hotspots. Note that Figure 4.6 do not have a separate process for carbon fiber production as in the other impact categories. The energy demand in the carbon fiber production and the CFRP production have been aggregated to a single process, which is represented by the CFRP production (inc. carbon fiber production).

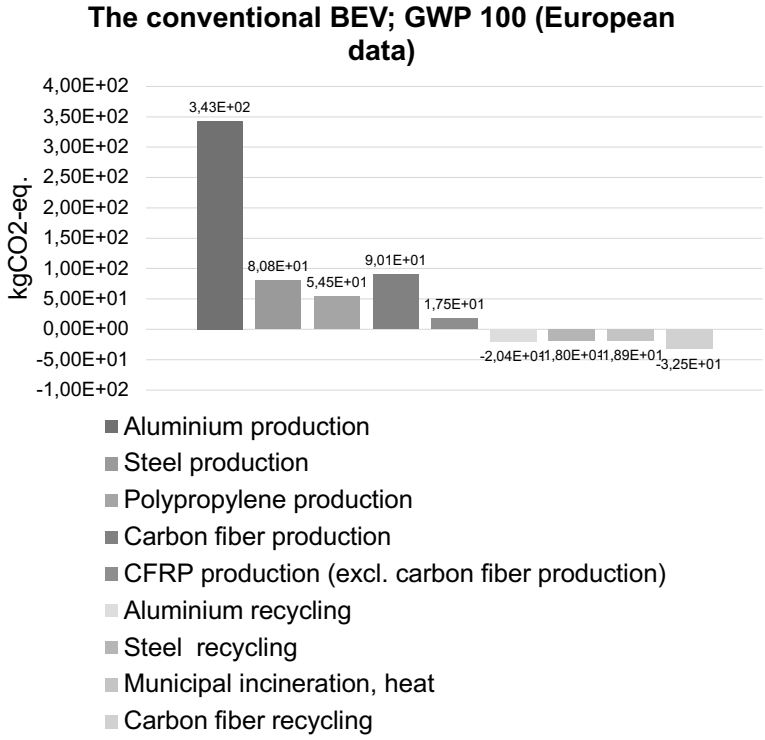

Figure 4.4: GWP 100 of the processes in the conventional BEV.

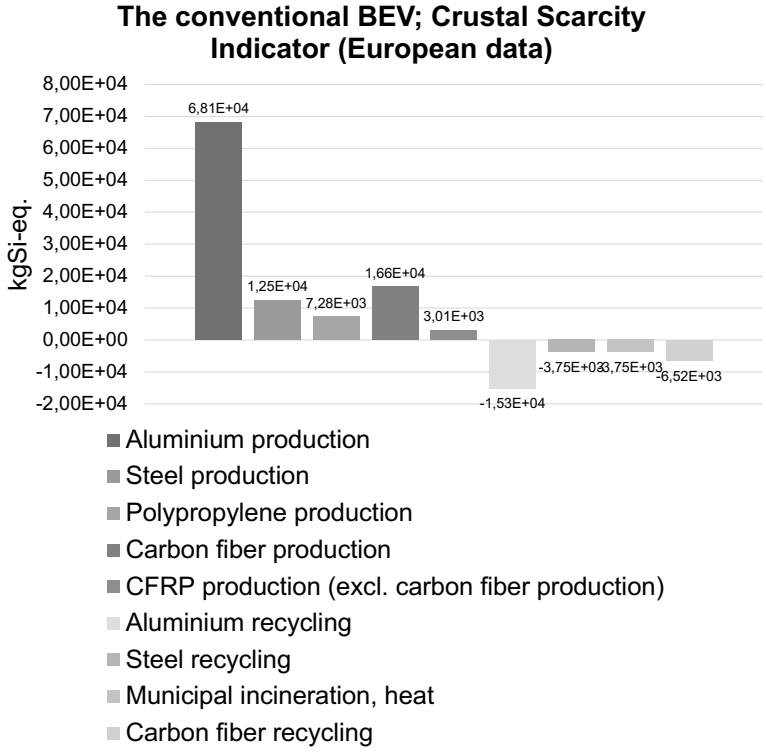

Figure 4.5: Crustal scarcity indicator of the processes in the conventional BEV.

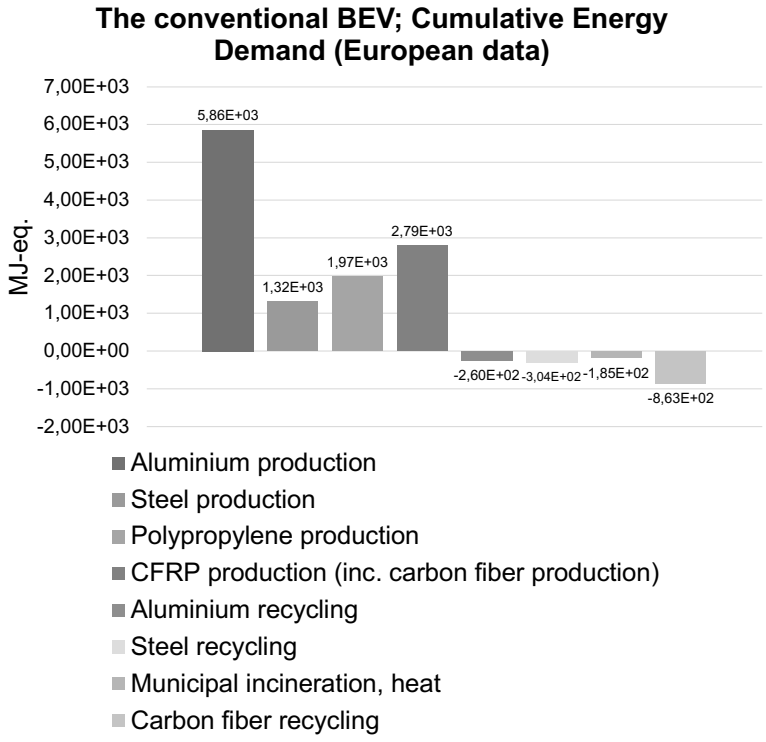

Figure 4.6: Cumulative energy demand of the processes in the conventional BEV.

The results show that the aluminium production causes the most impact in all three categories. This result is interesting considering that aluminum and steel constituted approximately equal shares of the total mass in the conventional BEV (Table 3.1). The credits from recycling of aluminium and steel are approximately the same in both the global warming potential and the cumulative energy demand. However, the credit from recycling of aluminium is much larger in the crustal scarcity indicator. As already explained, the total masses of steel and aluminium in the conventional BEV were approximately the same. This imply that there is another explanation to the result. The impact factors of aluminium and steel in the impact assessment method crustal scarcity indicator made by Arvidsson et al. [36] are also approximately the same ranging from 3 to 5. However, the Ecoinvent APOS version 3.7 for the market for aluminium cast alloy includes a process for zinc mine operation, which constitute approximately 17% of the total crustal scarcity impact from all processes. In the zinc mine operation process lead is a residual product from mining processes, and that has a really high impact for this impact category. This can be compared to the crustal scarcity impact from the steel production, which also constitute 17% of the total crustal scarcity impact. Depending on the type of zinc, the impact factor varies from 400 to 4000. However, it is unknown what type of zinc the zinc mine operation use, but this reasoning explains partly why the aluminium production as well as the aluminium recycling contribute with such a large impact on the crustal scarcity indicator.

Note that the proportion between the weight of aluminum and steel is not that common in a generic BEV, which usually has a larger portion of steel compared to aluminum [32]. However, many of the car manufactures are trying to find substitutes to steel with similar mechanical properties, which motivates a comparison between the materials. The modelling of both the production and recycling processes for aluminium and steel were done with processes in Ecoinvent APOS database version 3.7. This implies that the result should be representative of reality.

The carbon fiber production process causes the second most impact in all impact categories after aluminium production. The system also receives a credit from the recycling of carbon fibers. Aside from the crustal scarcity indicator, the recycling of carbon fibers give the largest credit to the system in all impact categories. For further information about the carbon fiber production and the CFRP production as well as the CFRP recycling, see Section 4.5.2.

The polypropylene production process causes relatively low impact on the global warming potential compared to the aluminium and steel production processes considering that polypropylene constituted two-thirds of their masses Table 3.1. However, the result for the cumulative energy demand shows that the energy demand for polypropylene is much higher than the energy demand for steel. Additionally, the credits from the municipal incineration process are similar for all impact categories. It should be mentioned that a generic vehicle often consist of several types of polymers. If the study had included other polymers, the result would most likely have looked different. The modelling of the recycling processes for aluminium, steel,

polypropylene and carbon fibers are based on a recycling rate of 95% according to EUs direction on recycling of metals and polymers [41]. However, the recycling rate can be discussed whether it is grounded in reality or not, but for this LCA study where a prospective approach was taken, the directive could be considered as reasonable.

4.5.2 The CFRP car

Figure 4.7, Figure 4.8 and Figure 4.9 presents the result per process (exl. the use phase of the vehicle) of the CFRP car for global warming potential, crustal scarcity indicator and cumulative energy demand. The appearance of the bars are rather similar between the impact categories and it can be seen that the carbon fiber production process is the hotspot of the system.

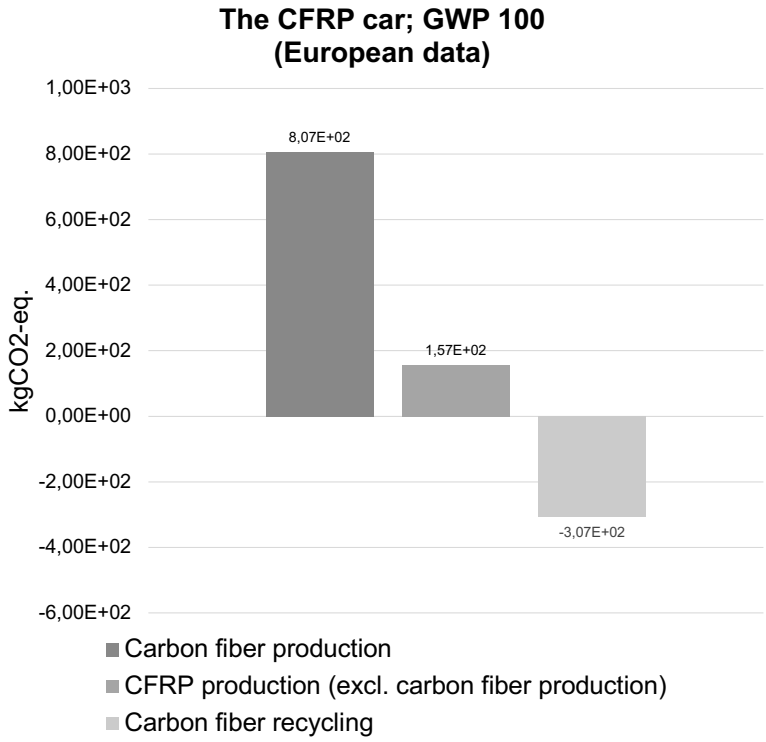

Figure 4.7: GWP 100 of the processes in the CFRP car.

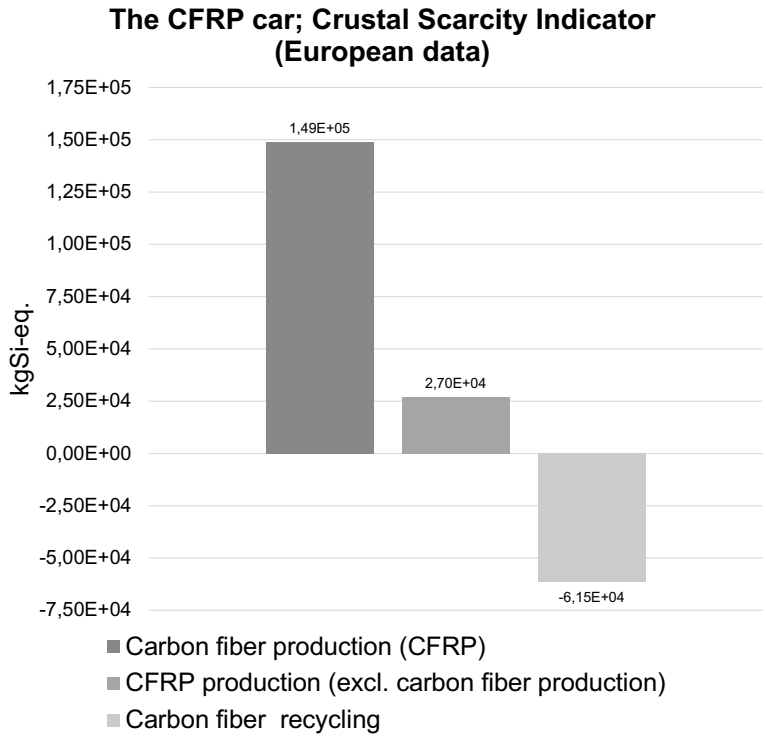

Figure 4.8: Crustal scarcity indicator of the processes in the CFRP car.

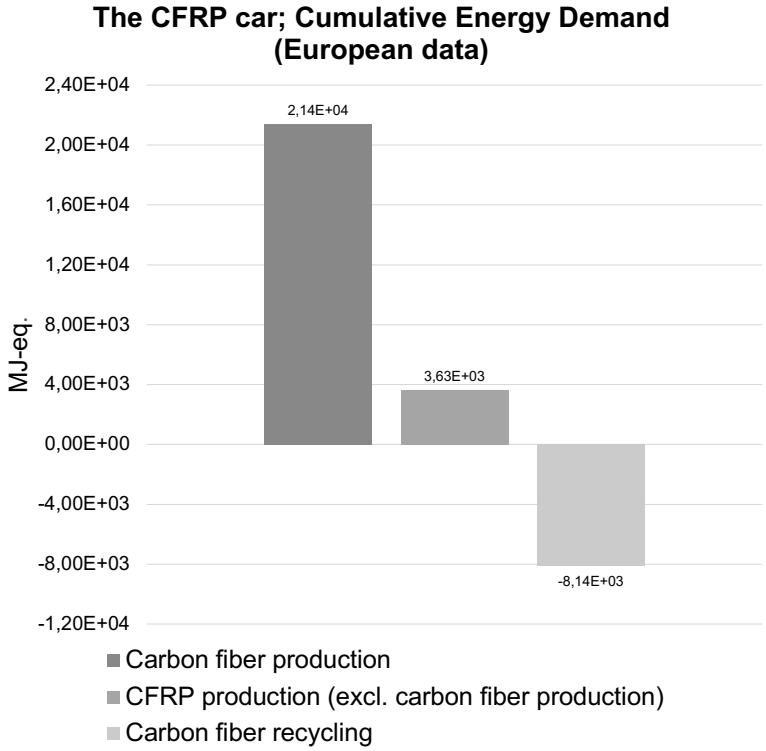

Figure 4.9: Cumulative energy demand of the processes in the CFRP car.

Carbon fibers are made of carbon-rich precursor material that undergoes a pyrolysis process where the precursor material is stabilized and carbonized. For this study, it was assumed that the precursor material was polyacrylonitrile fibers [35], which is a fossil-based polymer. The polyacrylonitrile fibers must first be stabilized, which is done through an oxidation process at an elevated temperature (180-300 °C). The stabilized fibers then undergoes a carbonization process where the fibers are heated at high temperatures (up to 1700 °C). This is done to remove non-carbon atoms from the polyacrylonitrile fibers. The carbonization process also requires nitrogen so that the fibers do not oxidize.

The processes have approximately the same type of energy requirements and emissions, but the concentration of the emissions are very different between the processes where the stabilization process emits high concentrations of nitrogen, while the carbonzation process emits high concentrations of hydrogen cyanide and ammonia [47]. Hydrogen cyanide is not included as an input factor in the global warming potential, crustal scarcity indicator or cumulative energy demand. This means that the environmental impact of hydrogen cyanide will not be included in the result. Hydrogen cyanide does have an impact on human health and other living organisms and would have had an impact on the result if human toxicity was chosen as an impact category. Furthermore, there are solutions on how to increase the energy efficiency and reduce the emission level of the carbon fiber production. Das [15] suggest that the polyacrylonitrile fibers can be substituted with lignin-based fibers, which could reduce the energy requirements and emission level by 5% and 22%, respectively. This suggestion is also in line with the findings by Janssen et al. [16] and Hermansson. [54] who also concluded that lignin could function as a substitution to polyacrylonitrile fibers and decrease the environmental impact of carbon fiber production. Furthermore, there are also solutions on processing technologies that would decrease the energy demand as well as the emissions. Lam et al. [55] suggest a microwave pyrolysis technology which provides a faster heating process resulting in a lower energy consumption.

The CFRPs was assumed to be recycled via pyrolysis process to recover the carbon fibers where only electricity was used. The modelling only included emissions related to the energy input, which means that other emissions were excluded. Meng et al. [11] discussed that recycling of carbon fiber with pyrolysis typically use a combination of electricity and natural gas in the combustion process. However, the authors did not specify the amount of electricity versus natural gas, but a slightly lower credit from the carbon fiber recycling process can be assumed according Meng et al.[11] energy set up.

Figure 4.10, Figure 4.11 and Figure 4.12 presents contribution graphs of the carbon fiber production in the CFRP car for global warming potential, crustal scarcity indicator and cumulative energy demand. Note that Figure 4.10 includes an input flow referred to as 'other emissions'. This input flow consists of particles released from the precursor material as it is processed during the stabilization and carbonization process. These particles only cause impact on global warming potential, which is

why the input flow is left out in Figure 4.10 and Figure 4.12.

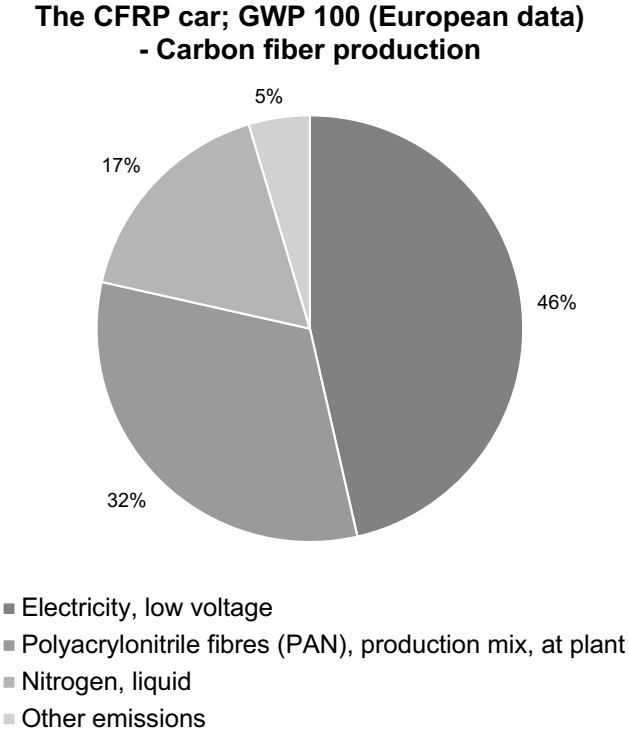

Figure 4.10: Cumulative energy demand of the processes in the CFRP car.

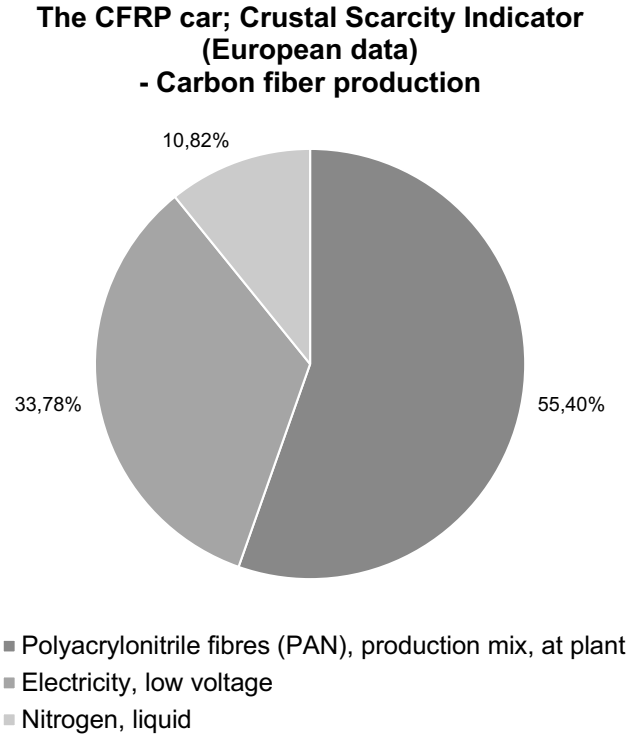

Figure 4.11: Crustal scarcity indicator of the processes in the CFRP car.

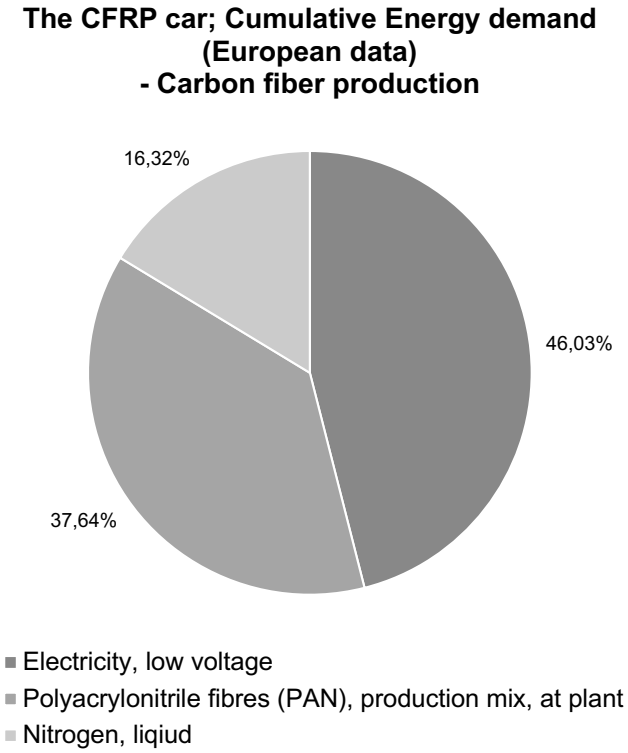

Figure 4.12: Cumulative energy demand of the processes in the CFRP car.

It can been seen that the electricity with low voltage constitute the largest share in both the global warming potential (Figure 4.10) and the cumulative energy demand (Figure 4.12), while the polyacrylonitrile fibers makes up the bulk in the crustal scarcity indicator (Figure 4.11). The high portion of electricity with low voltage is explained by the high energy use when the polyacrylonitrile fibers are stabilized and carbonized as described earlier, while the polyacrylonitrile fibers requires a lot of fossil-based resources in the production such as crude oil, brown and hard coal as well as sodium chloride, which explains its large share in the crustal scarcity indicator. Furthermore, the results for how much energy the polyacrylonitrile fibers require are in line with the findings by Das [15] who reported that the production of the precursor material typically constitutes 35% of the total energy use in carbon fiber production. However, it should be mentioned that the data set in this case for polyacrylonitrile fibers [35] is based on global data, while the other input flows are based on European data. This means that the polyacrylonitrile fibers would probably hold a slightly smaller share than Das [15] if all input flows were based on European data.

4.5.3 The SB car

Figure 4.13, Figure 4.14 and Figure 4.15 presents the environmental impact per process of the SB car for global warming potential, crustal scarcity indicator and cumulative energy demand. The results show that the carbon fiber production and the SB manufacturing (excl. carbon fiber production) are the hotspots in the system for all impact categories in addition to the battery production for the crustal scarcity indicator. For further information about the carbon fiber production, see Section 4.5.2.

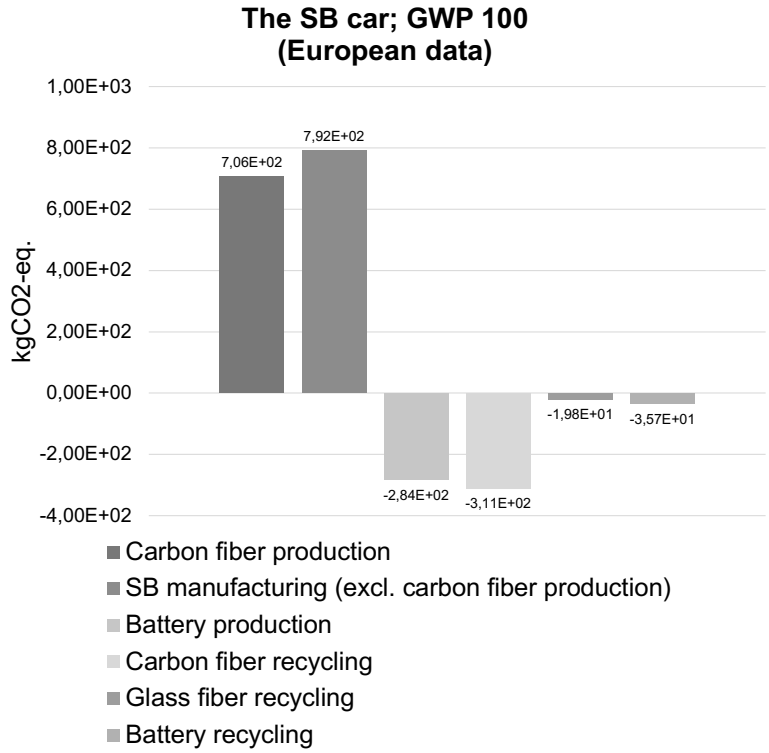

Figure 4.13: GWP 100 of the processes in the SB car.

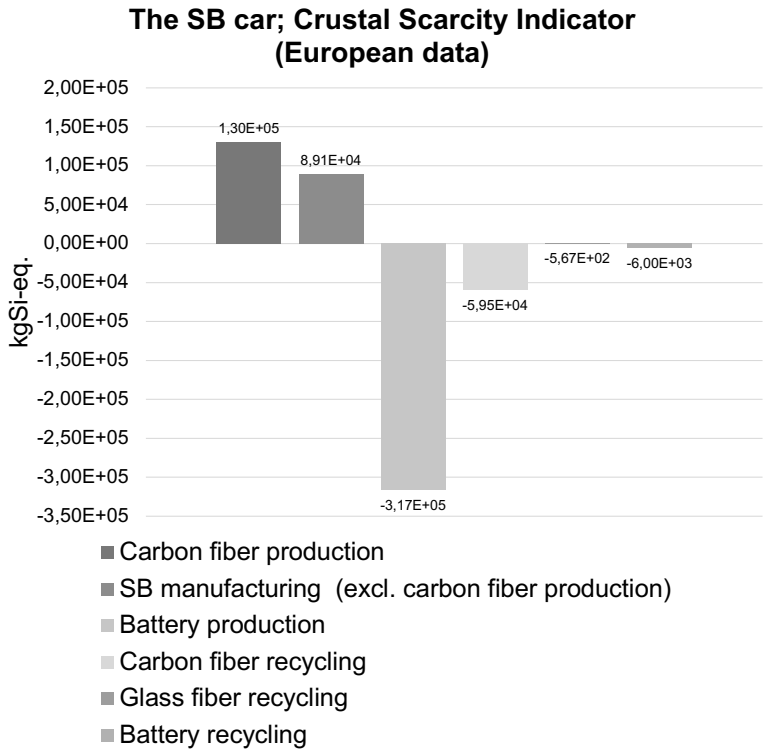

Figure 4.14: Crustal scarcity indicator of the processes in the SB car.

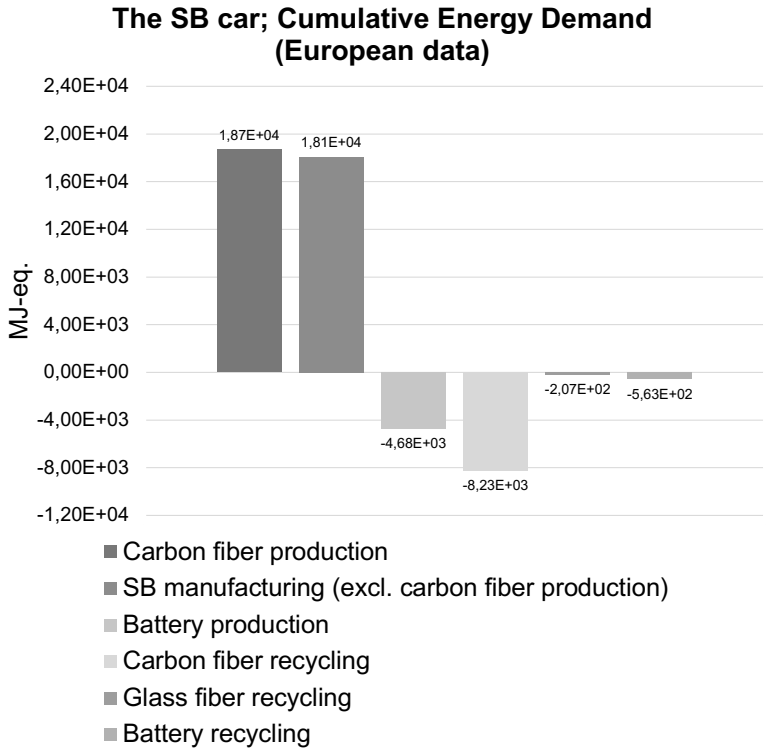

Figure 4.15: Cumulative energy demand of the processes in the SB car.

Credits from avoided production of batteries have a great impact on the environmen-

tal impact of the SB car. Manufacturing of the anode (graphite) and the cathode ($LiMn_2O_4$) in the Li-ion battery are the biggest contributors accounting for more than 50% of the total emissions from the battery production. The anode production process has an electrifying process of copper that causes the high climate impact, while the high climate impact from the cathode derives from the aluminum needed in the production process. The lack of European data in Ecoinvent APOS version 3.7, regarding battery production, can influence the reliability of the results. Although, manufacturing of batteries occurs on a global scale and includes many different materials and processes across the globe [53]. By choosing global data for this type of production process, the result will be much authentic. However, one could imagine that battery production is moving towards increased energy efficiency and reduced emissions. This would give the SBs a lower credit from the battery production process.

The recycling process of the Li-ion batteries only includes the hydrometallurgical process and the climate impact from this energy intensive process. These emissions are calculated as a credit for the system because of the chosen allocation method. No material recovery are included from the recycling process of the batteries in the system. However, the hydrometallurgical process, as described by Wang and Friedrich [46], also recovers graphite, cathode and lithium carbonate, which could be used to manufacture new batteries. These materials could have been included in the study, which would have resulted in a negative credit to the system. This affects the results, which can be considered as a weakness of the result.

The recycling of SBs was assumed to be done via a pyrolysis process to recover the carbon and glass fibers. However, this is something that is not taking place today. The same type of reasoning applies for the recycling of carbon fibers in the SB car as for the carbon fibers in the CFRP car (Section 4.5.2). The credit to the system for the recycling process of carbon fiber also has a large impact in the system, as for the CFRP car. Furthermore, the recycling of glass fibers was assumed to also be be recovered via a pyrolysis process as the carbon fibers. The recovery rate was assumed to be the same for the carbon fibers and glass fibers. This assumption can be questioned as to whether it is reasonable or not. Other studies [45, 33] have used a lower recovery rate for carbon fibers than for glass fibers. If the modelling of the recycling processes had been done with a lower recovery rate for the carbon fibers as in the other studies, the SB car would have received a lower credit from the recycling process. However, it is reasonable to imagine that the recovery rate of carbon fibers improves in the future, which motivates a similar rate to the glass fiber.

Figure 4.16, Figure 4.17 and Figure 4.18 presents contribution graphs of the SB manufacturing process (excluding the carbon fiber production) of the SB car for all impact categories.

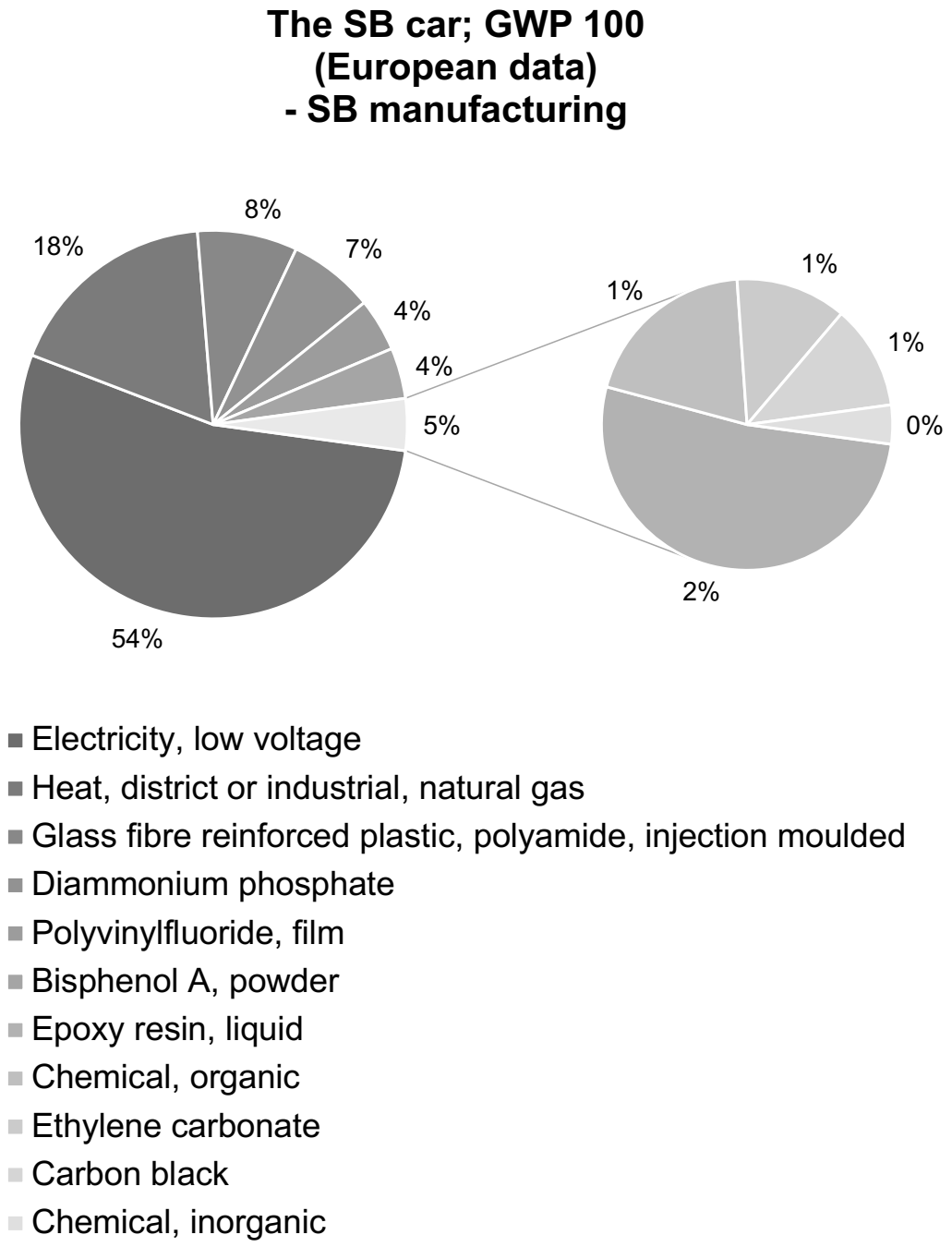

Figure 4.16: GWP 100 of the processes in the SB car.

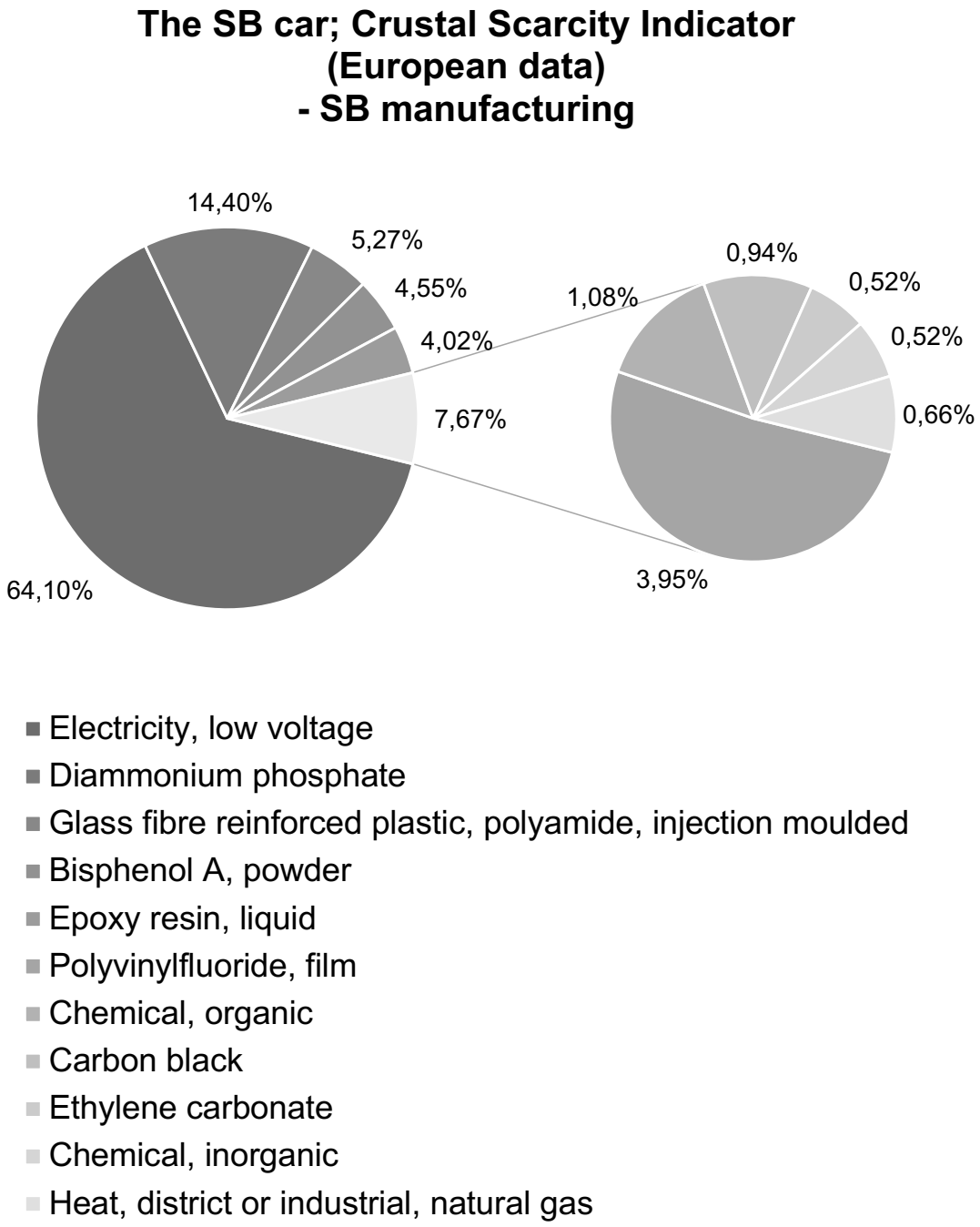

Figure 4.17: Crustal scarcity indicator of the processes in the SB car.

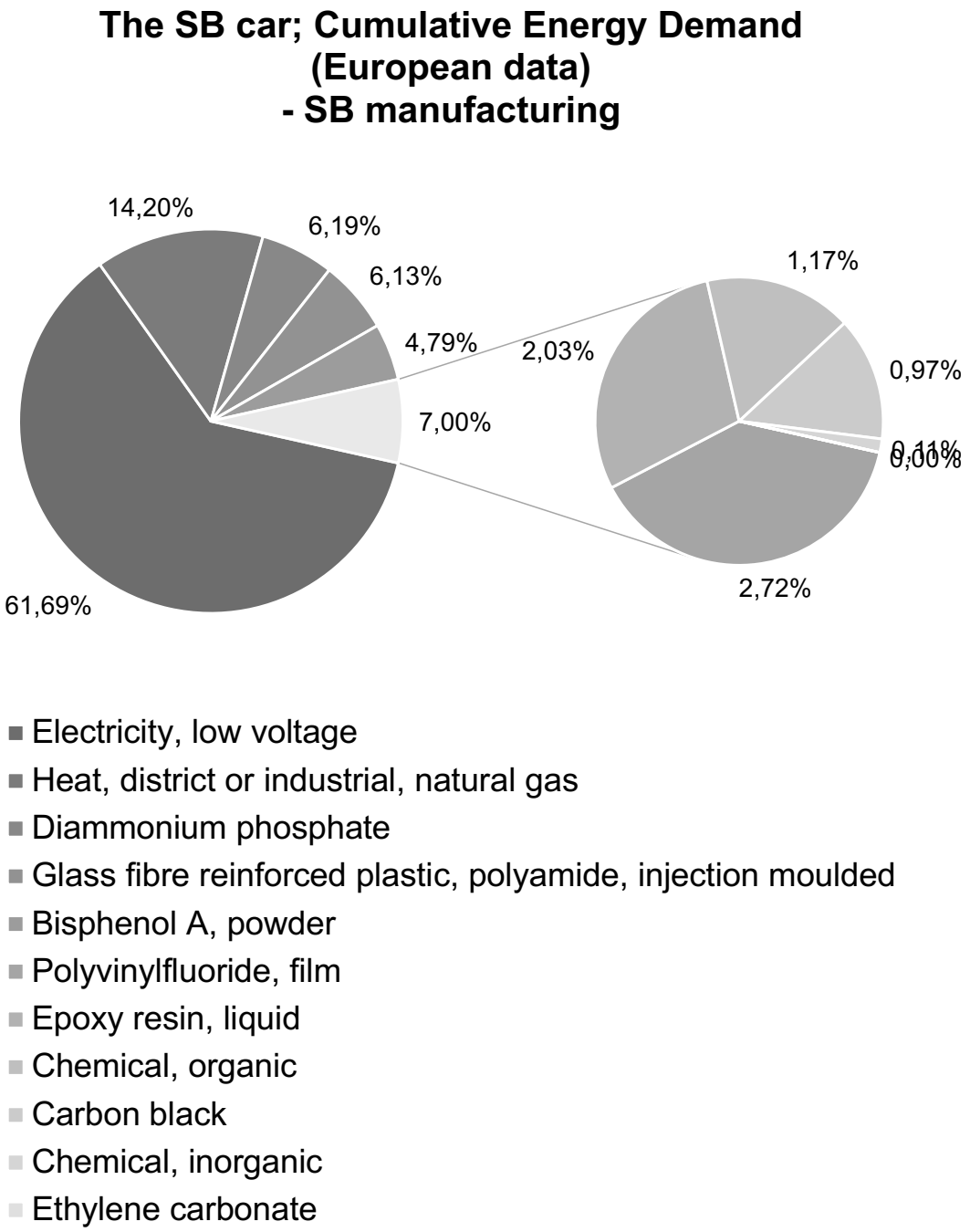

Figure 4.18: Cumulative energy demand of the processes in the SB car.

The results show that the electricity with low voltage constitute the largest share of the impact on the system for all impact categories. Figure 4.16 and Figure 4.18 have similar distribution of the most crucial input flows where the only difference is the glass fiber reinforced plastic and diammonium phosphate. However, it should be mentioned that the electricity consumption are only estimations based on the production environment of Li-ion batteries. As discussed in the method section (3.6.3.3), two important aspects of the manufacturing process are the primary energy needed in the manufacturing plant and how many processing steps that requires

dry room conditions. The study assumed that the energy requirement is 11.7 kWh electricity and 8.8 kWh gas per kg structural battery, which corresponds to 150 MJ primary energy [10]. However, the actual energy requirement will depend on how much of the manufacturing that must be done under clean room conditions. Additionally, dry room conditions is modelled with natural gas that has high climate impact for all the impact categories, except for crustal scarcity indicator, where natural gas only contribute to less then one percent of the total impacts (Figure 4.17). However, it is not known if natural gas will be needed in the future and if so, to which extend. It is reasonable to think that electricity mixes with high amount of renewable energy sources will be affected by the amount of natural gas.

The modelling of the structural battery electrolyte Table 3.8 included several constitutes that could not be found in the Ecoinvent APOS database version 3.7. These constituents were modelled as either inorganic or organic chemicals. Additionally, the diammonium phosphate was used to represent the $LiFePO_4$ in the negative electrode of the structural battery cell. These approximations may have affected the results. However, previous studies have used the same assumptions for modelling, which increase the reliability [49, 50].

4.6 Sensitivity Analysis

The following section includes sensitivity analysis of the lightweighting as well as the lifetime of the vehicles. Furthermore, the hotspots in the CFRP car and the SB car are also examined based on global and Swedish data for all impact categories.

4.6.1 The Result of Lightweighting Normalized to Swedish and Global data

Table 4.3 presents the result from the sensitivity analysis of the lightweighting, GWP100, where the credit from using lightweight materials based on European data is normalized to Swedish and global data. It can be seen that the credit would be 89% lower if the data was based on Swedish data and 78% higher if it was based on global data, see Figure D.8 and Figure D.2. This means that the CFRP car and the SB car will be credited differently depending on where the vehicles are used. Consequently, in regions with low emissions from the energy production, the credit will be lower compared to a region with the opposite conditions. This observation was also made by Zackrisson et al. [10] who have the same conclusion.

Table 4.3: Lightweighting normalized to Swedish and global data for global warming potential 100.

	Swedish data	European data	Global data
The CFRP car	0.11	1	1.78
The SB car	0.11	1	1.78

4.6.2 Break-even Analysis of the Use Phase of Global Warming Potential

In Figure 4.3, it can be seen that the net global warming potential is lower for the conventional BEV in comparison SB car including the credits from using lightweight materials and avoided production of batteries. For the CFRP car, the net global warming potential is lower for the CFRP car (Figure 4.3) including the credits from lightweighting. However, the credits from the lightweighting was based on a lifetime of 200,000 km as suggested by Hottle et al. [52], but there are ambitions that the lifetime of a vehicle will be increased as technologies continue to develop. Petrovic et al. [56] states that autonomous vehicles have great potential to reduce traffic accidents. If traffic accidents decreased in the future, the average lifetime of a vehicle would increase as a consequence. This motivates a sensitivity analysis where the lifetime of the vehicles is varied. Figure 4.19 presents the result from the break-even analysis where the SB car reach a lower global warming potential than the conventional BEV, this happens at about 335,000 km. The CFRP car reaches break-even at about 160,000 km, which is lower than the assumed driving range for a electric vehicle.

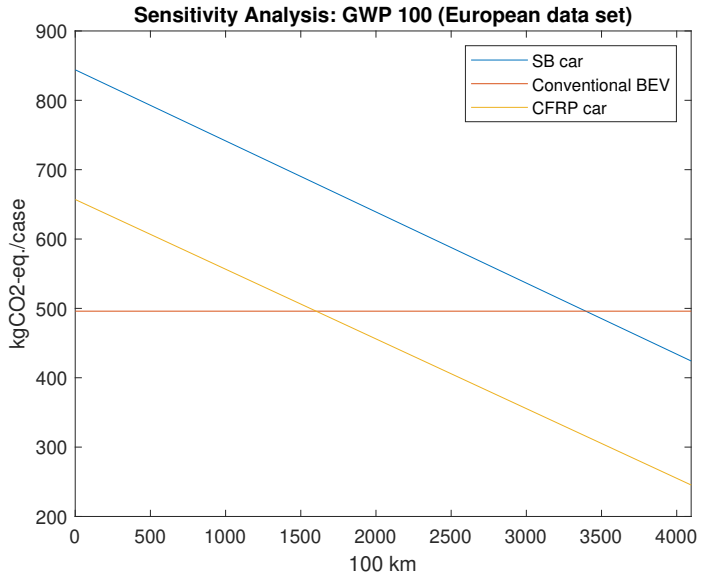

Figure 4.19: Break-even analysis of the global warming potential for the CFRP car and the SB car. Data is based on European data.

The result means that there are vehicles that are particularly suitable for CFRPs and SBs such as buses, taxicabs or trucks (i.e., vehicles with a high utilization rate). However, this presupposes that the lifetime of the vehicle is sufficiently high. This sensitivity analysis is based on European data, which means that the lightweighting results in a much larger credit in comparison to the same analysis with Swedish data. As presented in Table 4.3, the credit from using lightweight materials is 89% lower if the data is based on Swedish data instead of European. The result shows that the energy mix has a huge impact on the credit from lightweigting, which imply that

credits from lightweighting is much central to vehicles used in geographical areas where the energy mix is less clean.

4.6.3 Hotspots in the CFRP Car and the SB Car

In the following sections, the impact for the hotspots in the CFRP car (Section 4.5.2) and the SB car (Section 4.5.3) are normalized to global and Swedish data.

4.6.3.1 Global Warming Potential

Table 4.4 presents the sensitivity analysis of the hotspots in the CFRP and the SB car for global warming potential. From the Table 4.4, it can be seen that the climate impact varies approximately the same whether the calculations are based on Swedish or global data. Aside from the CFRP production in the CFRP car, the relative difference is greater for all processes if the data is based on Swedish data. The sensitivity analysis implies that the production of CFRP cars and SB cars would benefit significantly if the production was based on a Swedish energy mix, particularly the carbon fiber production in the CFRP car and the SB car, which reduced its impacts by 64% relative to the result based on European data. By using a Swedish energy mix, the net global warming potential becomes lower for the SB car including the credits from lightweighting and avoided battery production. For the CFRP car, this was already the case when the data was based on European. However, it can be seen that the net global warming potential becomes even lower. For further information about this sensitivity analysis, see Figure D.8 and Figure D.2

Table 4.4: The climate impact for the hotspots in the CFRP and the SB car normalized to Swedish and global data.

	Swedish data set	European data set	Global data set
CF production - CFRP car	0.44	1	1.51
CF production - SB car	0.44	1	1.52
CFRP production - CFRP car	0.67	1	1.36
SB manufacturing - SB car	0.52	1	1.40

4.6.3.2 Crustal Scarcity Indicator

In Table 4.5, the sensitivity analysis of the hotspots in the CFRP and the SB car with respect to crustal scarcity indicator is presented. It can be seen that the crustal scarcity impact becomes much smaller for all processes in the CFRP and the SB car when the data is based on Swedish data in comparison to when the data been based on European data. Furthermore, the SB manufacturing process in the SB car receives the largest relative difference in crustal scarcity impact. As explained earlier, this is related to the high energy requirements of the production. For further information about the sensitivity analysis, see Figure E.8 and Figure E.2.

Table 4.5: The crustal scarcity impact for the hotspots in the CFRP car and the SB car normalized to Swedish and global data.

	Swedish data set	European data set	Global data set
CF production - CFRP car	0.67	1	1.14
CF production - SB car	0.67	1	1.15
CFRP production - CFRP car	0.75	1	1.11
SB manufacturing - SB car	0.53	1	1.19

4.6.3.3 Cumulative Energy Demand

Table 4.6 presents the results for the hotspots from the sensitivity analysis. The table shows that there are small differences in cumulative energy demand if the modelling are based on European, Swedish or global data. This is reasonable because the only difference between the data sets are energy losses that occur within the electrical infrastructure of the geographical area, see Appendix F.

Table 4.6: The cumulative energy demand for the hotspots in the CFRP and the SB car normalized to Swedish and global data.

	Swedish data set	European data set	Global data set
CF production - CFRP car	0.89	1	1.04
CF production - SB car	0.89	1	1.04
CFRP production - CFRP car	0.89	1	1.04
SB manufacturing - SB car	0.90	1	1.02

5
Conclusion

This thesis designed a conceptual BEV with conventional materials which were replaced with either CFRPs or SBs. The thesis also assessed the life cycle impact of the conventional BEV and the composite vehicles. The results showed that CFRPs and SBs have the potential to reduce the weight of a conventional BEV while not deteriorating the modulus of elasticity or energy storage of the system. A total vehicle weight reduction of approximately 33 % and 47 % could be found in the CFRP and the SB car, respectively. The result also showed that the SB car provided a surplus of electrochemical capacity in comparison to the conventional BEV, which resulted in additional energy storage.

From the results, it is obvious that the carbon fiber production and the structural batteries manufacturing counteract the credits from lightweighting as well as the avoided battery production. The result shows that the CFRP car does provide an environmental benefit over the conventional BEV, while the SB car causes more environmental impact. However, the result indicates that the CFRP car and SB car could decrease the environmental impact drastically if the energy use was reduced in the carbon fiber production as well as the structural batteries manufacturing. Another possible solution to achieve environmental benefit for the CFRP car and SB car is to manufacture the vehicles in geographical areas where the energy system is fossil carbon lean. This leads to quite drastic reductions in environmental impact for the CFRP and the SB car.

The main methodological issue in assessing technologies like SBs using LCA is the definition of a functional unit as SBs stimulate two functions simultaneously. An additional problem was to model the system for the conventional BEV and composite vehicles as the materials and its manufacturing and recycling processes have different technology maturity level. This may have had implications for the comparative assessment of the vehicles.

The break-even analysis demonstrates that SBs should be implemented in vehicles with high utilization rates and long lifetimes. The high utilization rate could be improved by changing the way the vehicles are used today. Implementing circular economy is one way to handle the issue where car sharing is a strategy that could be used. For the lifetime, a possible scenario could be the implementation of autonomous driving, which would probably reduce the traffic accident rates. However, it can be concluded that the credit from lightweighting is heavily influenced by the energy mix where a fossil carbon lean energy system decreases the size of the credit.

However, the break-even analysis shows that for the CFRP car the importance of high utilization and long lifetime is not as important as for the SB car, which entails better prerequisites for CFRPs to be used in applications other then buses, taxicab or trucks.

5.1 Future Research

Future studies should focus on the modelling of the vehicle components, particularly for SBs. This study only used secondary data and some constituents in the SBs that could not be found in the Ecoinvent APOS version 3.7 were replaced with similar materials. It would also be interesting if future studies did a similar study, but where precursor materials was on lignin fibers instead of polyacrylonitrile fibers to see what impact it has on the result. Additionally, there is no method to recycle SBs at the moment. Future studies should therefore focus on this aspect to increase the knowledge of its impact. There seems also to be lack of European data for production and recycling of batteries. Further analysis in this area would be useful to give a more representative result of the impact from the batteries.

Bibliography

[1] Ralph Sims et al. *Transport. In: Climate Change 2014: Mitigation of Climate Change. Contribution of Working Group III to the Fifth Assessment Report of the Intergovernmental Panel on Climate Change*. Tech. rep. June 2014. DOI: 10.1017/CBO9781107415416.005.

[2] European Environment Agency. *Progress of EU transport sector towards its environment and climate objectives [Internet]*. 2018. URL: https://www.eea.europa.eu/publications/progress-of-eu-transport-sector-1/term-briefing-2018.

[3] European Commission. *Transport emissions [Internet]*. 2016. URL: https://ec.europa.eu/clima/policies/transport_en.

[4] K. Jagath Narayana and Ramesh Gupta Burela. "A review of recent research on multifunctional composite materials and structures with their applications". In: *Materials Today: Proceedings*. Vol. 5. 2. Elsevier Ltd, 2018, pp. 5580–5590. DOI: 10.1016/j.matpr.2017.12.149.

[5] Barton Bennett. *Future multifunctional structures: Composites needed | CompositesWorld*. Nov. 2010. URL: https://www.compositesworld.com/columns/future-multifunctional-structures-composites-needed.

[6] Ronald F. Gibsson. "A review of recent research on mechanics of multifunctional composite materials and structures". In: *Composite Structures* 92.12 (Nov. 2010), pp. 2793–2810. ISSN: 02638223. DOI: 10.1016/j.compstruct.2010.05.003.

[7] David Carlstedt and Leif E. Asp. "Performance analysis framework for structural battery composites in electric vehicles". In: *Composites Part B: Engineering* 186 (Apr. 2020). ISSN: 13598368. DOI: 10.1016/j.compositesb.2020.107822.

[8] Wilhelm Johannisson et al. "A residual performance methodology to evaluate multifunctional systems". In: *Multifunctional Materials* 3.2 (June 2020). ISSN: 23997532. DOI: 10.1088/2399-7532/ab8e95.

[9] Wilhelm Johannisson, Dan Zenkert, and Göran Lindbergh. "Model of a structural battery and its potential for system level mass savings". In: *Multifunctional Materials* 2.3 (Sept. 2019). ISSN: 23997532. DOI: 10.1088/2399-7532/ab3bdd.

[10] Mats Zackrisson et al. "Prospective life cycle assessment of a structural battery". In: *Sustainability (Switzerland)* 11.20 (Oct. 2019). ISSN: 20711050. DOI: 10.3390/su11205679.

[11] Fanran Meng et al. "Comparing Life Cycle Energy and Global Warming Potential of Carbon Fiber Composite Recycling Technologies and Waste Management Options". In: *ACS Sustainable Chemistry and Engineering* 6.8 (Aug. 2018), pp. 9854–9865. ISSN: 21680485. DOI: 10.1021/acssuschemeng.8b01026.

[12] Ronald F. Gibson. "A review of recent research on mechanics of multifunctional composite materials and structures". In: *Composite Structures* 92.12 (Nov. 2010), pp. 2793–2810. ISSN: 02638223. DOI: 10.1016/j.compstruct.2010.05.003.

[13] H. Ahmad et al. "A review of carbon fiber materials in automotive industry". In: *IOP Conference Series: Materials Science and Engineering*. Vol. 971. 3. IOP Publishing Ltd, Nov. 2020. DOI: 10.1088/1757-899X/971/3/032011.

[14] Leif E. Asp et al. "Structural battery composites: A review". In: *Functional Composites and Structures* 1.4 (Dec. 2019). ISSN: 26316331. DOI: 10.1088/2631-6331/ab5571.

[15] Sujit Das. "Life cycle assessment of carbon fiber-reinforced polymer composites". In: *International Journal of Life Cycle Assessment* 16.3 (Mar. 2011), pp. 268–282. ISSN: 09483349. DOI: 10.1007/s11367-011-0264-z.

[16] Matty Janssen et al. "Life cycle assessment of lignin-based carbon fibres". In: (2019). URL: http://urn.kb.se/resolve?urn=urn:nbn:se:ri:diva-40763.

[17] Dervis Ozkan, Mustafa Sabri Gok, and Abdullah Cahit Karaoglanli. "Carbon Fiber Reinforced Polymer (CFRP) Composite Materials, Their Characteristic Properties, Industrial Application Areas and Their Machinability". In: *Advanced Structured Materials* 124 (2020), pp. 235–253. ISSN: 18698441. DOI: 10.1007/978-3-030-39062-4{_}20.

[18] D. J. O'Brien, D. M. Baechle, and E. D. Wetzel. "Design and performance of multifunctional structural composite capacitors". In: *Journal of Composite Materials* 45.26 (Dec. 2011), pp. 2797–2809. ISSN: 00219983. DOI: 10.1177/0021998311412207.

[19] Michael F Ashby. *Materials selection mechanical design*. Tech. rep. Cambridge: Department of Engineering, Cambridge University, 1992.

[20] James P. Thomas and Muhammad A. Qidwai. "Mechanical design and performance of composite multifunctional materials". In: *Acta Materialia* 52.8 (May 2004), pp. 2155–2164. ISSN: 13596454. DOI: 10.1016/j.actamat.2004.01.007.

[21] R. Kanno et al. "Carbon as negative electrodes in lithium secondary cells". In: *Journal of Power Sources* 26.3-4 (May 1989), pp. 535–543. ISSN: 03787753. DOI: 10.1016/0378-7753(89)80175-2.

[22] James F. Snyder, Eric D. Wetzel, and Cara M. Watson. "Improving multifunctional behavior in structural electrolytes through copolymerization of structure- and conductivity-promoting monomers". In: *Polymer* 50.20 (Sept. 2009), pp. 4906–4916. ISSN: 00323861. DOI: 10.1016/j.polymer.2009.07.050.

[23] Maria H. Kjell et al. "PAN-Based Carbon Fiber Negative Electrodes for Structural Lithium-Ion Batteries". In: *Journal of The Electrochemical Society* 158.12 (2011), A1455. ISSN: 00134651. DOI: 10.1149/2.053112jes.

[24] Giulia Fredi et al. "Graphitic microstructure and performance of carbon fibre Li-ion structural battery electrodes". In: *Multifunctional Materials* 1.1 (Aug. 2018), p. 015003. ISSN: 2399-7532. DOI: 10.1088/2399-7532/aab707. URL: https://iopscience.iop.org/article/10.1088/2399-7532/aab707.

[25] Eric Jacques et al. "Impact of electrochemical cycling on the tensile properties of carbon fibres for structural lithium-ion composite batteries". In: *Composites Science and Technology* 72.7 (Apr. 2012), pp. 792–798. ISSN: 02663538. DOI: 10.1016/j.compscitech.2012.02.006.

[26] Eric Jacques et al. "Expansion of carbon fibres induced by lithium intercalation for structural electrode applications". In: *Carbon* 59 (Aug. 2013), pp. 246–254. ISSN: 00086223. DOI: 10.1016/j.carbon.2013.03.015.

[27] Leif E. Asp et al. "A Structural Battery and its Multifunctional Performance". In: *Advanced Energy and Sustainability Research* 2.3 (Mar. 2021), p. 2000093. ISSN: 2699-9412. DOI: 10.1002/aesr.202000093.

[28] Greg Peters and Magdalena Svanström. "Environmental Assessment of Products and Processes". In: *Environmental Sustainability for Engineers and Applied Scientists*. Cambridge University Press, Mar. 2019, pp. 139–169. DOI: 10.1017/9781316711408.008.

[29] Joachim Starke. *Carbon composites in automotive structural applications [PowerPoint presentation].* URL: https://eucia.eu/userfiles/files/Starke-Eucia%202016-V4-Druck%20b.pdf.

[30] Tesla. *Model S Premium Electric Sedan [powerPoint presentation].* URL: https://www.tesla.com/sites/default/files/tesla-model-s.pdf.

[31] Rishab Rangarajan. *Structural Battery Composites in Electric Vehicle Design: A Feasibility study.* Tech. rep. 2018. URL: https://hdl.handle.net/20.500.12380/256368.

[32] Erik Emilsson, Lisbeth Dahllöf, and Maria Ljunggren Söderman. "Plastics in passenger cars A comparison over types and time In cooperation with : Volvo Cars". In: (2019). URL: www.ivl.se.

[33] Frida Hermansson et al. "The environmental benefits and challenges of a composite car with structural battery materials". In: *Resource efficient vehicle conference* (2021).

[34] Ecoinvent. *Ecoinvent 3.7 [PowerPoint presentation].* URL: https://www.ecoinvent.org/database/ecoinvent-371/ecoinvent-37/ecoinvent-37.html.

[35] David Fazio Simone; Pennington. "Polyacrylonitrile fibres (PAN); from acrylonitrile and methacrylate; production mix, at plant; PAN without additives (Location: EU-27)." In: *European Commission, Joint Research Centre (JRC)* (2005). URL: http://data.europa.eu/89h/jrc-eplca-db00901a-338f-11dd-bd11-0800200c9a66.

[36] Rickard Arvidsson et al. "A crustal scarcity indicator for long-term global elemental resource assessment in LCA". In: *International Journal of Life Cycle Assessment* 25.9 (Sept. 2020), pp. 1805–1817. ISSN: 16147502. DOI: 10.1007/s11367-020-01781-1.

[37] Rickard Arvidsson et al. "Environmental Assessment of Emerging Technologies: Recommendations for Prospective LCA". In: *Journal of Industrial Ecology* 22.6 (Dec. 2018), pp. 1286–1294. ISSN: 15309290. DOI: 10.1111/jiec.12690.

[38] Frida Hermansson, Matty Janssen, and Magdalena Svanström. "Allocation in life cycle assessment of lignin". In: *International Journal of Life Cycle Assessment* 25.8 (Aug. 2020), pp. 1620–1632. ISSN: 16147502. DOI: 10.1007/s11367-020-01770-4.

[39] Mats Zackrisson et al. “Life cycle assessment of lithium-air battery cells”. In: *Journal of Cleaner Production* 135 (Nov. 2016), pp. 299–311. ISSN: 09596526. DOI: 10.1016/j.jclepro.2016.06.104.

[40] Julien Matheys and Wout Van Autenboer. “SUBAT: Sustainable Batteries. WP5 Final public report”. In: (2006).

[41] Eur-LEX. *Official Journal of the European Union [Internet]*. URL: https://eur-lex.europa.eu/legal-content/EN/TXT/?uri=CELEX%3A32000L0053.

[42] Amelie Gustafsson. *Mapping and investigation of carbon emissions from incineration of plastics A thesis investigation on common polymers and how they should be managed*. Tech. rep.

[43] Tetsuya Suzuki and Jun Takahashi. *The Ninth Japan International Sampe symposium prediction of energy intensity of carbon fiber reinforced plastics for mass-produced passenger cars*. Tech. rep.

[44] Robert A. Witik et al. “Assessing the life cycle costs and environmental performance of lightweight materials in automobile applications”. In: *Composites Part A: Applied Science and Manufacturing* 42.11 (Nov. 2011), pp. 1694–1709. ISSN: 1359835X. DOI: 10.1016/j.compositesa.2011.07.024.

[45] S. J. Pickering. “Recycling technologies for thermoset composite materials-current status”. In: *Composites Part A: Applied Science and Manufacturing* 37.8 (Aug. 2006), pp. 1206–1215. ISSN: 1359835X. DOI: 10.1016/j.compositesa.2005.05.030.

[46] Honggang Wang and Bernd Friedrich. “Development of a Highly Efficient Hydrometallurgical Recycling Process for Automotive Li–Ion Batteries”. In: *Journal of Sustainable Metallurgy* 1.2 (June 2015), pp. 168–178. ISSN: 21993831. DOI: 10.1007/s40831-015-0016-6.

[47] Yuriy Alexander Romaniw. “The relationship between lightweighting with carbon fiber reinforces polymers and the life cycle environmental impacts of orbital launch rockets a dissertation.” In: (2013).

[48] European Commission. *European Platform on Life Cycle Assessment [Internet]*. URL: https://eplca.jrc.ec.europa.eu/.

[49] Mats Zackrisson et al. *Supplementary material*. URL: http://www.mdpi.com/2071-1050/11/20/5679/s1.

[50] Sampatrao Manjare and Rajendra Mohite. “Application life cycle assessment to diammonium phosphate production”. In: *Advanced Materials Research*.

Vol. 354-355. 2012, pp. 256–265. ISBN: 9783037852668. DOI: 10.4028/www.scientific.net/AMR.354-355.256.

[51] J. B. Dunn et al. "The significance of Li-ion batteries in electric vehicle life-cycle energy and emissions and recycling's role in its reduction". In: *Energy and Environmental Science* 8.1 (Jan. 2015), pp. 158–168. ISSN: 17545706. DOI: 10.1039/c4ee03029j.

[52] Troy Hottle et al. "Critical factors affecting life cycle assessments of material choice for vehicle mass reduction". In: *Transportation Research Part D: Transport and Environment* 56 (Oct. 2017), pp. 241–257. ISSN: 13619209. DOI: 10.1016/j.trd.2017.08.010.

[53] European Union. *Lithium-ion batteries for mobility and stationary storage applications scenarios for costs and market growth Implications of growth on costs and market size*. Tech. rep. DOI: 10.2760/87175. URL: https://europa.eu/!FF86WW.

[54] Frida Hermansson. *Thesis for the degree of licentiate of engineering assessing the future of environmental impact of lignin-based and recycled carbon fliers in composites using life cycle assessment*. Tech. rep.

[55] Su Shiung Lam et al. "Cleaner conversion of bamboo into carbon fibre with favourable physicochemical and capacitive properties via microwave pyrolysis combining with solvent extraction and chemical impregnation". In: *Journal of Cleaner Production* 236 (Nov. 2019). ISSN: 09596526. DOI: 10.1016/j.jclepro.2019.117692.

[56] Dorde Petrovic, Radomir Mijailović, and Dalibor Pešić. "Traffic Accidents with Autonomous Vehicles: Type of Collisions, Manoeuvres and Errors of Conventional Vehicles' Drivers". In: *Transportation Research Procedia*. Vol. 45. Elsevier B.V., 2020, pp. 161–168. DOI: 10.1016/j.trpro.2020.03.003.

A

Calculations of the Effective Modulus of Elasticity

A.1 Cell Design with 8 laminates

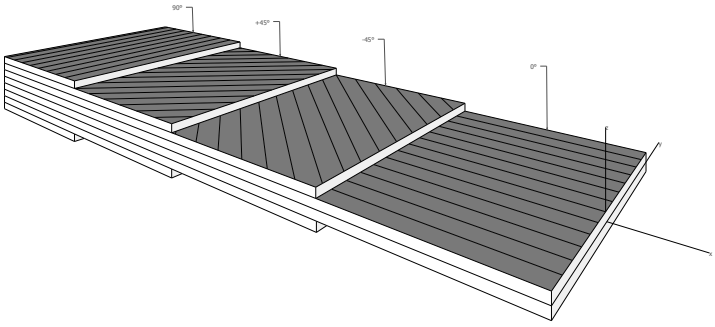

(a)

Figure A.1: Cell with 8 laminates and laminate orientation code $[0/\text{-}45/45/90]_s$.

B

Inventory Analysis

B.1 Modelling of the conventional BEV

Table B.1: Providers for the modelling of the conventional BEV including processes for production. Data is based on the database Ecoinvent APOS 3.7 and ELCD.

Process	Provider
Aluminum production	aluminium alloy production, AlMg3 | aluminium alloy, AlMg3 | APOS U
	impact extrusion of aluminium, 5 strokes | impact extrusion of aluminium, 5 strokes | APOS U
	sheet rolling, aluminium | sheet rolling, aluminium | APOS U
Steel production	steel production, low-alloyed, hot rolled | steel, low-alloyed, hot rolled | APOS U
	impact extrusion of steel, hot, 5 strokes | impact extrusion of steel, hot, 5 strokes | APOS U
Polypropylene production	injection moulding | injection moulding | APOS U
	polypropylene production, granulate | polypropylene, granulate | APOS U
Carbon fiber production	market for electricity, low voltage | electricity, low voltage | APOS U
	market for nitrogen, liquid | nitrogen, liquid | APOS U
	Polyacrylonitrile fibres (PAN), production mix, at plant, from acrylonitrile and methacrylate, PAN without additives
CFRP production	market for electricity, low voltage | electricity, low voltage | APOS U
	market for epoxy resin, liquid | epoxy resin, liquid | APOS U

Table B.2: Providers for the modelling of the conventional BEV including processes regarding recycling. Data is based on the database Ecoinvent APOS 3.7 and ELCD.

Process	Provider
Recycling of carbon fibers	Same as for Carbon fiber production
	market for electricity, low voltage | electricity, low voltage | APOS U
Recycling of PP	treatment of waste polystyrene, municipal incineration | heat, for reuse in municipal waste incineration only | APOS U
Steel recycling	steel production, electric, low-alloyed | steel, low-alloyed | APOS U
Aluminium recycling	treatment of aluminium scrap, post-consumer, by collecting, sorting, cleaning, pressing | aluminium scrap, post-consumer | APOS U

B.2 Modelling of the CFRP car

Table B.3: Providers for the modelling of the CFRP car. Data is based on the database Ecoinvent APOS 3.7 and ELCD.

Process	Provider
Carbon fiber production	market for electricity, low voltage | electricity, low voltage | APOS, U
	market for nitrogen, liquid | nitrogen, liquid | APOS, U
	Polyacrylonitrile fibres (PAN), production mix, at plant, from acrylonitrile and methacrylate, PAN without additives
CFRP production	market for electricity, low voltage | electricity, low voltage | APOS, U
	market for epoxy resin, liquid | epoxy resin, liquid | APOS, U
Recycling of carbon fibers	Same as for Carbon fiber production
	market for electricity, low voltage | electricity, low voltage | APOS, U

B.3 Modelling of the SB car

Table B.4: Providers for the modelling of the SB car. Data is based on the database Ecoinvent APOS 3.7 and ELCD.

Process	Provider
Carbon fiber production	market for electricity, low voltage | electricity, low voltage | APOS, U
	market for nitrogen, liquid | nitrogen, liquid | APOS, U
	Polyacrylonitrile fibres (PAN), production mix, at plant, from acrylonitrile and methacrylate, PAN without additives
SB production	glass fibre reinforced plastic production, polyamide, injection moulded | glass fibre reinforced plastic, polyamide, injection moulded | APOS, U
	market for epoxy resin, liquid | epoxy resin, liquid | APOS, U
	market for polyvinylfluoride, film | polyvinylfluoride, film | APOS, U
	market group for heat, district or industrial, natural gas | heat, district or industrial, natural gas | APOS, U
	market for electricity, low voltage | electricity, low voltage | APOS, U
Carbon fiber recycling	Same as for carbon fiber production
	market for electricity, low voltage | electricity, low voltage | APOS, U
Battery production	battery production, Li-ion, rechargeable, prismatic | battery, Li-ion, rechargeable, prismatic | APOS, U
Battery recycling	EcoSpold 2 intermediate exchange, ID = e3c4c750-7765-43b6-802b-8dbe05270f05
Recycled glass fiber	glass fibre reinforced plastic production, polyamide, injection moulded | glass fibre reinforced plastic, polyamide, injection moulded | APOS, U

Table B.5: Providers for the modelling of the SBE adapted from [49]. Data is based on providers in Ecoinvent APOS version 3.7.

Constituent	Provider	Comment
Bisphenol A dimethacrylate	Market for bisphenol A, powder | bisphenol A, powder | APOS, U	-
Lithium trifluoromethane-sulfonate	Market for chemicals, inorganic | chemical, inorganic | APOS, U	Corresponds to salt. Approximated as inorganic chemicals.
Ethylene carbonate	Market for ethylene carbonate | ethylene carbonate | APOS, U	-
Dimethyl methylphosphonate	Market for chemical, organic | chemical, organic | APOS, U	Corresponds to organic substance. Approximated as organic chemicals.
2,2'(Ethylenedioxy)-diethanethiol	Market for chemical, organic | chemical, organic | APOS, U	Corresponds to organic substance. Approximated as organic chemicals.
Tris(N-nitroso-N-phenyl-hydroxy-laminato)al.	Market for chemical, organic | chemical, organic | APOS, U	Corresponds to organic substance. Approximated as organic chemicals.
2,2'-Azobis(2-methyl-propionitrile)	Market for chemical, organic | chemical, organic | APOS, U	Corresponds to organic substance. Approximated as organic chemicals.

B.4 Modelling of the Use Phase

Table B.6: Provider for the modelling of the use phase of the vehicles. Data is based on providers in Ecoinvent APOS version 3.7.

Provider	Comment
Market group for electricity, low voltage | electricity, low voltage | APOS, U - EU	Represent the propulsion of the vehicles.

C
Sensitivity Analysis

C.1 Adjustments in the Sensitivity Analysis based on Swedish data

C.1.1 The Conventional BEV

Table C.1: Manually changed in the processes for the sensitivity analysis of the conventional BEV. Data is based on Ecoinvent APOS version 3.7.

Process	Provider
Aluminum production	Market for alkylbenzene sulfonate, linear, petrochemical GLO to market for alkylbenzene, linear, petrochemical RER
	Market group for electricity RER to market for electricity SE
Steel production	2nd provider steel, low-alloyed: market group for electricity GLO to market for electricity SE
	2nd provider steel, low-alloyed: market from electric arc furnace converter GLO to electric arc furnace converter RER
	2nd provider steel, low-alloyed: market anode, for metal electrolysis GLO to anode production, for metal electrolysis RER
Polypropylene production	2nd provider polypropylene, granulate: market for polypropylene, granulate GLO to polypropylene production, granulate RER
Polypropylene forming	2nd provider injection moulding: market group for electricity RER to market for electricity SE
	2nd provider injection moulding: market for kaoling GLO to kaoling production RER
	2nd provider injection moulding: market for malusil GLO to malusil production RER
Carbon fiber production	Market group for electricity RER to market for electricity SE
	2nd provider nitrogen liquid: market group for electricity RER
CFRP production	Market group for electricity RER to market for electricity SE
Recycling of carbon fibers	Market group for electricity RER to market for electricity SE
	2nd provider nitrogen liquid: market group for electricity RER
Recycling of CFRP	Market group for electricity RER to market for electricity SE

C.1.2 The CFRP car

Table C.2: Manually changes in the processes for the sensitivity analysis of the CFRP car.

Process	Provider
Carbon fiber production	Market group for electricity RER to market for electricity SE
	2nd provider nitrogen liquid: market group for electricity RER to market for electricity SE
CFRP production	Market group for electricity RER to market for electricity SE
Recycling of carbon fibers	Market group for electricity RER to market for electricity SE
	2nd provider nitrogen liquid: market group for electricity RER to market for electricity SE
Recycling of CFRP	Market group for electricity RER to market for electricity SE

C.1.3 The SB car

Table C.3: Manually changes in the processes for the sensitivity analysis of the SB car.

Process	Provider
Carbon fiber production	Market group for electricity RER to market for electricity SE
	2nd provider nitrogen liquid: market group for electricity RER to market for electricity SE
SB manufacturing	Market group for electricity RER to market for electricity SE
Battery production	2nd provider: market group for electricity GLO to market for electricity SE
	2nd provider: metal for metal working factory GLO to metal working factory construction RER
	2nd provider: market for reinforced steel GLO to reinforced steel production EU without Austria
	2nd provider: market for sheet rolling steel GLO to sheet rolling steel RER
Recycling of carbon fibers	Market group for electricity RER to market for electricity SE
	2nd provider nitrogen liquid: market group for electricity RER to market for electricity SE
Recycling of glass fibers	Market group for electricity RER to market for electricity SE
Recycling of battery	2nd provider: market for chemical factory. organics GLO to chemical factory, organics RER
	2nd provider: market group for electricity GLO to market for electricity SE
	2nd provider: market for lime hydrated packed ROW to market for lime hydrated packed RER
	2nd provider: market for sulfuric acid ROW to market for sulfuric acid RER

D

Global Warming Potential

D.1 European data

D.1.1 The SB car

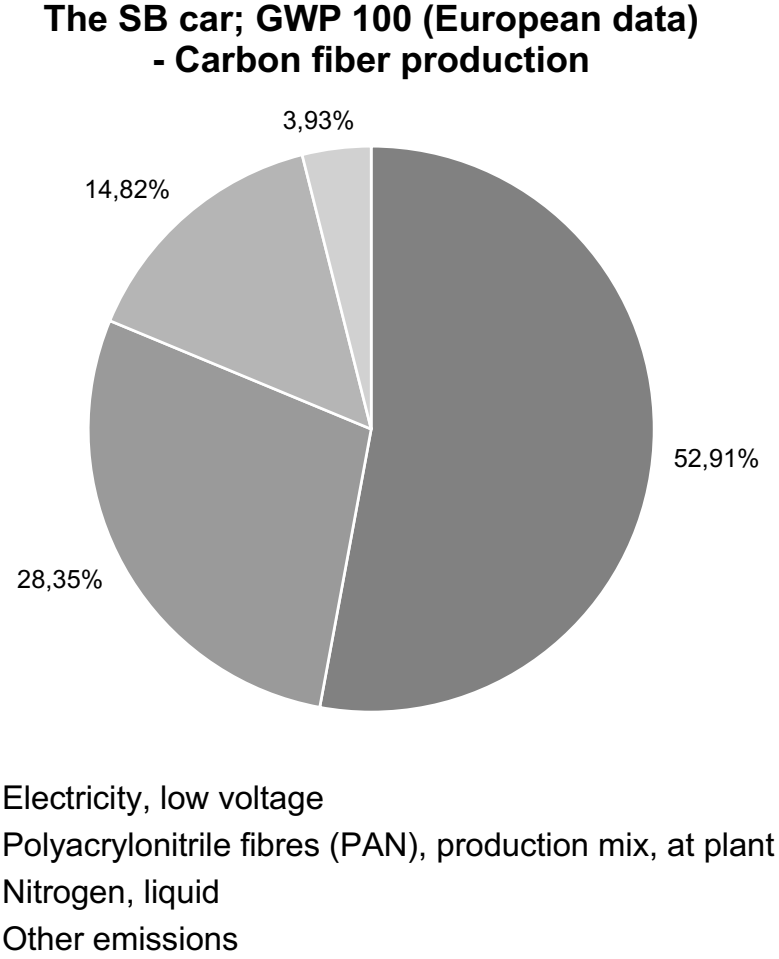

Figure D.1: Contribution graph for global warming potential of the carbon fiber production for the SB car based on European data. The result was achieved by an LCA where the inventory was based on a conceptual design of the vehicle. The functional unit included the function of the car components as well as the battery of the electric vehicle where the lifetime was set to 200,000 km.

D.2 Global data

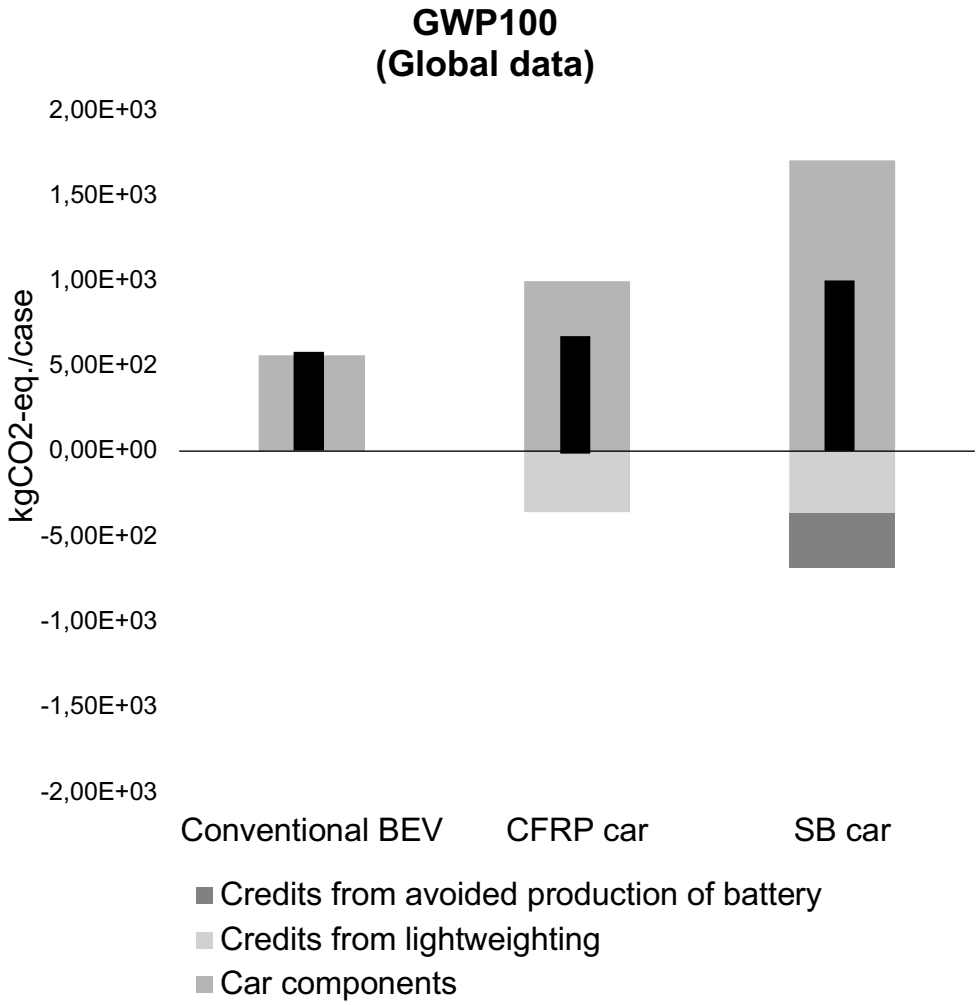

Figure D.2: Global warming potential of the three vehicles based on global data. Black bars shows the net climate impact. The result was achieved by an LCA where the inventory was based on a conceptual design of the three vehicles. The functional unit included the function of the car components as well as the battery of the electric vehicle where the lifetime was set to 200,000 km.

D.2.1 The conventional BEV

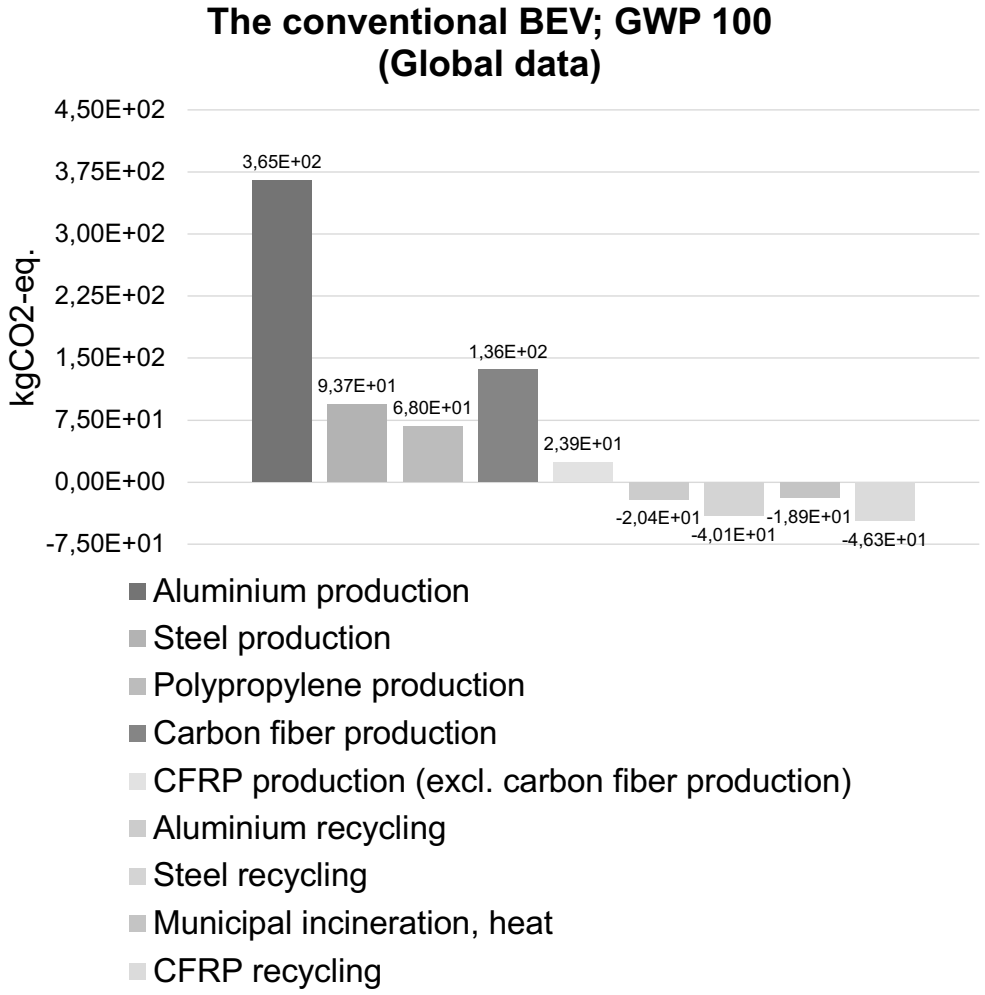

Figure D.3: Global warming potential per process for the conventional BEV based on global data. The result was achieved by an LCA where the inventory was based on a conceptual design of the vehicle. The functional unit included the function of the car components as well as the battery of the electric vehicle where the lifetime was set to 200,000 km.

D.2.2 The CFRP car

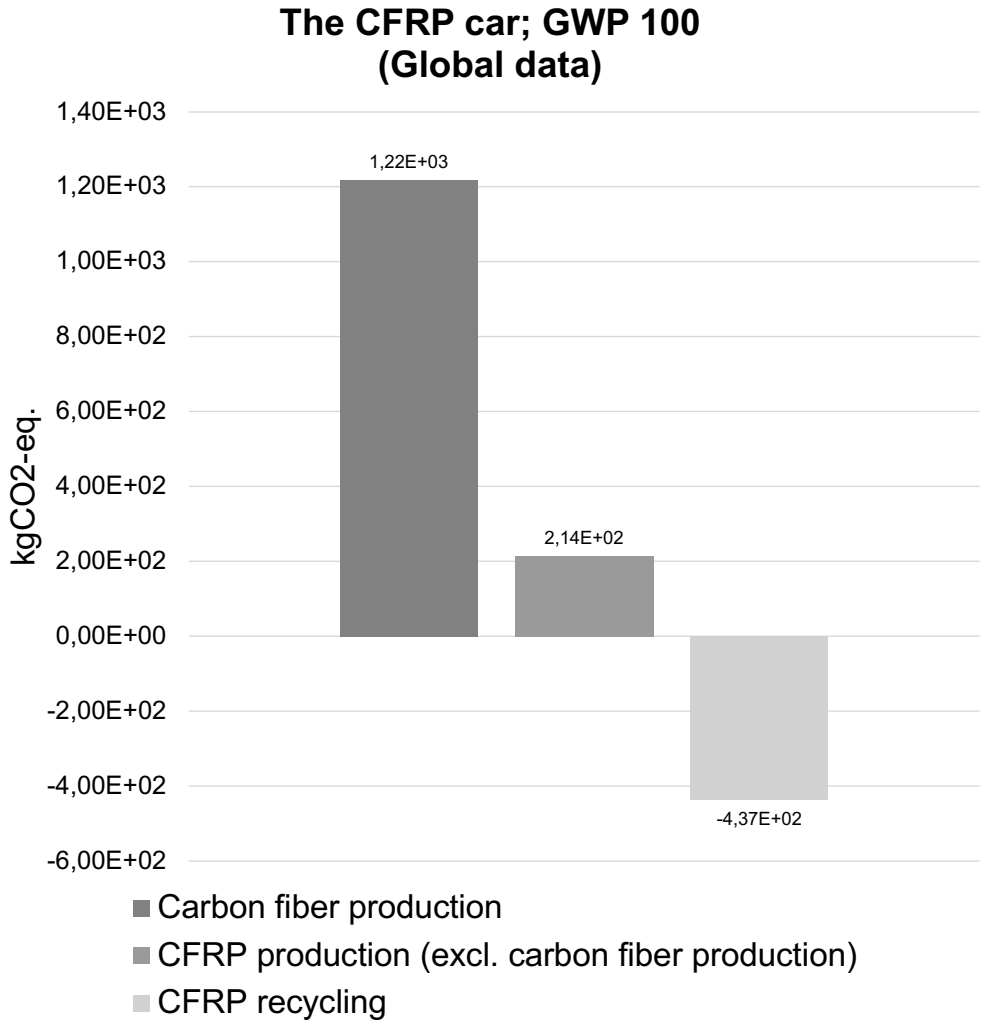

Figure D.4: Global warming potential per process for the CFRP car based on global data. The result was achieved by an LCA where the inventory was based on a conceptual design of the vehicle. The functional unit included the function of the car components as well as the battery of the electric vehicle where the lifetime was set to 200,000 km.

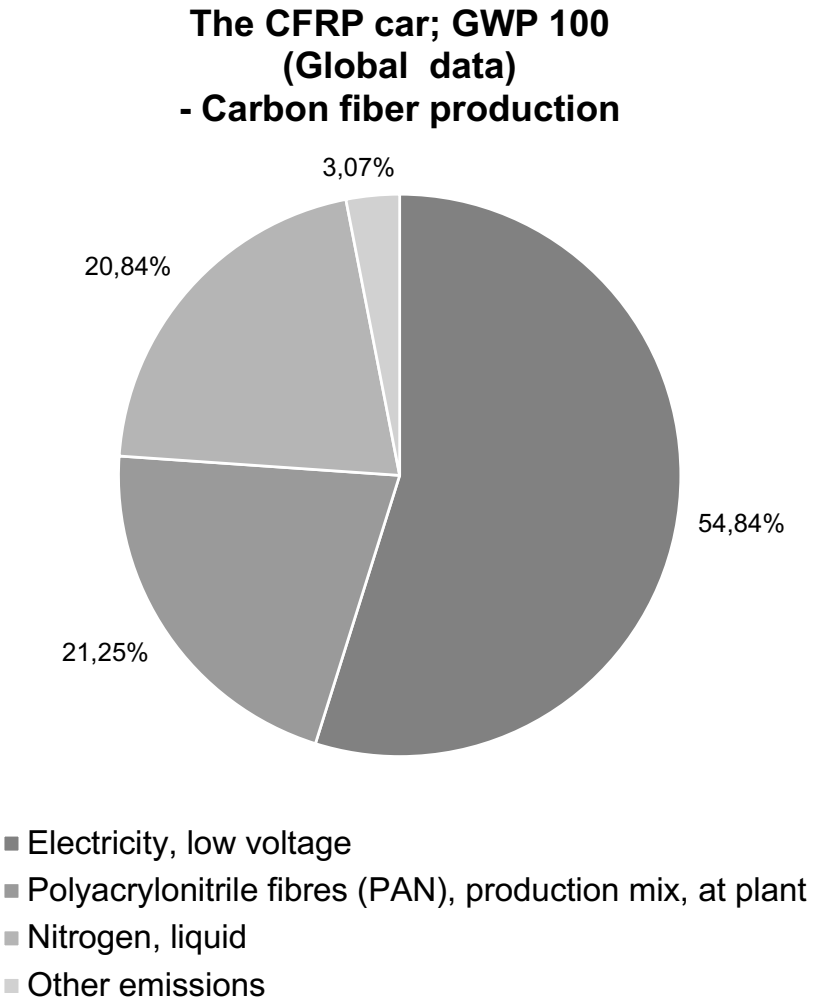

Figure D.5: Contribution graph for global warming potential of the carbon fiber production for the CRFP car based on global data. The result was achieved by an LCA where the inventory was based on a conceptual design of the vehicle. The functional unit included the function of the car components as well as the battery of the electric vehicle where the lifetime was set to 200,000 km.

D.2.3 The SB car

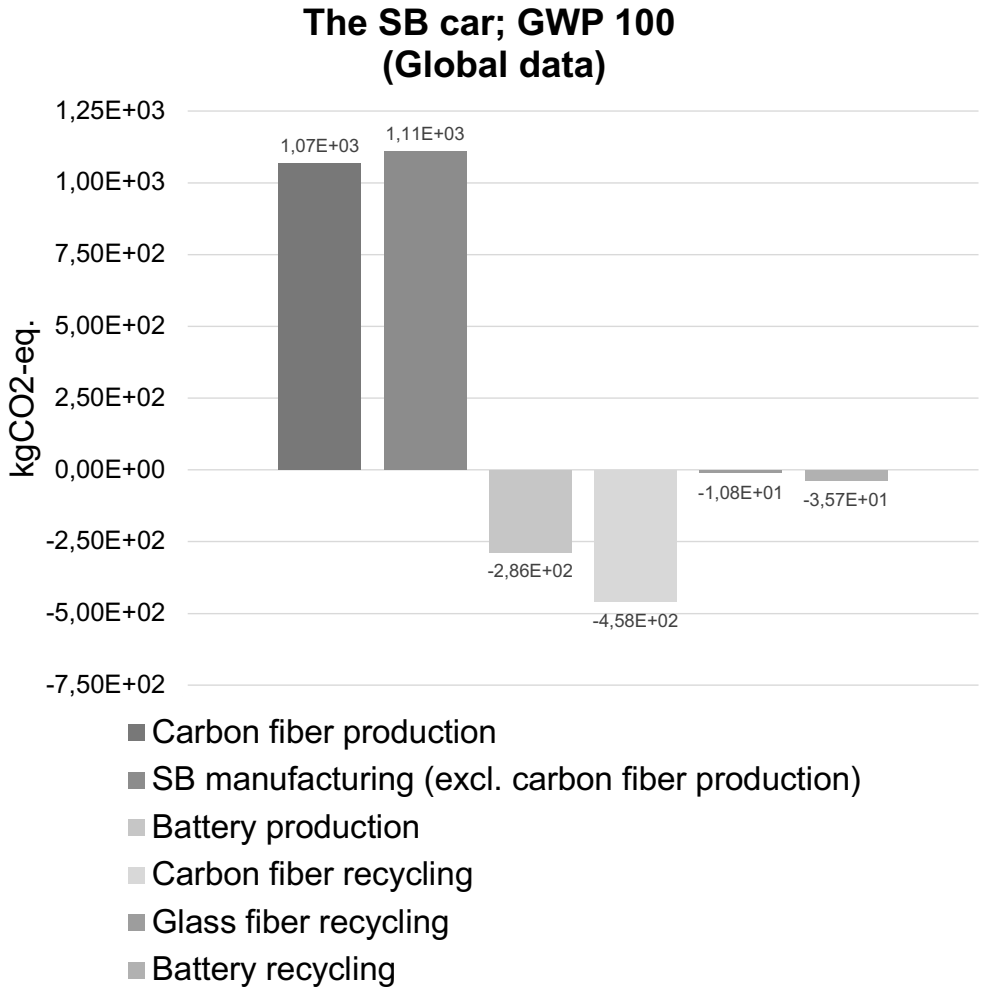

Figure D.6: Global warming potential per process for the SB car based on global data. The result was achieved by an LCA where the inventory was based on a conceptual design of the vehicle. The functional unit included the function of the car components as well as the battery of the electric vehicle where the lifetime was set to 200,000 km.

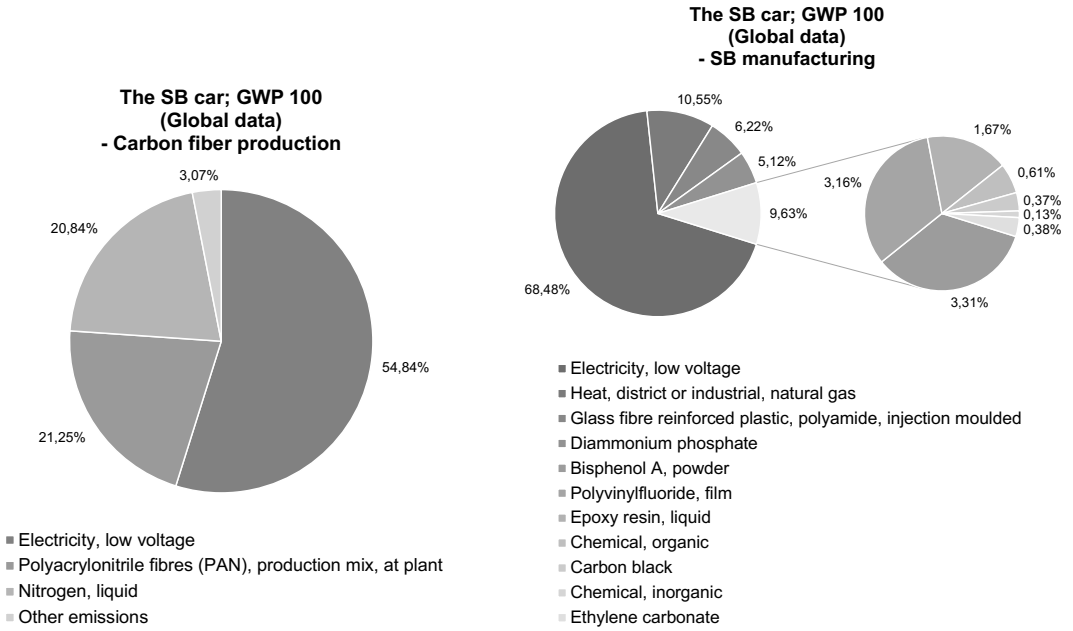

Figure D.7: Contribution graphs for global warming potential of the carbon fiber production and the SB manufacturing for the SB car based on global data. The result was achieved by an LCA where the inventory was based on a conceptual design of the vehicle. The functional unit included the function of the car components as well as the battery of the electric vehicle where the lifetime was set to 200,000 km.

D.3 Swedish data

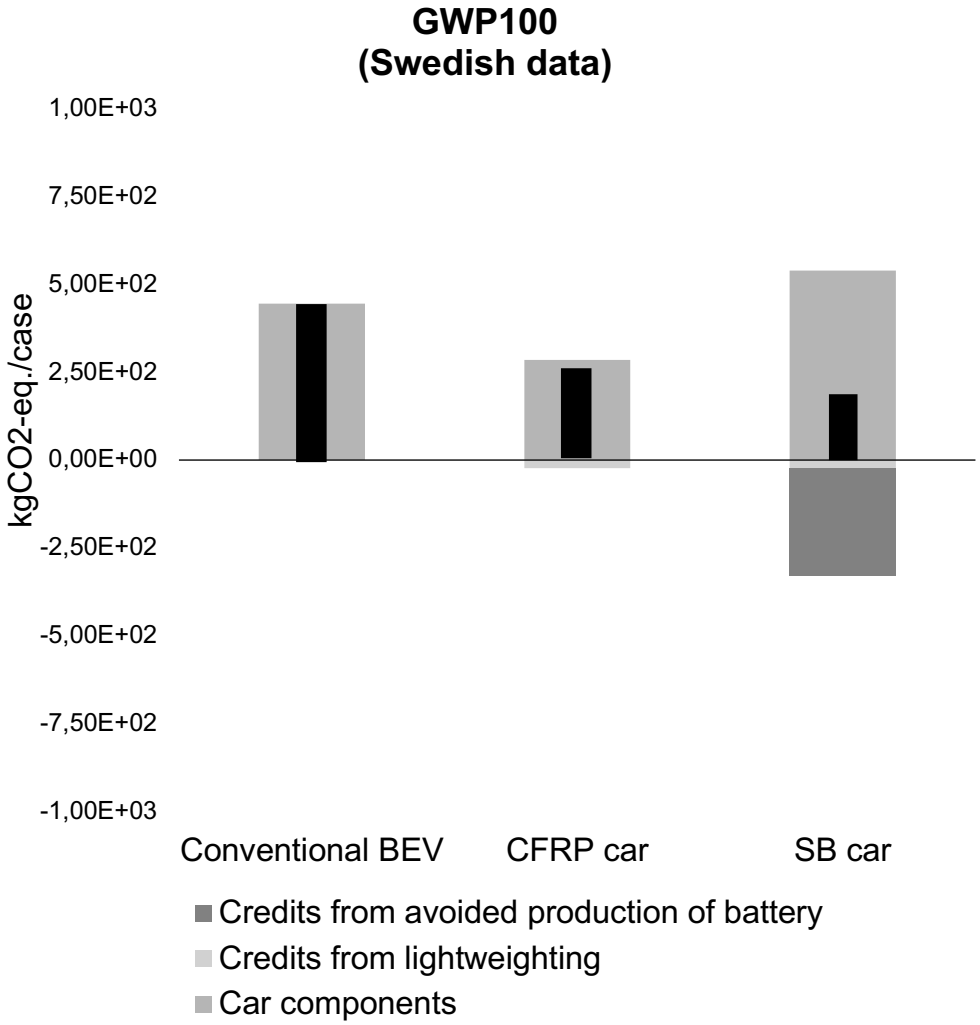

Figure D.8: Global warming potential of the three vehicles based on Swedish data. Black bars shows the net climate impact. The result was achieved by an LCA where the inventory was based on a conceptual design of the vehicles. The functional unit included the function of the car components as well as the battery of the electric vehicle where the lifetime was set to 200,000 km.

D.3.1 The conventional BEV

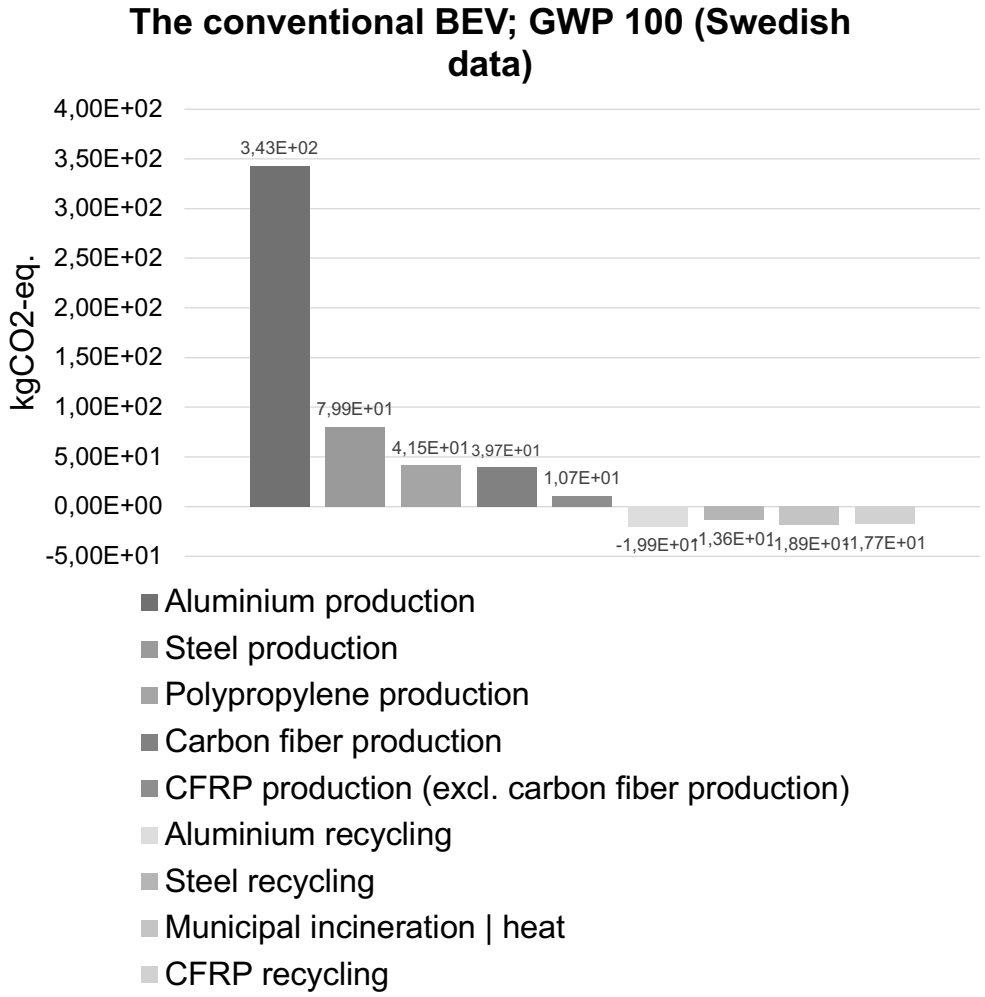

Figure D.9: Global warming potential per process for the conventional BEV based on Swedish data. The result was achieved by an LCA where the inventory was based on a conceptual design of the vehicle. The functional unit included the function of the car components as well as the battery of the electric vehicle where the lifetime was set to 200,000 km.

D.3.2 The CFRP car

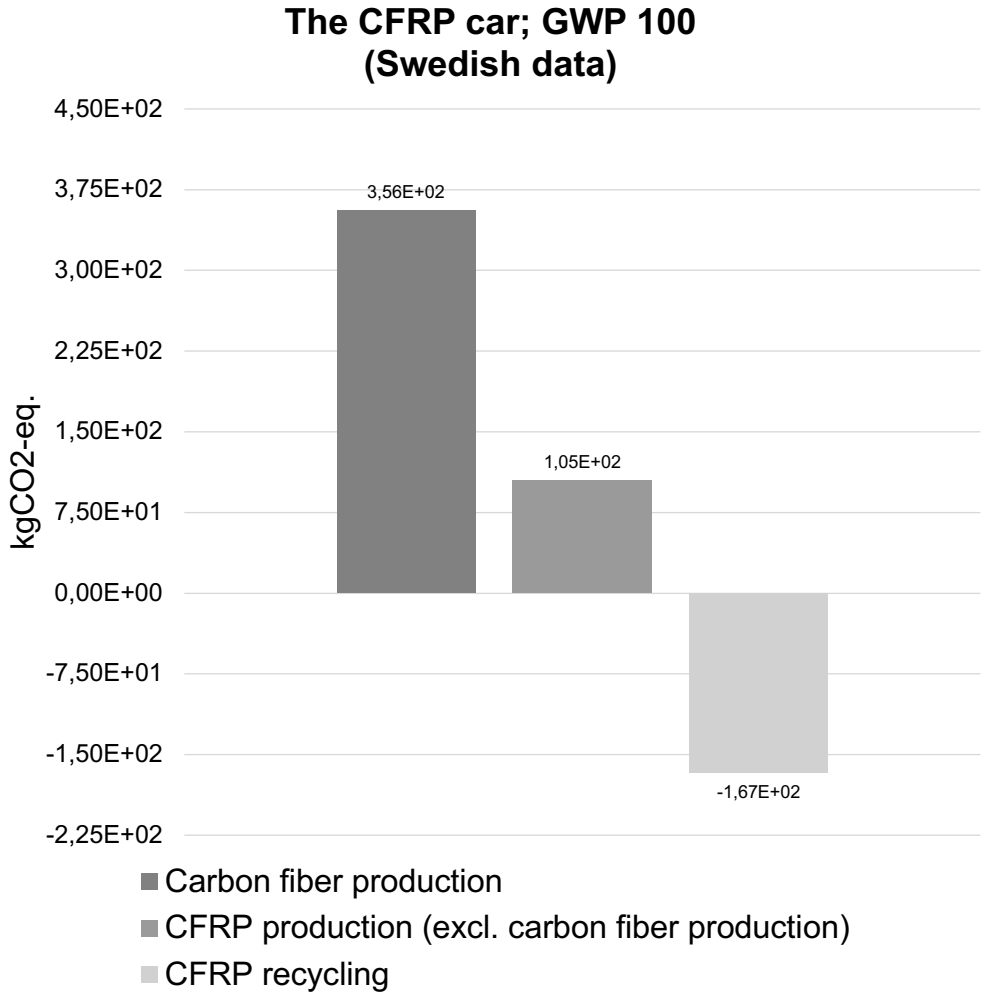

Figure D.10: Global warming potential per process for the CFRP car based on Swedish data. The result was achieved by an LCA where the inventory was based on a conceptual design of the vehicle. The functional unit included the function of the car components as well as the battery of the electric vehicle where the lifetime was set to 200,000 km.

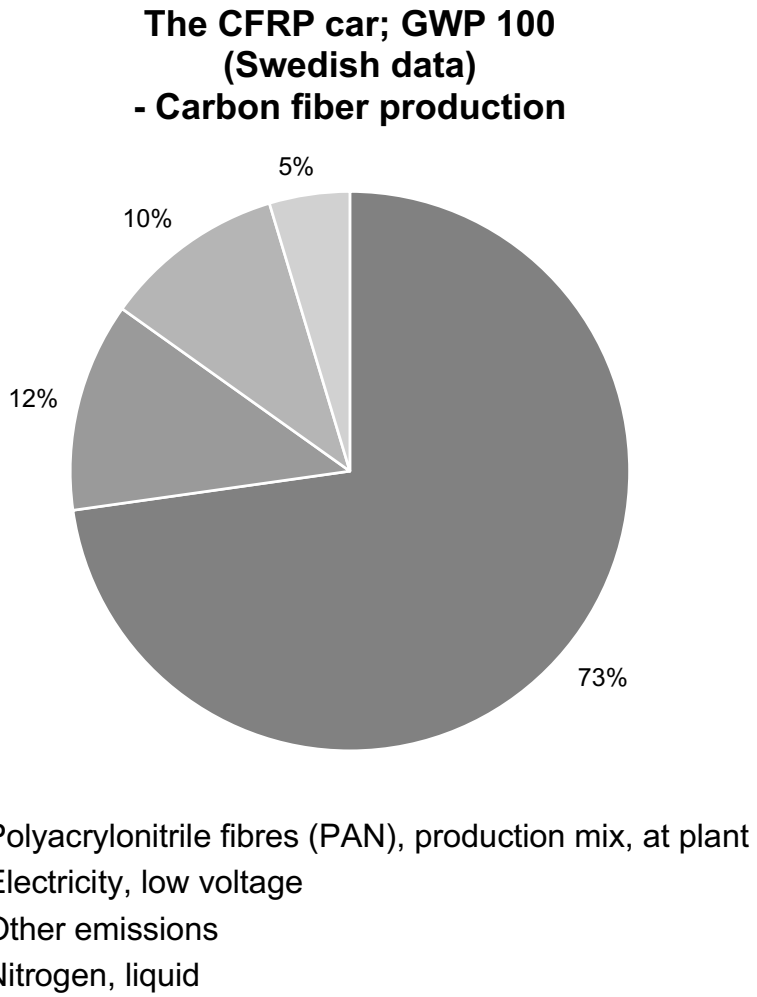

Figure D.11: Contribution graph for global warming potential of the carbon fiber production for the CRFP car based on Swedish data. The result was achieved by an LCA where the inventory was based on a conceptual design of the vehicle. The functional unit included the function of the car components as well as the battery of the electric vehicle where the lifetime was set to 200,000 km.

D.3.3 The SB car

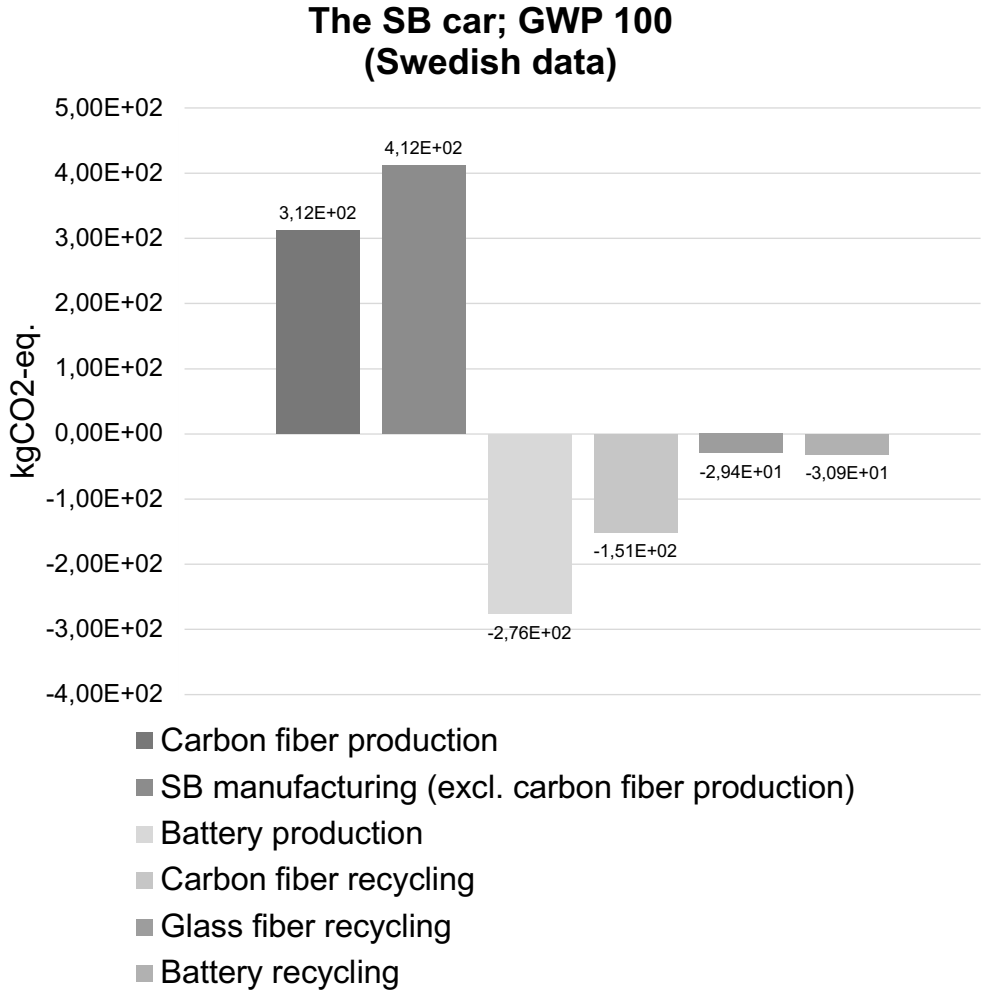

Figure D.12: Global warming potential per process for the SB car based on Swedish data. The result was achieved by an LCA where the inventory was based on a conceptual design of the vehicle. The functional unit included the function of the car components as well as the battery of the electric vehicle where the lifetime was set to 200,000 km.

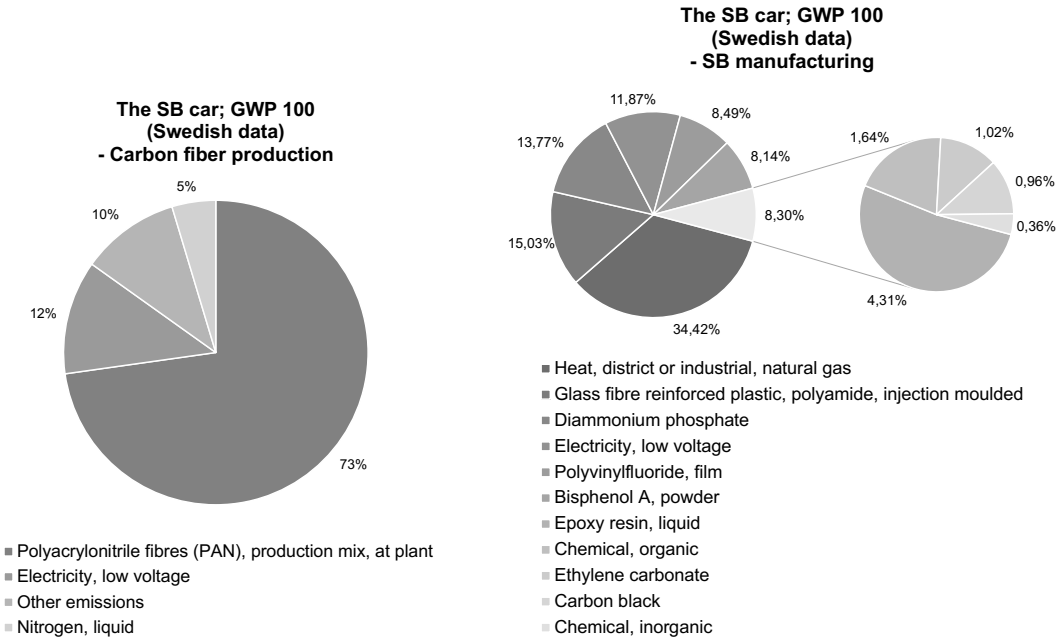

Figure D.13: Contribution graphs for global warming potential of the carbon fiber production and the SB manufacturing for the SB car based on Swedish data. The result was achieved by an LCA where the inventory was based on a conceptual design of the vehicle. The functional unit included the function of the car components as well as the battery of the electric vehicle where the lifetime was set to 200,000 km.

E

Crustal Scarcity Indicator

E.1 European data

E.1.1 The SB car

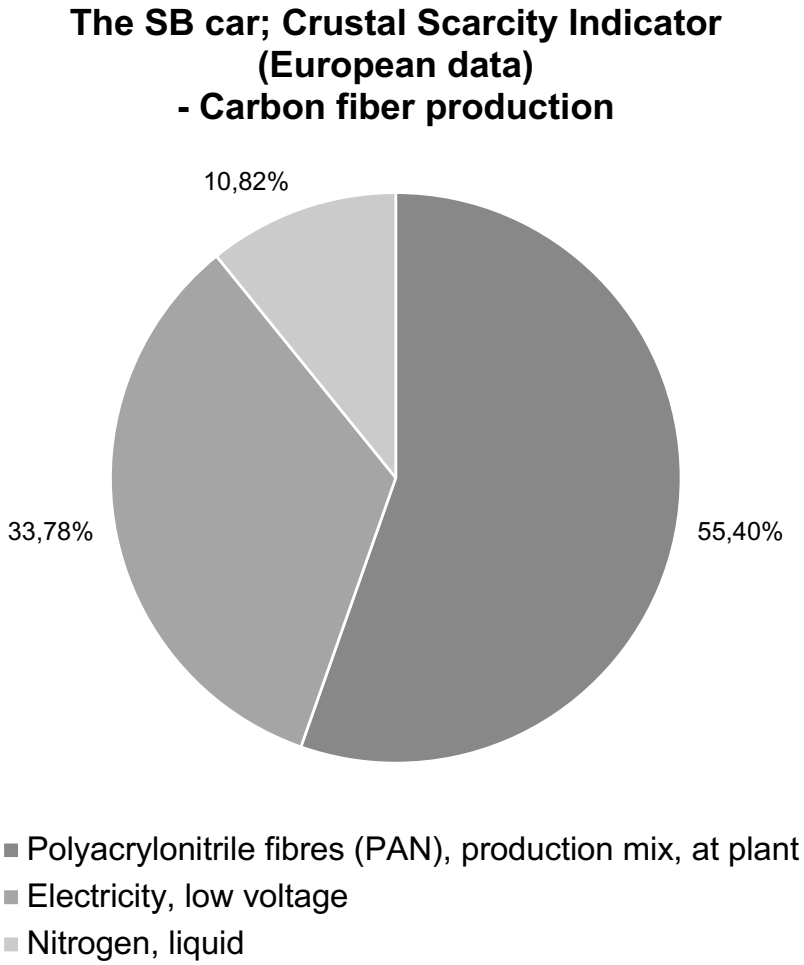

Figure E.1: Contribution graph for crustal scarcity indicator of the carbon fiber production for the SB car based on European data. The result was achieved by an LCA where the inventory was based on a conceptual design of the vehicle. The functional unit included the function of the car components as well as the battery of the electric vehicle where the lifetime was set to 200,000 km.

E.2 Global Data

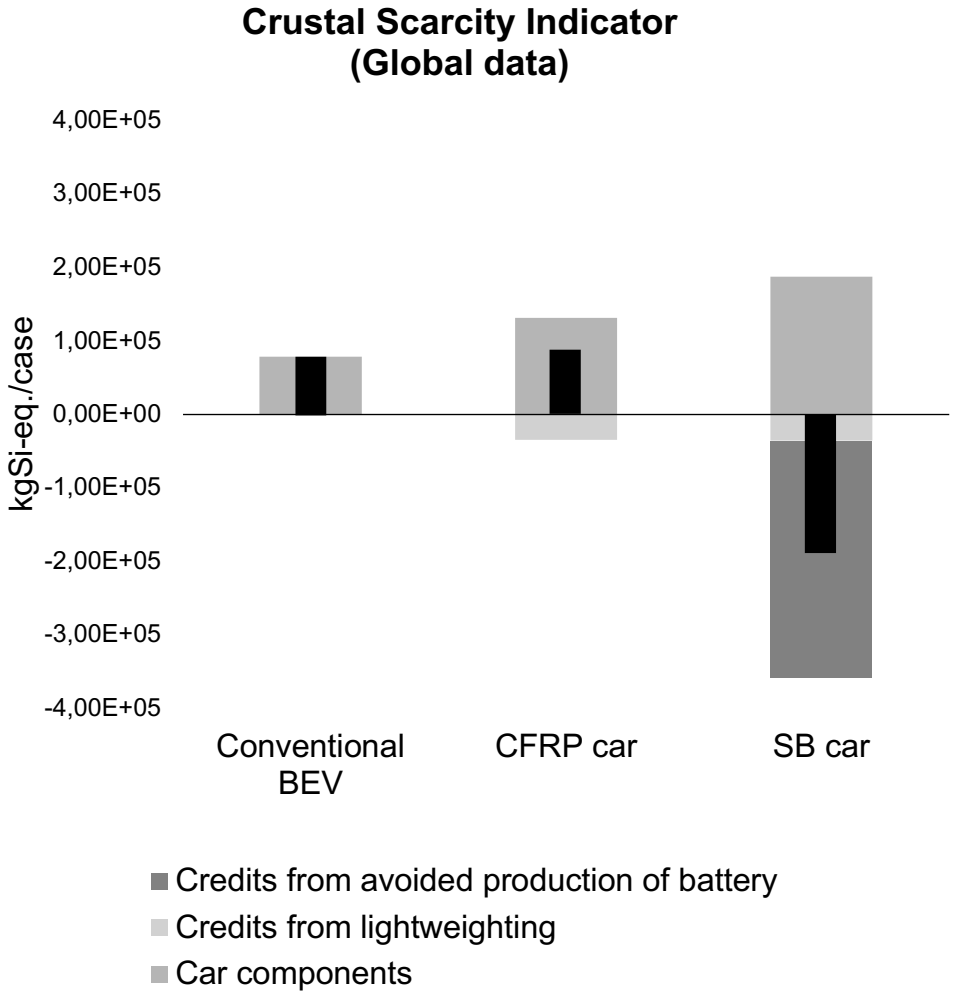

Figure E.2: Crustal scarcity impact of the three vehicles based on global data. Black bars shows the net climate impact. The result was achieved by an LCA where the inventory was based on a conceptual design of the vehicles. The functional unit included the function of the car components as well as the battery of the electric vehicle where the lifetime was set to 200,000 km.

E.2.1 The conventional BEV

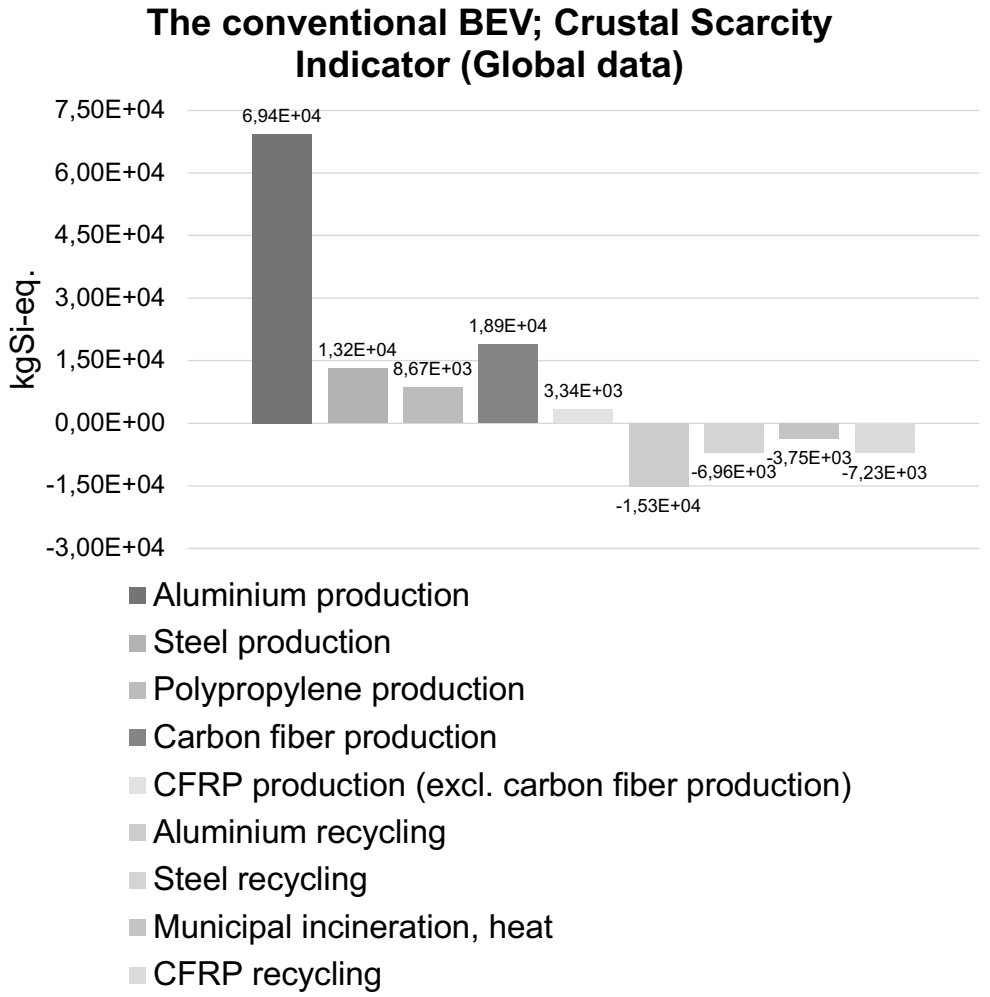

Figure E.3: Crustal scarcity impact per process for the conventional BEV based on global data. The result was achieved by an LCA where the inventory was based on a conceptual design of the vehicle. The functional unit included the function of the car components as well as the battery of the electric vehicle where the lifetime was set to 200,000 km.

E.2.2 The CFRP car

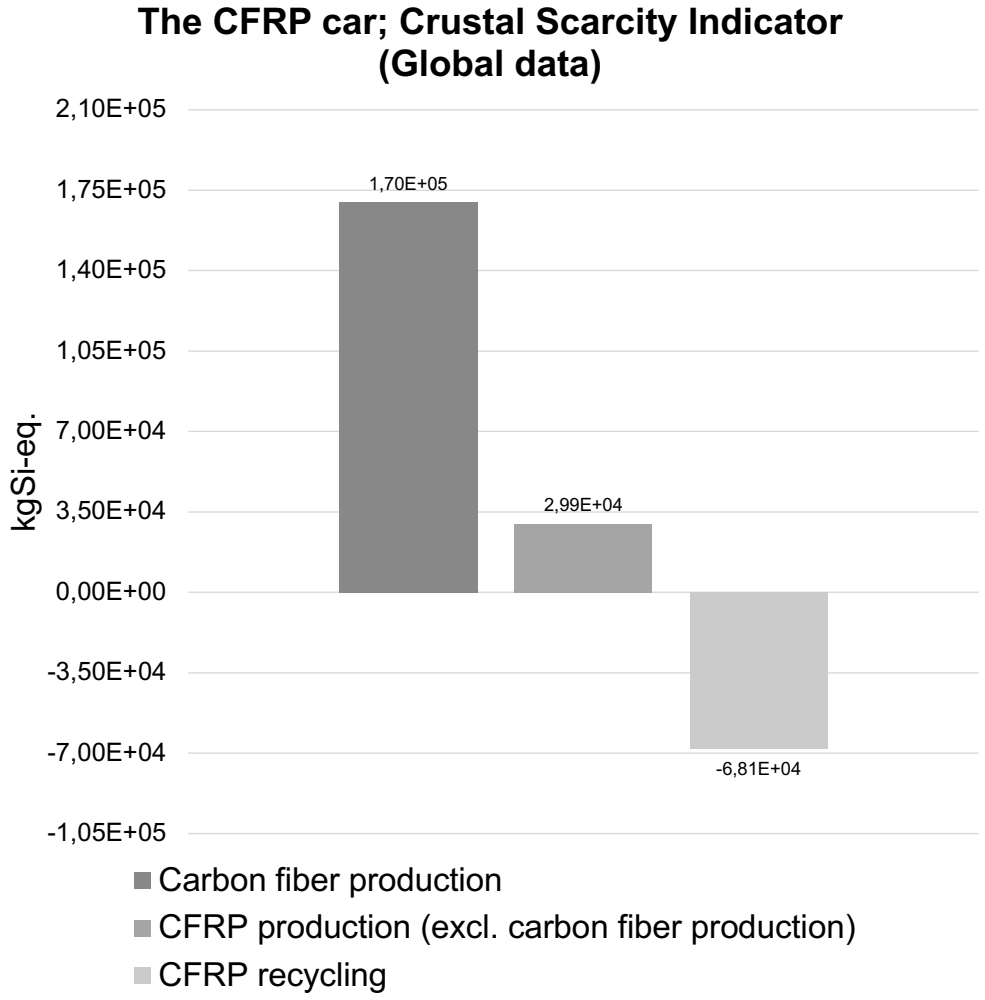

Figure E.4: Crustal scarcity impact per process for the CFRP car based on global data. The result was achieved by an LCA where the inventory was based on a conceptual design of the vehicle. The functional unit included the function of the car components as well as the battery of the electric vehicle where the lifetime was set to 200,000 km.

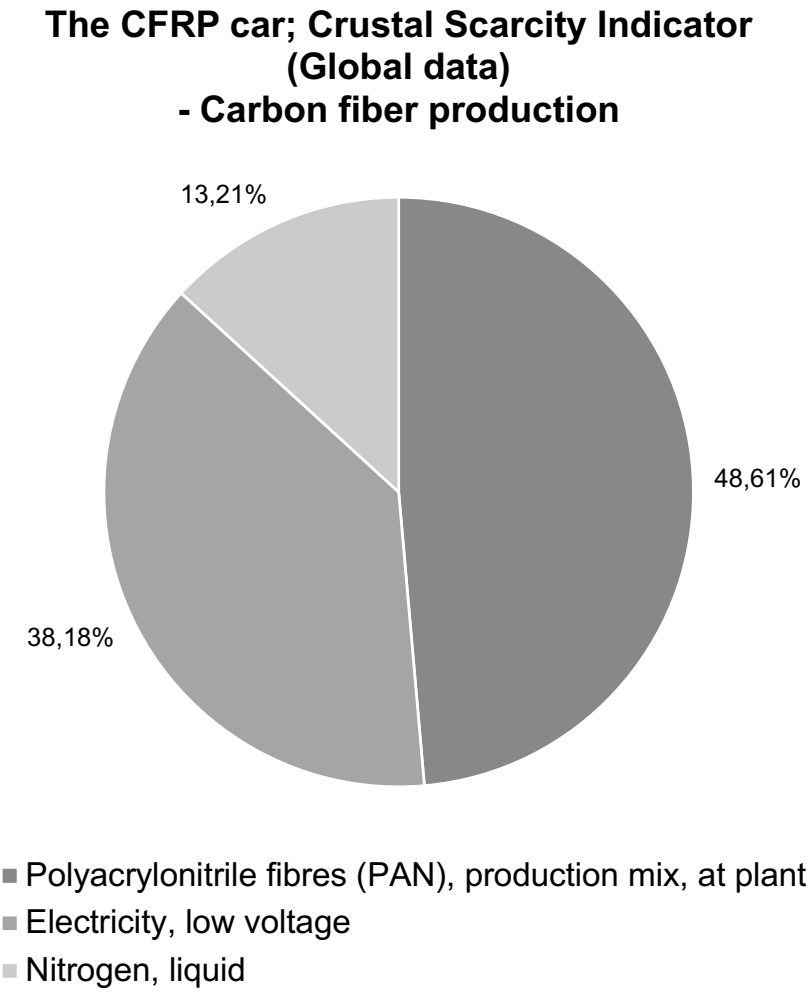

Figure E.5: Contribution graph for crustal scarcity indicator of the carbon fiber production for the CRFP car based on global data. The result was achieved by an LCA where the inventory was based on a conceptual design of the vehicle. The functional unit included the function of the car components as well as the battery of the electric vehicle where the lifetime was set to 200,000 km.

E.2.3 The SB Car

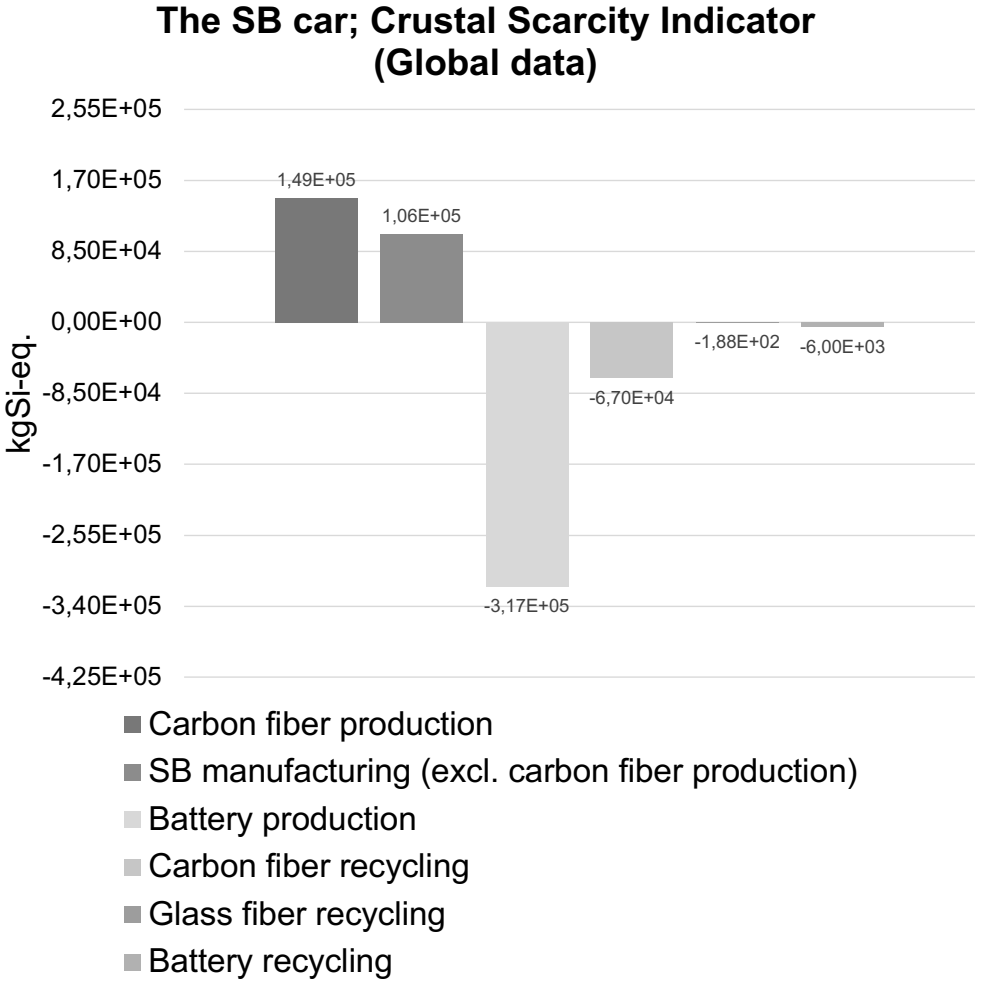

Figure E.6: Crustal scarcity impact per process for the SB car based on global data. The result was achieved by an LCA where the inventory was based on a conceptual design of the vehicle. The functional unit included the function of the car components as well as the battery of the electric vehicle where the lifetime was set to 200,000 km.

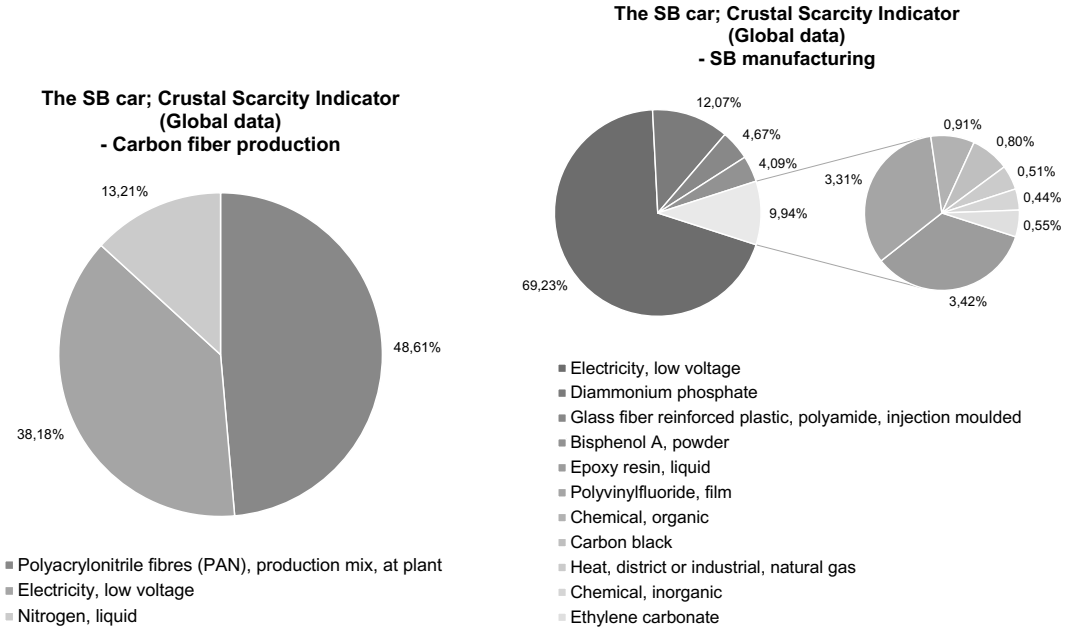

Figure E.7: Contribution graphs for crustal scarcity indicator of the carbon fiber production and the SB manufacturing for the SB car based on global data. The result was achieved by an LCA where the inventory was based on a conceptual design of the vehicle. The functional unit included the function of the car components as well as the battery of the electric vehicle where the lifetime was set to 200,000 km.

E.3 Swedish Data

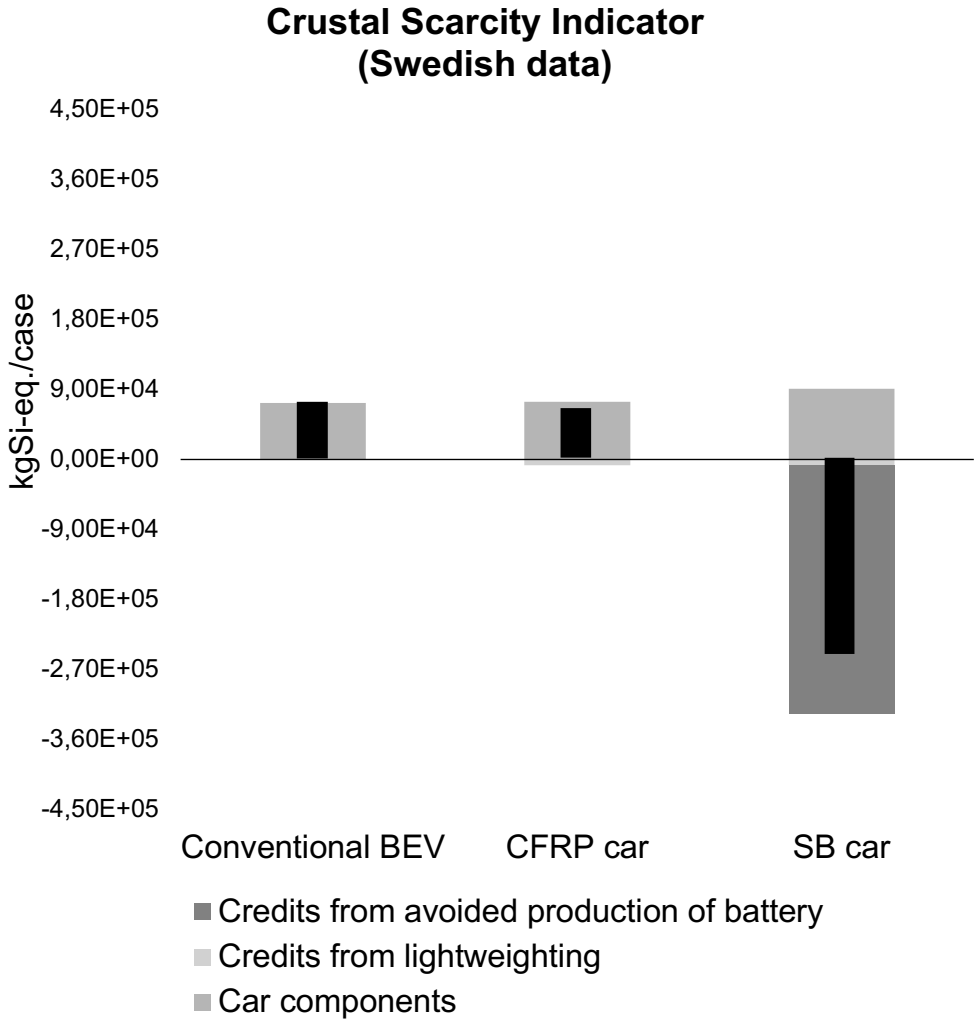

Figure E.8: Crustal scarcity impact of the three vehicles based on Swedish data. Black bars shows the net climate impact. The result was achieved by an LCA where the inventory was based on a conceptual design of the vehicles. The functional unit included the function of the car components as well as the battery of the electric vehicle where the lifetime was set to 200,000 km.

E.3.1 The conventional BEV

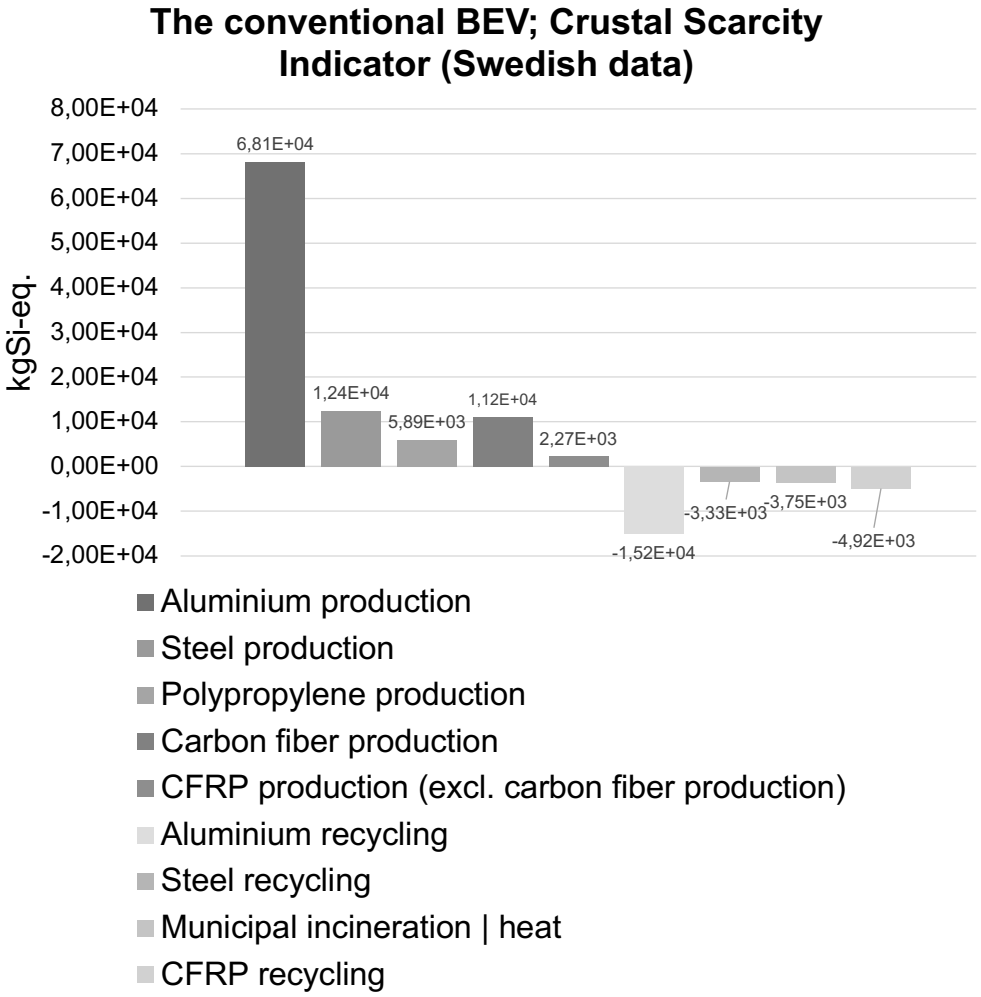

Figure E.9: Crustal scarcity impact per process for the conventional BEV based on Swedish data. The result was achieved by an LCA where the inventory was based on a conceptual design of the vehicle. The functional unit included the function of the car components as well as the battery of the electric vehicle where the lifetime was set to 200,000 km.

E.3.2 The CFRP car

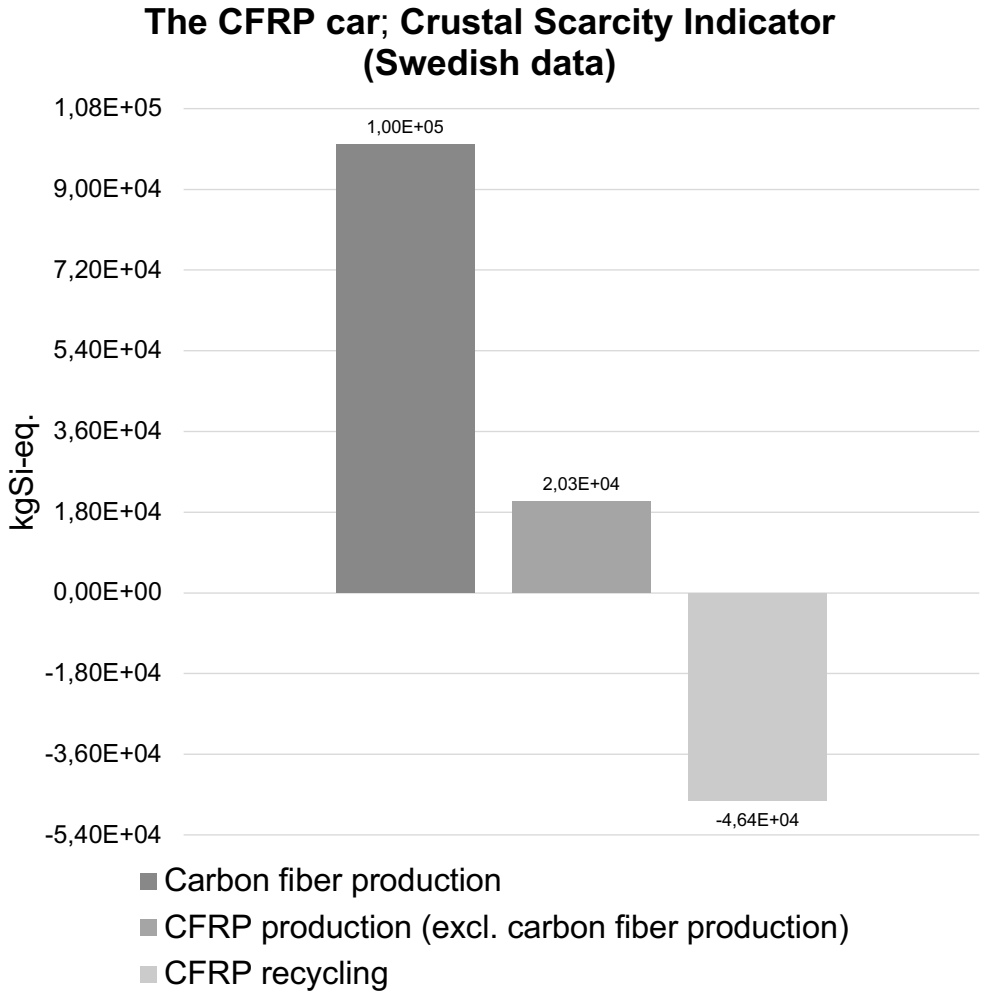

Figure E.10: Crustal scarcity impact per process for the CFRP car based on Swedish data. The result was achieved by an LCA where the inventory was based on a conceptual design of the vehicle. The functional unit included the function of the car components as well as the battery of the electric vehicle where the lifetime was set to 200,000 km.

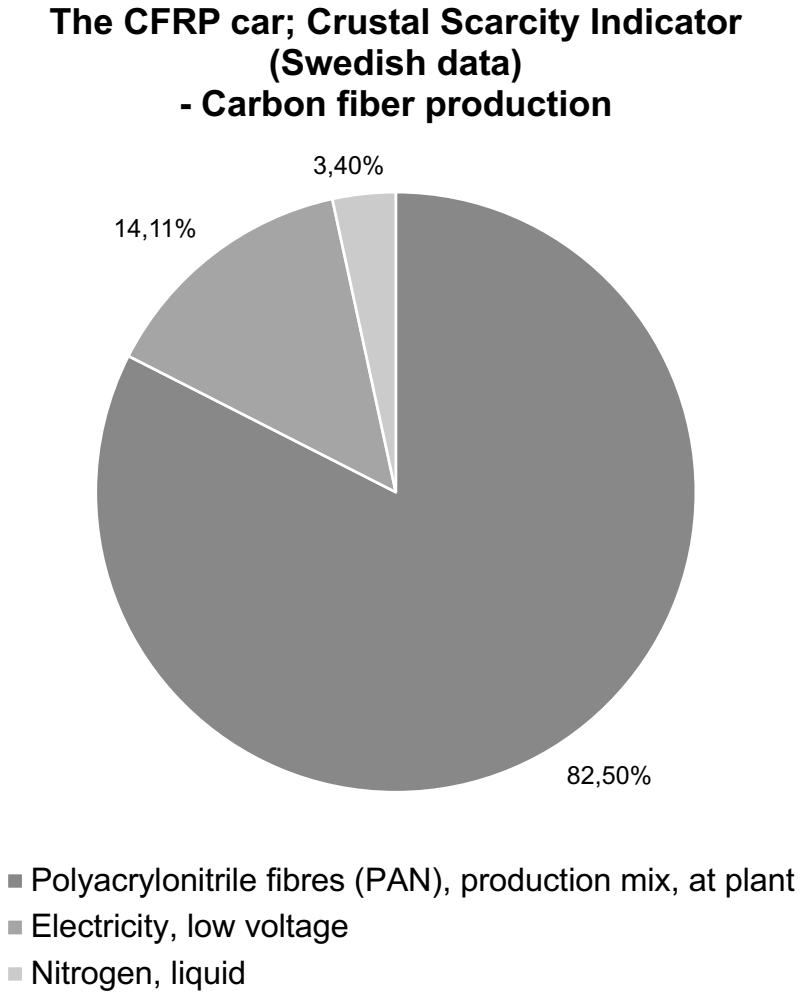

Figure E.11: Contribution graph for crustal scarcity indicator of the carbon fiber production for the CRFP car based on Swedish data. The result was achieved by an LCA where the inventory was based on a conceptual design of the vehicle. The functional unit included the function of the car components as well as the battery of the electric vehicle where the lifetime was set to 200,000 km.

E.3.3 The SB Car

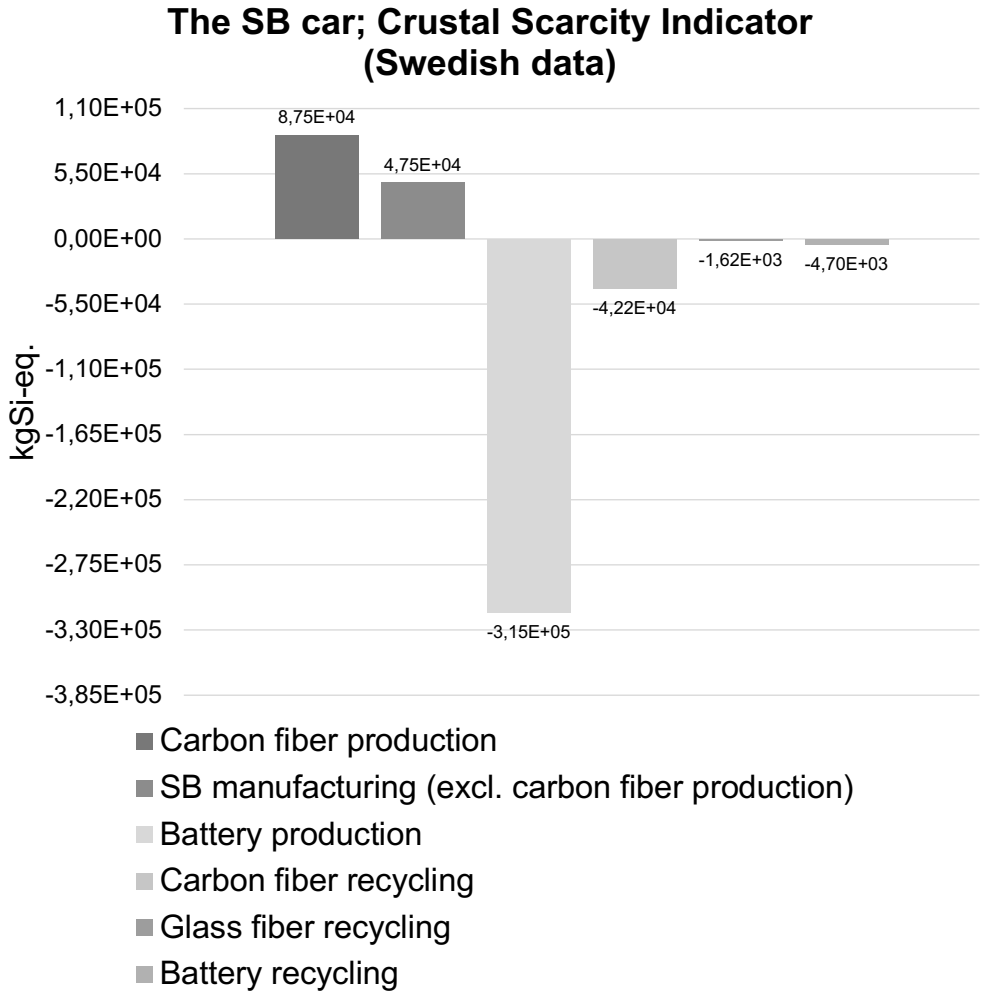

Figure E.12: Crustal scarcity impact per process for the SB car based on Swedish data. The result was achieved by an LCA where the inventory was based on a conceptual design of the vehicle. The functional unit included the function of the car components as well as the battery of the electric vehicle where the lifetime was set to 200,000 km.

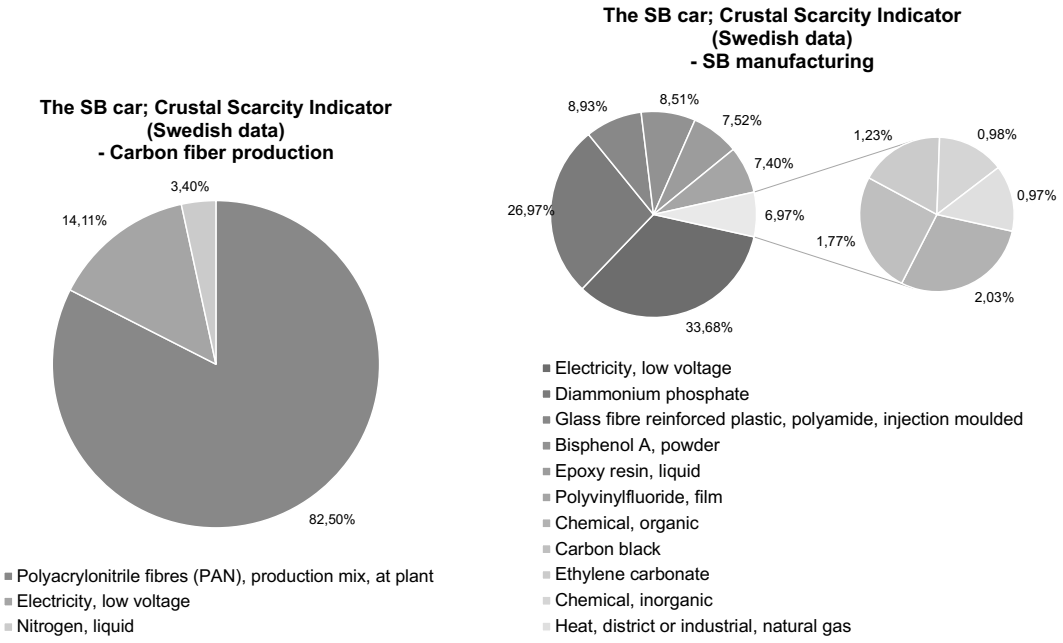

Figure E.13: Contribution graphs for crustal scarcity indicator of the carbon fiber production and the SB manufacturing based on Swedish data. The result was achieved by an LCA where the inventory was based on a conceptual design of the vehicle. The functional unit included the function of the car components as well as the battery of the electric vehicle where the lifetime was set to 200,000 km.

F

Cumulative Energy Demand

F.1 European data

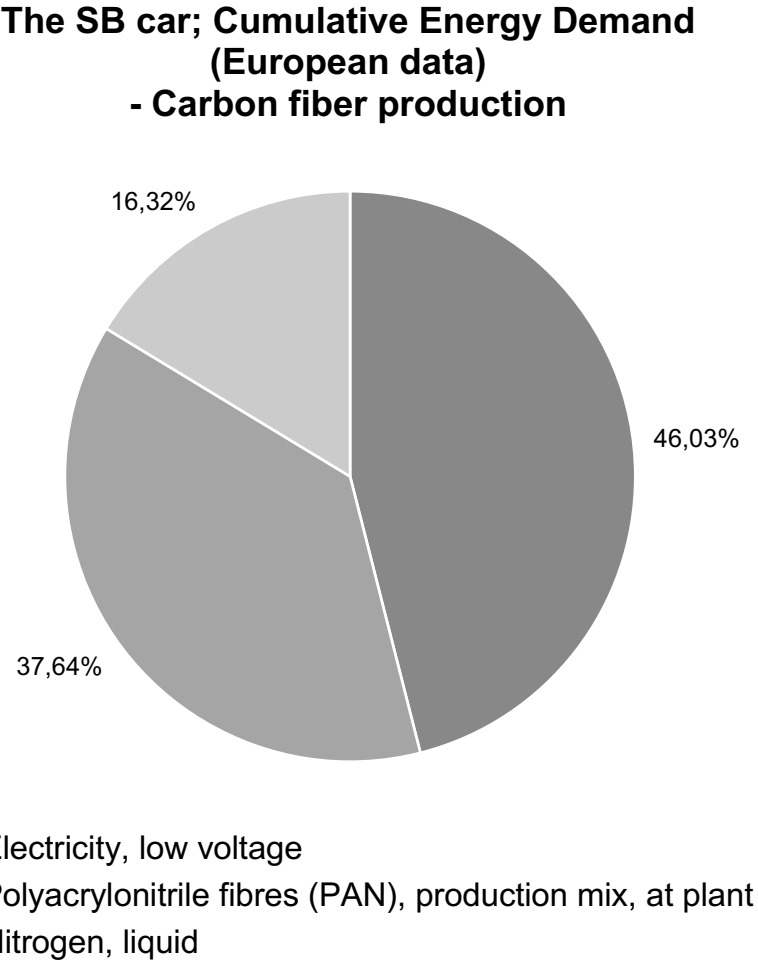

Figure F.1: Contribution graph for cumulative energy demand of the carbon fiber production for the SB car based on European data. The result was achieved by an LCA where the inventory was based on a conceptual design of the vehicle. The functional unit included the function of the car components as well as the battery of the electric vehicle where the lifetime was set to 200,000 km.

F.2 Global Data

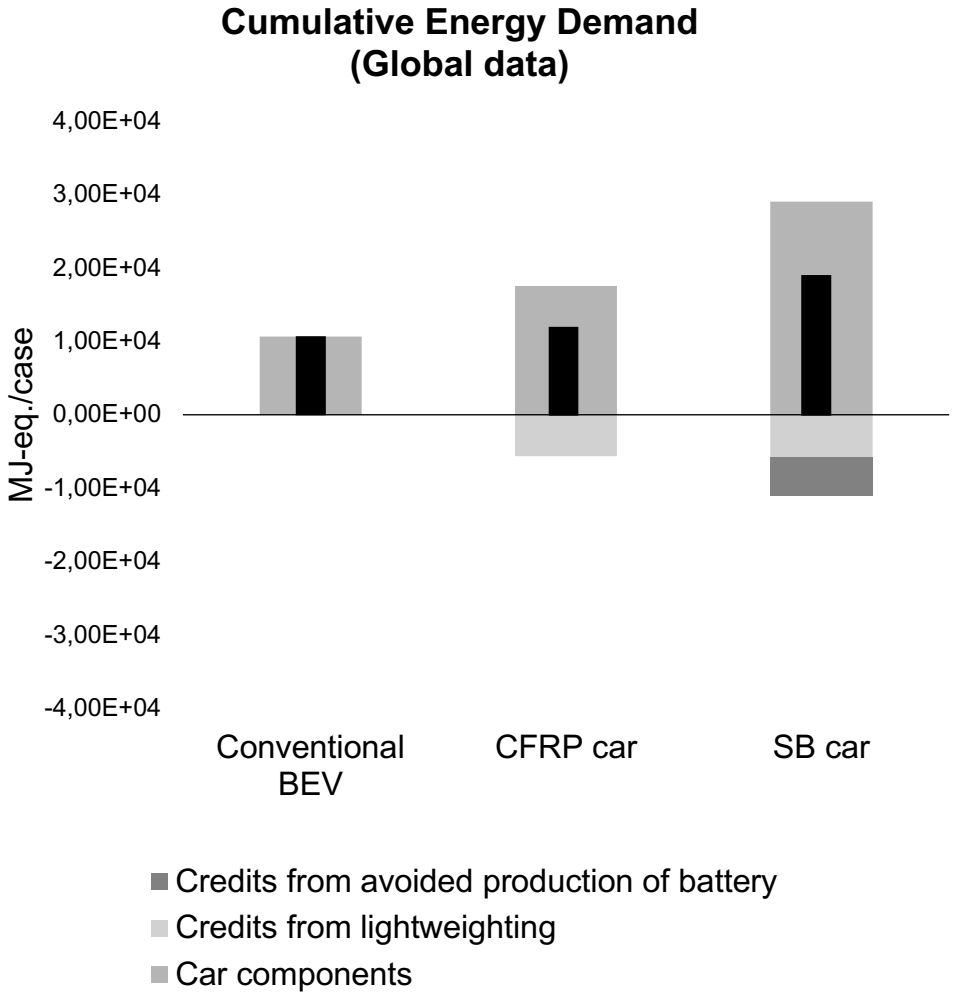

Figure F.2: Cumulative energy demand of the three vehicles based on global data. Black bars shows the net climate impact. The result was achieved by an LCA where the inventory was based on a conceptual design of the vehicles. The functional unit included the function of the car components as well as the battery of the electric vehicle where the lifetime was set to 200,000 km.

F.2.1 The conventional BEV

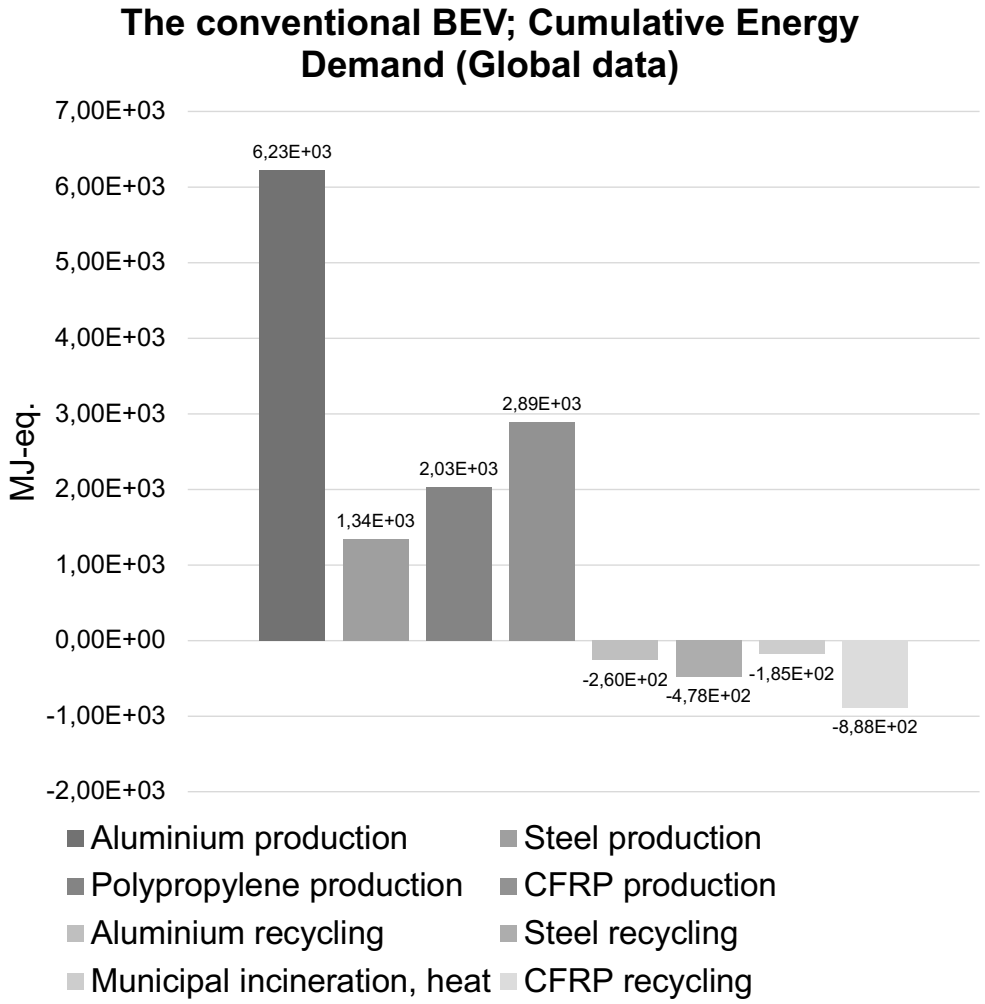

Figure F.3: Cumulative energy demand per process for the conventional BEV based on global data. The result was achieved by an LCA where the inventory was based on a conceptual design of the vehicle. The functional unit included the function of the car components as well as the battery of the electric vehicle where the lifetime was set to 200,000 km.

F.2.2 The CFRP car

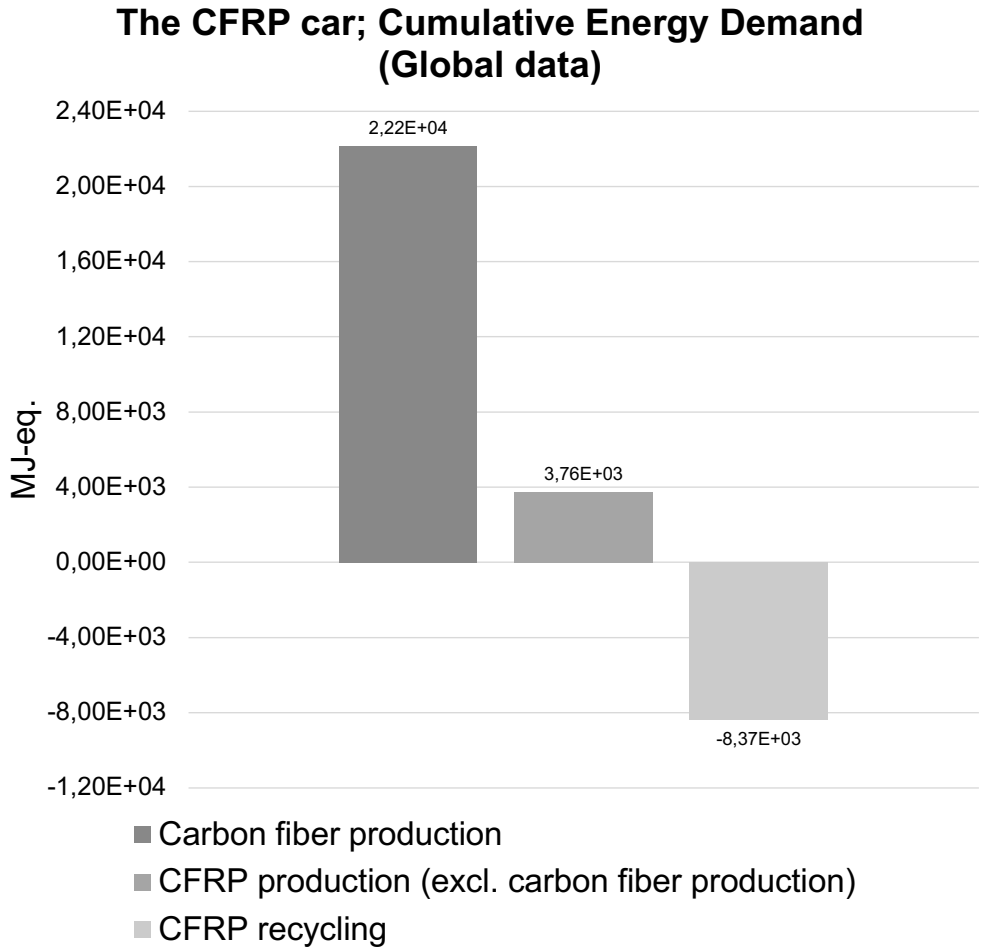

Figure F.4: Cumulative energy demand per process for the CFRP car based on global data. The result was achieved by an LCA where the inventory was based on a conceptual design of the vehicle. The functional unit included the function of the car components as well as the battery of the electric vehicle where the lifetime was set to 200,000 km.

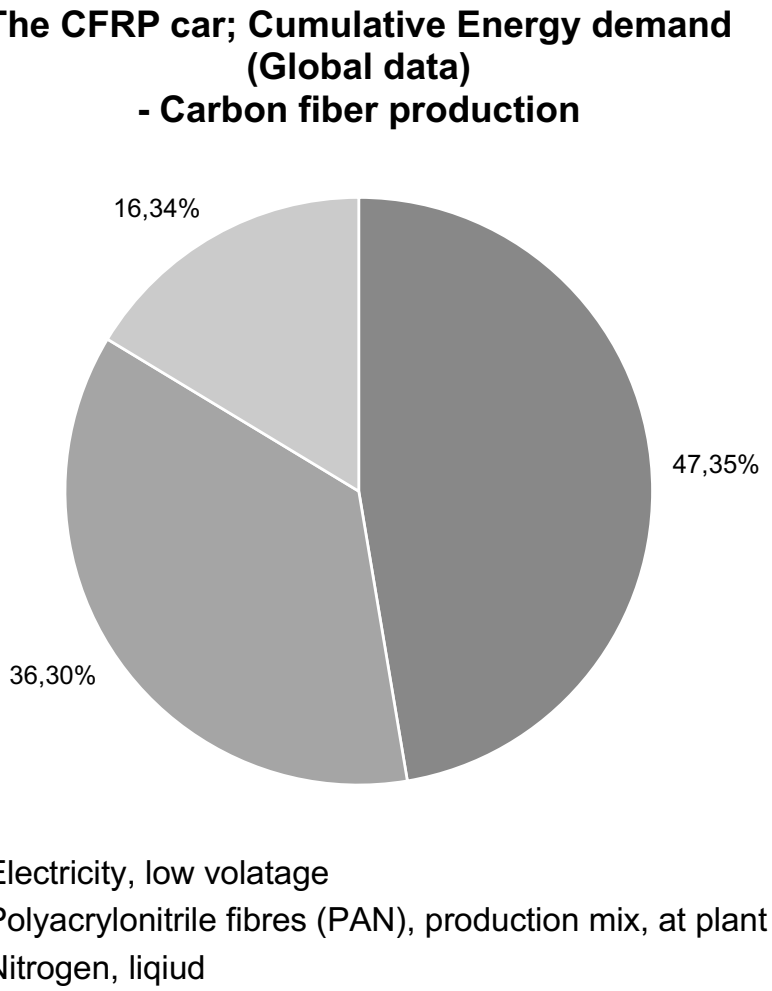

Figure F.5: Contribution graph for cumulative energy demand of the carbon fiber production for the CRFP car based on global data. The result was achieved by an LCA where the inventory was based on a conceptual design of the vehicle. The functional unit included the function of the car components as well as the battery of the electric vehicle where the lifetime was set to 200,000 km.

F.2.3 The SB Car

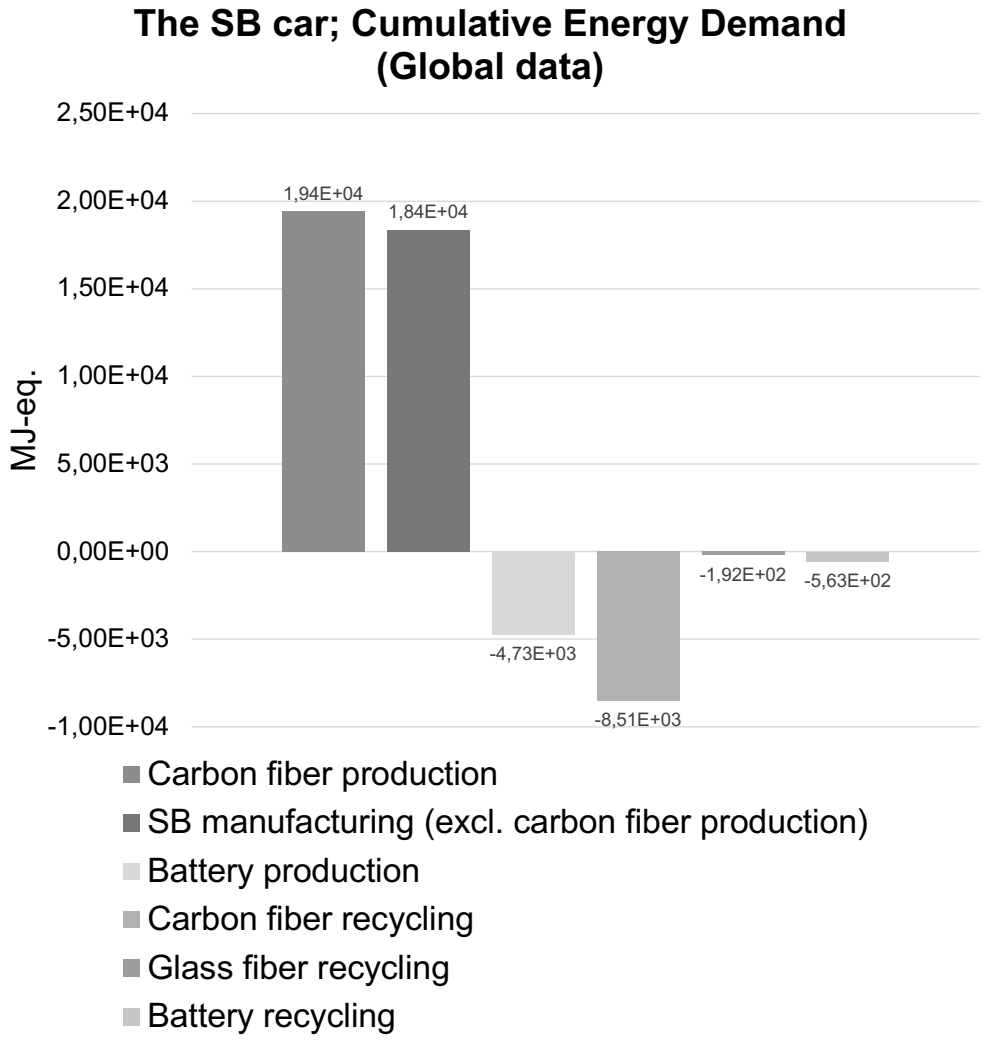

Figure F.6: Cumulative energy demand per process for the SB car based on global data. The result was achieved by an LCA where the inventory was based on a conceptual design of the vehicle. The functional unit included the function of the car components as well as the battery of the electric vehicle where the lifetime was set to 200,000 km.

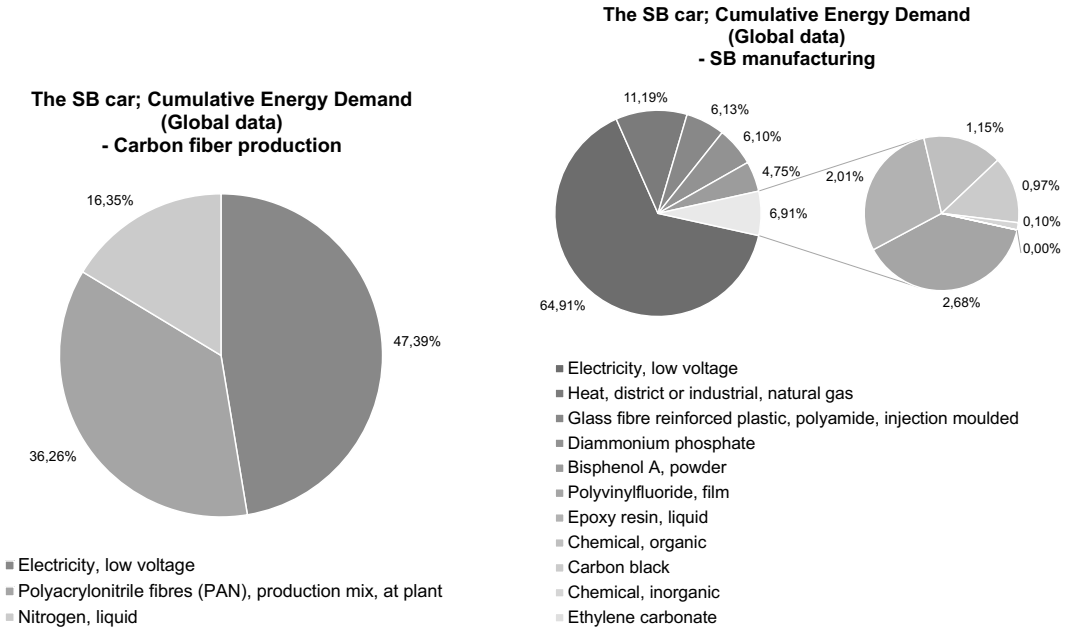

Figure F.7: Contribution graphs for cumulative energy demand of the carbon fiber production and the SB manufacturing for the SB car based on global data. The result was achieved by an LCA where the inventory was based on a conceptual design of the vehicle. The functional unit included the function of the car components as well as the battery of the electric vehicle where the lifetime was set to 200,000 km.

F.3 Swedish Data

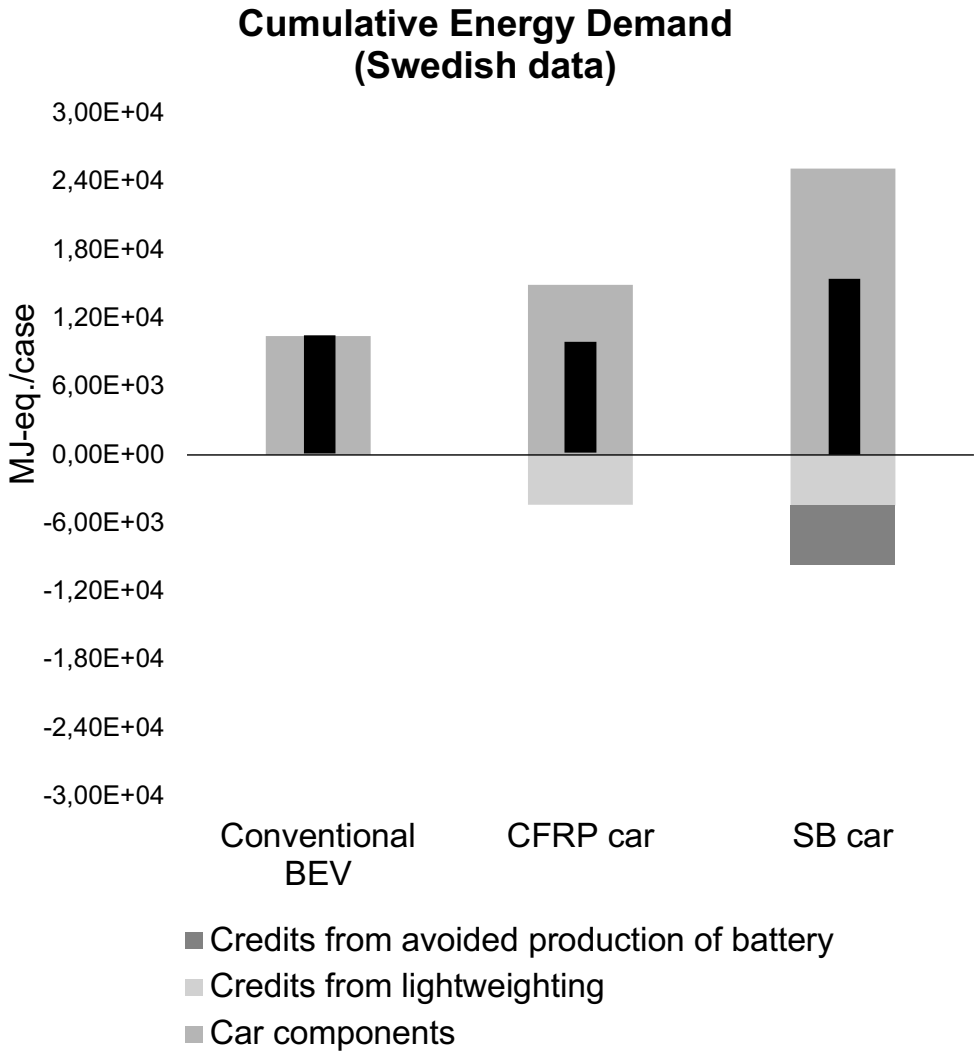

Figure F.8: Cumulative energy demand of the three vehicles based on Swedish data. Black bars shows the net climate impact. The result was achieved by an LCA where the inventory was based on a conceptual design of the vehicles. The functional unit included the function of the car components as well as the battery of the electric vehicle where the lifetime was set to 200,000 km.

F.3.1 The conventional BEV

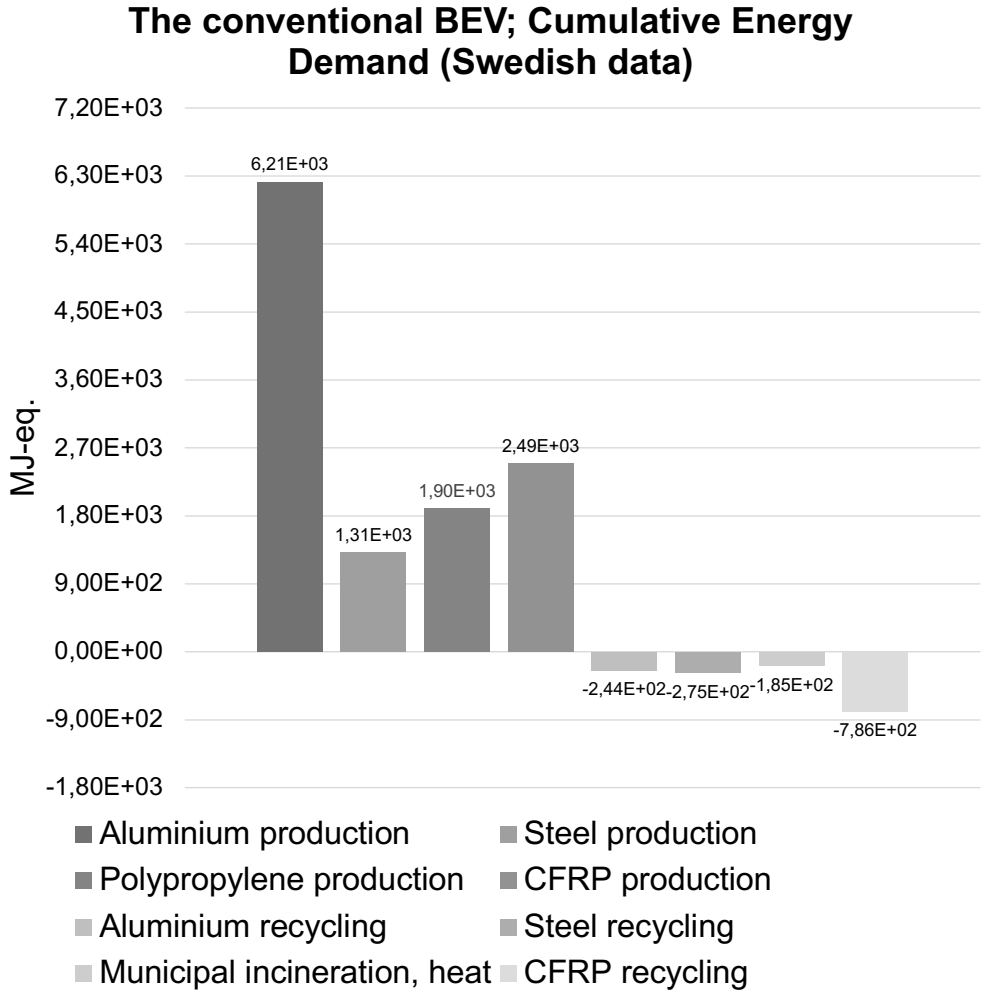

Figure F.9: Cumulative energy demand per process for the conventional BEV based on Swedish data. The result was achieved by an LCA where the inventory was based on a conceptual design of the vehicle. The functional unit included the function of the car components as well as the battery of the electric vehicle where the lifetime was set to 200,000 km.

F.3.2 The CFRP car

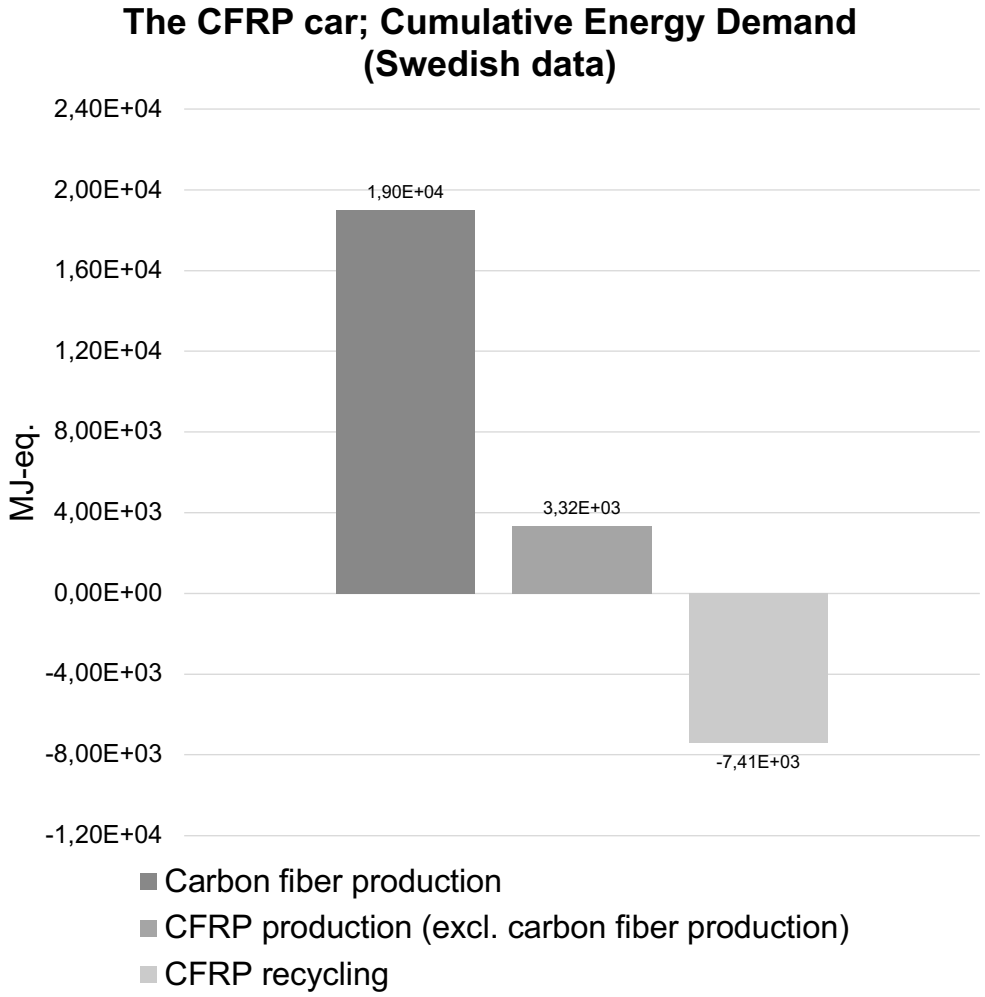

Figure F.10: Cumulative energy demand per process for the CFRP car based on Swedish data. The result was achieved by an LCA where the inventory was based on a conceptual design of the vehicle. The functional unit included the function of the car components as well as the battery of the electric vehicle where the lifetime was set to 200,000 km.

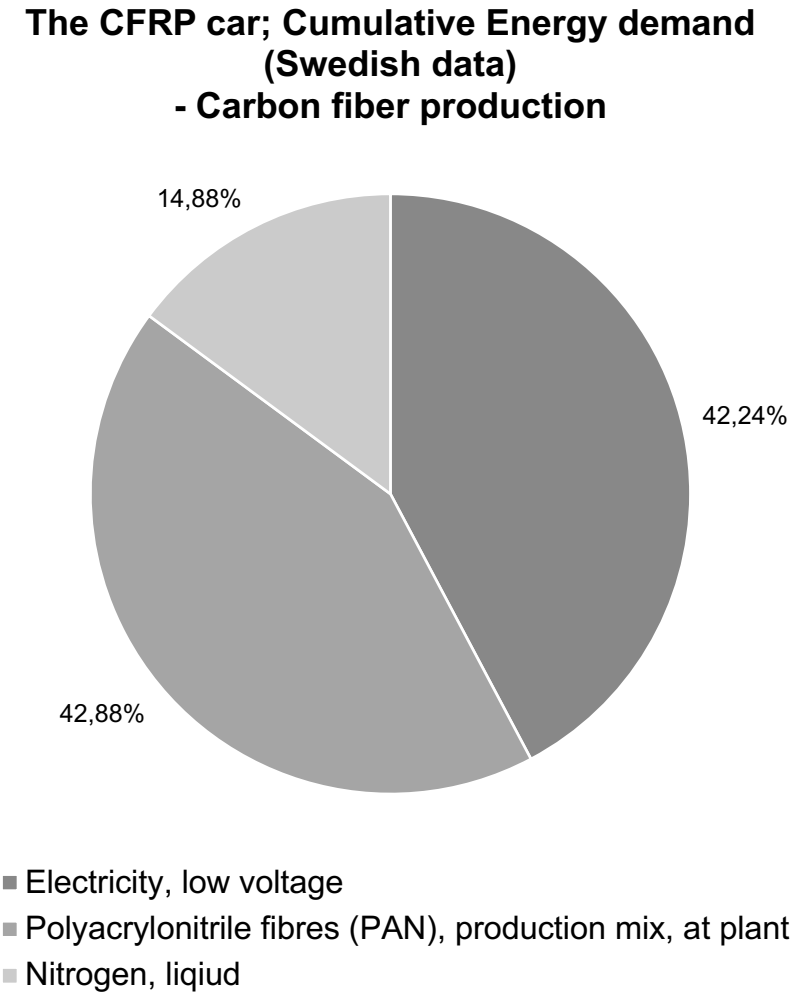

Figure F.11: Contribution graph for cumulative energy demand of the carbon fiber production for the CRFP car based on Swedish data. The result was achieved by an LCA where the inventory was based on a conceptual design of the vehicle. The functional unit included the function of the car components as well as the battery of the electric vehicle where the lifetime was set to 200,000 km.

F.3.3 The SB Car

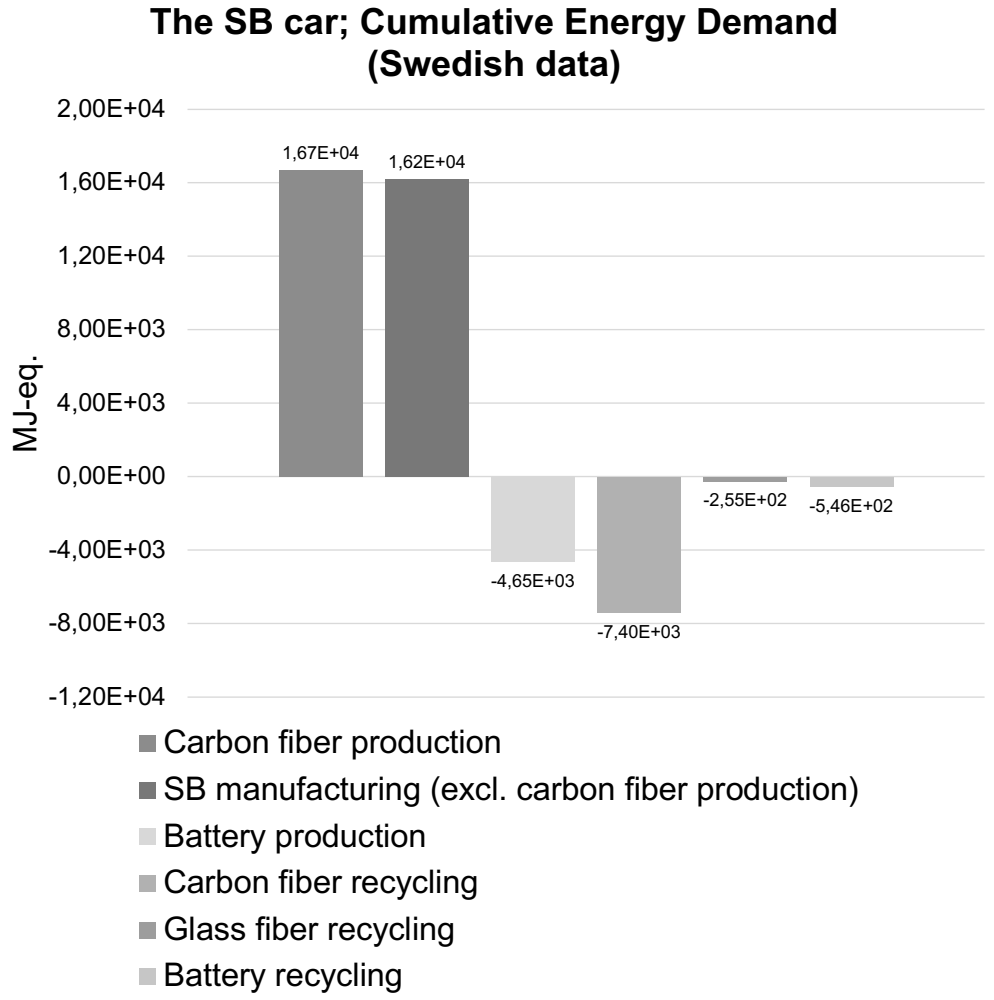

Figure F.12: Cumulative energy demand per process for the SB car based on Swedish data. The result was achieved by an LCA where the inventory was based on a conceptual design of the vehicle. The functional unit included the function of the car components as well as the battery of the electric vehicle where the lifetime was set to 200,000 km.

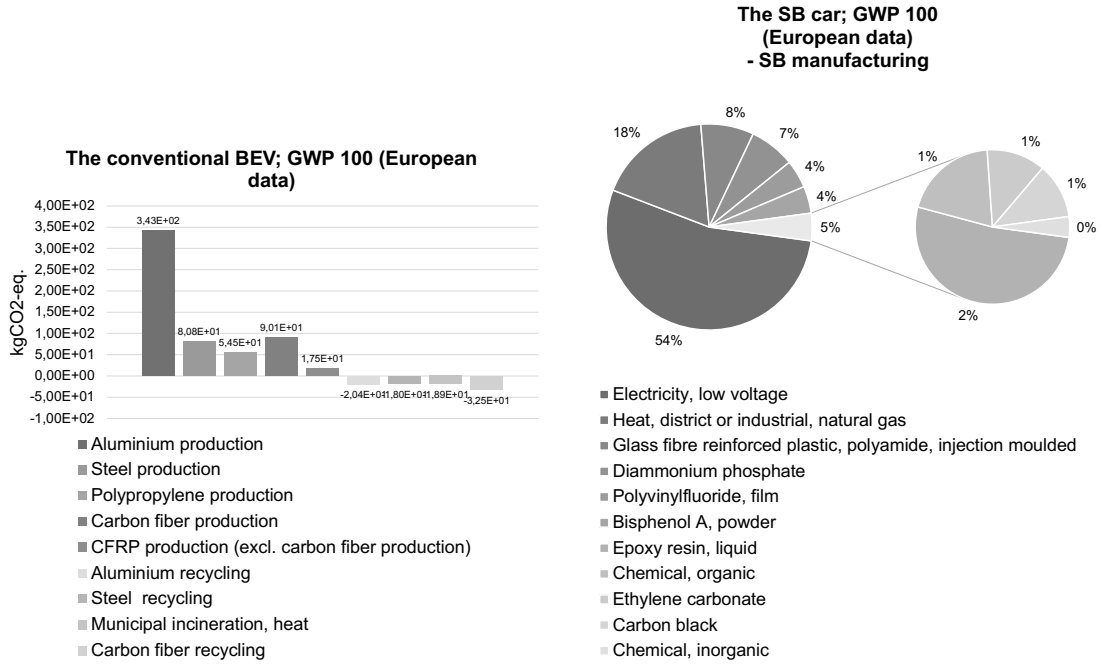

Figure F.13: Contribution graphs for cumulative energy demand of the carbon fiber production and the SB manufacturing for the SB car based on Swedish data. The result was achieved by an LCA where the inventory was based on a conceptual design of the vehicle. The functional unit included the function of the car components as well as the battery of the electric vehicle where the lifetime was set to 200,000 km.

DEPARTMENT OF TECHNOLOGY MANAGEMENT AND ECONOMICS
DIVISION OF ENVIRONMENTAL SYSTEMS ANALYSIS
CHALMERS UNIVERSITY OF TECHNOLOGY
Gothenburg, Sweden
www.chalmers.se

CHALMERS
UNIVERSITY OF TECHNOLOGY